Post-Translational Regulation of Autophagy

in *Saccharomyces Cerevisiae*

by

Yuchen Feng

A dissertation submitted in partial fulfillment
of the requirements for the degree of
Doctor of Philosophy
(Molecular, Cellular and Developmental Biology)
in the University of Michigan
2018

Doctoral Committee:

Professor Daniel J. Klionsky, Chair
Professor Anuj Kumar
Professor Lois Weisman
Professor Haoxing Xu

Yuchen Feng

yuchenf@umich.edu

ORCID iD: 0000-0002-5140-6364

Dedication

To my parents and grandparents

Acknowledgements

Completion of this doctoral dissertation is impossible without the support of many people. I sincerely appreciate your contributions in one way or another that makes me who I am.

First and foremost, thank you to my awesome advisor Dr. Daniel J. Klionsky for his fundamental role in my doctoral work since 2013. My deep gratitude is beyond words. As a distinguished scientist, you are a role model who demonstrated an enthusiastic, persistent and dedicated scientist from every day. I am grateful for your enormous guidance and support, invaluable training of critical thinking and experimental design, with your immense knowledge. As a Ph.D. mentor, you are also a humorous life coach sharing research experience, career development ideas, who always encourages and supports me to be the person I want to be. You made my journey oriented and enjoyable. I have learned substantially from you and will keep learning. Thank you for granting the one-of-a-kind Klionsky's 'trademark' that lasts a lifetime.

I am grateful for my thesis committee who guided me continuously since 2015. In particular, I thank Dr. Lois Weisman for her constructive and critical questions, Dr. Haoxing Xu for bringing an insightful mammalian perspective and Dr. Anuj Kumar for sharing yeast work experience and being a great listener. Special thanks goes to Dr. Ann Miller, the mentor of my first rotation, for your understanding, patience and tremendous help to get me over difficulties. I also thank my prelim committee Dr. Anuj Kumar, Dr. Ann Miller and Dr. Kwoon Wong for insightful suggestions and comments to kick off my research on the right track.

I am extremely fortunate to have joined the Klionsky lab and have worked with so many amazing and talented people. I started my rotation in January 2013 and have felt like home ever since. I sincerely thank the past and current lab members for your brilliant minds and loving souls that make the lab a cutting-edge research group as well as a welcoming home. I would never have imagined getting so many wonderful friends here. First, I thank Kai Mao for his tremendous help to start my rotation, training on all the experiments, techniques, and discussion of the Atg9 phosphorylation project. I thank Xu Liu for having me in the peroxisome project, endless help in lots of experiments and being a great friend. I also received constructive suggestions and inspirations from Amelie Bernard, Meiyan Jin, and Hana Popelka. I thank Zhiyuan Yao for sharing all the graduate school life being in the same cohort, lab and working on a few papers together. I thank Damian Gatica for his sense of humor. I give special thanks to Aileen Ariosa for her extreme kindness and being a true friend. Thank you for being knowledgeable, creative and constantly willing to help. It is my fortunate to share a bay, an apartment and special moments in life. Thanks to other members Ke Wang, Steven Backues, Katie Parzych, Daniel Orban, Xin Wen, Elizabeth Delorme-Axford, Zhangyuan Yin, Clarence Pascual, Ying Yang, Vikramjit Lahiri and Ziheng Xu for making a positive and collaborative working environment together and of course lots of game-night fun!

Last but not least, deepest gratitude goes to my families, my parents and grandparents, without whom I would never have been here. Thank you for giving me the freedom to choose what I wanted. Your unconditional and endless love, support, care and sacrifice is what I would never be able to pay back. I also thank my beloved husband Ruiyang Li, for having my back no matter what and being my Superman. Lastly, I thank my furry friend Tabi for kindly sharing her keyboard, pillow and yoga mat.

Preface

This thesis summarizes the research projects I participated in while working in Dr. Daniel J. Klionsky's laboratory since January 20013. Through these projects we gain a better understanding of how autophagy-related (*ATG*) genes are regulated through post-translational modifications (PTMs), in particular phosphorylation and ubiquitination of Atg9.

Chapters 1 contains parts of two review papers published in *Cell Research* (doi:10.1038/cr.2013.168) and *Trends in Cell Biology* (doi: http://dx.doi.org/10.1016/j.tcb.2015.02.002) with some modifications. Ding He, Zhiyuan Yao and I contributed equally to the first. Zhiyuan Yao and I contributed equally to the second.

Chapter 2 characterizes of the molecular machinery of how phosphorylation of Atg9 facilitates autophagosome formation and increase autophagy activity. It is published in the journal *Autophagy* (doi: 10.1080/15548627.2016.1157237). Kai Mao and Ke Wang prepared samples for SILAC. Jin-mi Heo from J. Wade Harper's lab in Harvard Medical School did SILAC analysis. Misuzu Baba from Kogakuin University did electron microscopy. Steven K. Backues generated strains in Figure 4C. I generated all other data.

Chapter 3 characterizes of the molecular machinery of down-regulation of autophagy through Atg9 ubiquitination-mediated proteasome degradation. This manuscript is submitted and under revision. I designed and performed most experiments. Erpan Ahat helped with strain construction in E3 screen.

Chapter 4 summarizes the major implications of my thesis research and future directions. It contains part of review paper *Trends in Cell Biology* (doi: http://dx.doi.org/10.1016/j.tcb.2015.02.002) Zhiyuan and I contributed equally.

Table of Contents

List of Tables

List of Figures

Abstract

Macroautophagy/autophagy is primarily a self-eating process that recycles cytosolic components such as misfolded or aggregated proteins and dysfunctional organelles for homeostasis and survival in unfavorable conditions. This highly conserved and constitutive pathway has to be tightly regulated; either too much or too little autophagy can be detrimental. Dysregulation of this pathway is related to various diseases that include neurodegeneration, cancer and infection, as well as aging-related disorders. Autophagy is stringently regulated at different levels including transcriptionally, post-transcriptionally, translationally and post-translationally. A thorough understanding of the mechanisms involved is crucial to allow the manipulation of autophagy for the treatment of diseases. Although 41 autophagy-related (*ATG*) genes have been identified, we have a limited understanding of the complex network of regulatory factors that control this process.

Atg9 is the only transmembrane protein in the core autophagy machinery (and one of only two Atg membrane proteins in fungi), which is absolutely required for autophagosome biogenesis and autophagy activity. Unlike other Atg proteins, Atg9 has a distinctive feature with regard to its subcellular localization: This protein travels between peripheral sites and the phagophore assembly site (PAS) where the autophagosome is formed, presumably delivering membranes from different donors to the PAS for autophagosome biogenesis.

Post-translational modifications (PTMs) including phosphorylation, ubiquitination, glycosylation, methylation, represent a subset of regulatory mechanisms that are critical for

modulating autophagy in order to adapt to different types of environmental stress. Atg9 is a phosphoprotein that is regulated by the Atg1 kinase. We used stable isotope labeling by amino acids in cell culture (SILAC) to identify phosphorylation sites on this protein and identified an Atg1-independent phosphorylation site at serine 122. A nonphosphorylatable Atg9 mutant showed decreased autophagy activity, whereas the phosphomimetic mutant enhanced activity. Electron microscopy analysis suggests that the different levels of autophagy activity reflect differences in autophagosome formation, correlating with the delivery of Atg9 to the PAS. Finally, this phosphorylation regulates Atg9 interaction with Atg23 and Atg27.

Besides, we identified a second novel mechanism of Atg9 regulation in autophagy through ubiquitination. In growing conditions, Atg9 is synthesized at a basal level and cells are primed for autophagy. We show that in this situation Atg9 is ubiquitinated and targeted for degradation in a proteasome-dependent manner, thereby limiting autophagy to a basal level. However, when cells are deprived of nutrients, autophagy is highly induced, necessitating an increase in the amount of Atg9; the proteasome-dependent reduction of Atg9 protein levels is subsequently reduced to facilitate the increase in autophagy. Thus, the post-translational ubiquitination of Atg9 provides an additional mechanism that allows cells to maintain appropriate levels of autophagy, and—by ending this modification—to rapidly respond and adapt to environmental stresses.

Chapter 1 Introduction[1]

1.1 Overview of Autophagy

1.1.1 Definition

Autophagy is a cellular process in which cytoplasmic contents are degraded within the lysosome/vacuole, and the resulting macromolecular constituents are recycled [1]. Macroautophagy is one type of autophagic process in which the substrates are sequestered within cytosolic double-membrane vesicles termed autophagosomes. The substrates of macroautophagy include superfluous and damaged organelles, cytosolic proteins and invasive microbes. Following degradation, the breakdown products are released back into the cytosol in order to recycle the macromolecular constituents and to generate energy to maintain cell viability under unfavorable conditions, and to protect the cell during various conditions of stress [1-3]. Autophagy is highly conserved from yeast to mammals, both morphologically and with regard to the protein constituents that make up the core autophagy machinery.

1.1.2 Terms and structures

The most readily identifiable feature of macroautophagy is the sequestration of cargo within cytosolic double-membrane vesicles, and many researchers still consider the analysis of

[1] This chapter is reprinted partly from Yuchen Feng, Ding He, Zhiyuan Yao, Daniel J Klionsky (2014) *Cell Research* (doi:10.1038/cr.2013.168), and partly from Zhiyuan Yao, Daniel J Klionsky (2015) *Trends in Cell Biology* (doi: http://dx.doi.org/10.1016/j.tcb.2015.02.002), with minor modifications.

macroautophagy by electron microscopy to be the "gold standard" for verifying macroautophagy activity. Below, I present some of the most common terms describing the principle structures of macroautophagy (Figure 1.1).

Autophagic body: The inner-membrane-bound structure released into the vacuole lumen after the outer membrane of the autophagosome fuses with vacuolar membrane [4]. Note that autophagic bodies only appear in yeast and plants due to the large size of the vacuole, and are not found in mammalian lysosomes.

Autophagosome: The completed double-membrane bound compartment, the product of phagophore expansion and closure, which sequesters cytoplasmic cargos during macroautophagy [5, 6].

PAS: The phagophore assembly site; a peri-vacuolar location or compartment where the nucleation of the phagophore initiates. Most components of the macroautophagy core machinery locate at least transiently at the PAS in yeast; however, a mammalian equivalent of the PAS has not been identified [7-9].

Phagophore: The double-membrane structure that functions in the initial sequestering of cargo, and thus the active compartment of macroautophagy. The phagophore further elongates/expands and ultimately closes, generating a completed autophagosome [10].

1.1.3 Origin of the phagophore membrane

Atg8 was the first Atg protein characterized to mark the phagophore and autophagosome [11, 12]. Immunofluorescence microscopy revealed that in rich conditions, Atg8 is primarily dispersed in the cytoplasm as small puncta, while it forms larger puncta in the vicinity of the vacuole when yeast cells are switched to starvation conditions; the nature of the smaller puncta is not known, whereas the larger puncta correspond to nascent autophagosomes. Subsequent studies

with green fluorescent protein (GFP)-tagged chimeras demonstrated that most of the Atg proteins reside at this location, at least transiently [8]. Accordingly, this site is proposed to be where the phagophore assembles, and is thus termed the phagophore assembly site, or PAS [8, 9]. The precise nature of the PAS with regard to its protein and membrane composition, or the reason for its peri-vacuolar localization, is not known, but assembly of the Atg proteins at the PAS occurs in a hierarchical manner [13]. The PAS forms constitutively, and in vegetative conditions a key component that marks this site is Atg11; upon autophagy induction, the structure transitions into an autophagy specific PAS and the function of Atg11 is replaced by a ternary complex of Atg17-Atg31-Atg29 that assembles at the PAS along with Atg1 and Atg13 [14, 15]. Atg9, which shuttles between the PAS and peripheral sites, plays an important role in directing membrane to the PAS that is needed for autophagosome formation, and it localizes to the PAS at a similar time as the Atg1 kinase complex. Subsequently, the PtdIns3K and Atg12–Atg5-Atg16 complexes are recruited to the PAS; the latter acts in part as an E3 ligase to facilitate the formation of Atg8– PE, one of the last proteins that are recruited to the PAS. In mammalian cells, the colocalization of ATG proteins is observed at multiple sites [16-18], instead of a single PAS as in yeast.

Until recently, the dogma was that the phagophore and autophagosome formed de novo, meaning that the sequestering membrane does not form in “one step” from a pre-existing organelle already containing its cargo as occurs throughout the secretory pathway [19, 20]. Regardless of the specific mechanism, autophagosome formation is thought to occur by the expansion of the phagophore, that is, a sheet of membrane that would correspond to the size of a complete autophagosome does not separate from the endomembrane system and simply curl up to form an autophagosome. Rather, after nucleation the phagophore grows through the addition of membrane from one or more donor sources [1, 21]; however, the origin of the phagophore membrane is still

under debate. Various lines of data suggest a role for almost every membrane compartment in contributing to formation of the autophagosome, including the ER, mitochondria, the Golgi apparatus and the plasma membrane [22-26]. As discussed above, there is no absolute equivalent of the yeast PAS in mammalian cells. Instead, there is evidence that there may be at least two separate mechanisms for generating autophagosomes. One mechanism would involve the delivery of membrane from various organelles, as is thought to occur in yeast, and the second utilizes an omega-shaped membrane structure or cradle, derived from phosphatidylinositol-3-phosphate (PtdIns3P)-enriched ER subdomains, termed an omegasome [27].

1.2 Types of Autophagy

There are three primary types of autophagy: microautophagy, macroautophagy and a mechanistically unrelated process, chaperone-mediated autophagy that only occurs in mammalian cells. Both micro and macroautophagy can be selective or nonselective and these processes have been best characterized in yeast [28] (Table 1.1). As noted above, the most distinguishing feature of macroautophagy is the formation of the double-membrane bound phagophore and autophagosome (Figure 1.1). In contrast, during microautophagy the cargos are sequestered by direct invagination or protusion/septation of the yeast vacuole membrane [29]. Nonselective autophagy is used for the turnover of bulk cytoplasm under starvation conditions, whereas selective autophagy specifically targets damaged or superfluous organelles, including mitochondria and peroxisomes, as well as invasive microbes; each process involves a core set of machinery, as well as specific components, and accordingly is identified with a unique name — mitophagy for selective mitochondria degradation by autophagy, pexophagy for peroxisomes, xenophagy for microbes, etc. [30, 31]. In this chapter, I will mainly focus on macroautophagy, since the molecular or physiological studies of nonselective microautophagy are limited, and

selective microautophagy shares most of the same machinery with macroautophagy (hereafter autophagy).

1.3 Core molecular machinery of autophagosome formation

The transition of autophagy studies from morphology to molecular machinery relied on the identification of the ATG gene. As mentioned above, genetic screens for autophagy-defective mutants in yeast have led to the identification of over 40 ATG genes [32-35], many of which have known orthologs in higher eukaryotes.

Among these ATG genes, one subgroup, consisting of approximately 18 genes (Table 1.2), is shared among the various types of autophagy including nonselective macroautophagy, the cytoplasm-to-vacuole-targeting (Cvt) pathway (a biosynthetic autophagy-like pathway), mitophagy and pexophagy. More specifically, the corresponding gene products of this subgroup are required for autophagosome formation, and thus are termed the core autophagy machinery. The core Atg proteins can be divided into different functional subgroups: (A) the Atg1/ ULK complex (Atg1, Atg11, Atg13, Atg17, Atg29 and Atg31) is the initial complex that regulates the induction of autophagosome formation; (B) Atg9 and its cycling system (Atg2, Atg9 and Atg18) play a role in membrane delivery to the expanding phagophore after the assembly of the Atg1 complex at the PAS; (C) the PtdIns 3-kinase (PtdIns3K) complex (Vps34, Vps15, Vps30/Atg6, and Atg14) acts at the stage of vesicle nucleation, and is involved in the recruitment of PtdIns3P-binding proteins to the PAS; (D) two ubiquitin-like (Ubl) conjugation systems: the Atg12 (Atg5, Atg7, Atg10, Atg12 and Atg16) and Atg8 (Atg3, Atg4, Atg7 and Atg8) conjugation systems play roles in vesicle expansion [13, 36-38].

1.3.1 Yeast Atg1 kinase complex

The Atg1 kinase complex regulates the magnitude of autophagy [39-43]. This complex also plays a role in mediating the retrieval of Atg9 from the PAS [44]. The Atg1 kinase complex is extensively regulated, receiving input from several signaling pathways. In yeast, much of the regulation centers around nutrient signaling and involves kinases that sense the nutritional status of the cell including the target of rapamycin (TOR), protein kinase A (PKA), Gcn2 and Snf1. The yeast Atg1 kinase complex includes Atg1, a Ser/Thr protein kinase, Atg13, a regulatory subunit, and the Atg17-Atg31-Atg29 complex, which may function in part as a scaffold (Figure 1.2). Atg1 is the only kinase of the core autophagy machinery; however, despite the fact that it was the first Atg protein to be identified, the key physiological substrate of yeast Atg1 is not known. Atg1 kinase activity is required for autophagosome formation and the Cvt pathway, although there are conflicting data concerning the changes in kinase activity when yeast cells shift from vegetative growth to autophagy-inducing conditions [45-47]. Atg1 recruitment to the PAS may be regulated by PKA-dependent phosphorylation [48]. TOR also phosphorylates Atg1, and autophosphorylation is important in regulating Atg1 kinase activity [49, 50].

Atg13 is required for Atg1 kinase activity. Atg13 is hyperphosphorylated under nutrient-rich conditions, and its phosphorylation is regulated by TOR complex 1 (TORC1) [51] and/or PKA [52]. Atg13 is rapidly, but only partially, dephosphorylated upon autophagy induction [53]. These data, coupled with affinity isolation studies, led to a model suggesting that the interaction between Atg1 and Atg13 is controlled by Atg13 phosphorylation — dephosphorylation would lead to the formation of an Atg1-Atg13 complex, and subsequent activation of Atg1 kinase activity [42]. Recent data, however, suggest that Atg1 and Atg13 interact in a constitutive manner [54], which is similar to the situation in other organisms. Atg17-Atg31-Atg29 exists as a stable complex under

both vegetative and starvation conditions, suggesting that formation of the complex is not involved in autophagy induction. Atg31 bridges Atg17 and Atg29, Atg17 binds Atg13, and Atg29 binds Atg11; the latter is a scaffold protein that may also be considered part of the Atg1 kinase complex because it binds Atg1 and is involved in the transition of the PAS that occurs during the switch from vegetative to starvation conditions [14, 15, 39, 55-57]. Both Atg29 and Atg31 are phosphoproteins. The phosphorylation of Atg29 appears to be involved in regulation and is proposed to alter the conformation of an inhibitory C-terminal peptide to allow the protein to become active [15].

1.3.2 Yeast Atg9

In yeast cells, Atg9 is a transmembrane protein that transits between the PAS and peripheral sites (Figure 1.3); the latter have been termed Atg9 reservoirs or tubulovesicular clusters, and are proposed to represent sites from which membrane is delivered to the forming phagophore [23, 44, 58], although the exact role of Atg9 in this process is not clear. Atg9 is proposed to consist of six transmembrane domains, with both the amino and carboxyl termini exposed in the cytosol. Atg9 self-interacts and may exist in a complex [59]. Atg9 localization to the PAS from the peripheral sites (referred to as anterograde transport) depends on Atg11, Atg23 and Atg27 [44, 60-62]. Return to the peripheral sites (retrograde movement) requires Atg1-Atg13, Atg2 and Atg18; PAS recruitment of the latter involves binding to PtdIns3P and thus necessitates the function of Atg14 and the class III PtdIns3K complex [44]. Atg27 is a type I integral transmembrane protein, while the other components involved in Atg9 movement are soluble and/ or peripherally associated with membranes.

Atg9 was the first identified transmembrane protein in the Atg protein family, but detailed structural information is not available. Similarly, no structural information has been published for

the Atg11, Atg23 and Atg27 proteins, which are involved in Atg9 localization to the PAS [44, 60-62] (Figure 1.3). Atg18, together with Atg2, helps Atg9 cycle from the PAS to peripheral sites. Although the structure of Atg18 has not been solved, a paralog, Hsv2, which shares high sequence similarity with Atg18, has been studied in different yeast strains [63-65]. Both proteins belong to the "PROPPINs" family, which are defined by β propeller structures and the existence of phosphoinositide binding sites [65, 66]. Hsv2 displays the typical propeller fold that consists of seven β blades. In addition, Hsv2 (and Atg18 along with a second paralog, Atg21) harbor an FRRG motif, which is required for phosphoinositide binding. Detailed analysis indicates that Hsv2 possesses two PtdIns3P binding sites, located in blade 5 and blade 6. Mutations in the corresponding sites in Atg18 result in loss of Atg18 localization. Moreover, the blade 6 β3-β4 loop of Hsv2 proves to be important for protein docking to the membrane. When several hydrophobic residues in this region, or the corresponding residues in Atg18, are mutated, the binding of the protein to liposomes is eliminated [65]. These results suggest a potential Atg18-docking model: the disk-like Atg18 touches the membrane with its edge; two binding sites interact with PtdIns3P on the membrane surface and the hydrophobic loop penetrates the membrane to stabilize the interaction.

The Atg18 β1-β2 loop and β2-β3 loop in blade 2 are important for PAS targeting [64]. Blade 2 is located at the opposite position to blade 5 and blade 6, and thus is not involved in membrane docking. Additional studies indicate that the loops in blade 2 are important forAtg18-Atg2 interaction [64, 67], allowing a refinement of the model for Atg18 membrane binding. While Atg18 binds to the membrane through blades 5 and 6, blade 2, which is located on the opposite side of the protein, interacts with Atg2. The structural data further suggest that the Atg18-Atg2 interaction is independent of membrane docking. Detailed information about the Atg18-Atg2

interaction awaits progress on the crystallization of Atg2, which may also provide insight into their interdependent localization to the PAS.

1.3.3 Yeast PtdIns3K complexes I and II

In yeast, Vps15 (a putative regulatory protein kinase that is required for Vps34 membrane association), Vps30/Atg6, Vps34 (the PtdIns3K), Atg14 and Atg38, form the autophagy-specific class III PtdIns3K complex I (Figure 1.4), which localizes at the PAS [68-70]. One key role of the PtdIns3K complex, the generation of PtdIns3P, is presumably to recruit PtdIns3P-binding proteins such as Atg18 to the PAS. Vps15, Vps34 and Vps30 are generation of PtdIns3P, is presumably to recruit PtdIns3P-binding proteins such as Atg18 to the PAS. Vps15, Vps34 and Vps30 are present in a second complex that includes Vps38 instead of Atg14. Thus, the latter protein appears to determine the specificity of the PtdIns3K complex I for macroautophagy.

1.3.4 Yeast Ubl conjugation systems

There are two Ubl protein conjugation systems that participate in macroautophagy [48]. These include two Ubl proteins, Atg8 and Atg12, which are used to generate the conjugation products Atg8–PE and Atg12–Atg5, respectively (Figure 1.5). The Ubl conjugation systems participate in phagophore expansion, although their functions are not fully understood. The Atg12–Atg5 conjugate, along with a third component, Atg16, may act in part as an E3 ligase to facilitate the conjugation of Atg8 to PE, and the amount of Atg8 can regulate the size of autophagosomes [71]; however, Atg8 also functions in cargo binding during selective autophagy [72]. Yeast Atg8 is initially synthesized with a C-terminal arginine residue that is removed by Atg4, a cysteine protease [38, 100]. During autophagy, Atg8 is released from Atg8–PE by a second Atg4-dependent cleavage referred to as deconjugation [73], whereas there is no similar cleavage that separates Atg12 from Atg5. Both of the Ubl protein conjugation systems share a single E1-like activating

enzyme, Atg7 [74-77]. The E2-like conjugating enzymes are Atg3 for Atg8, and Atg10 for Atg12 [75, 78].

1.4 Selective autophagy

In selective autophagy, the overall morphology is largely the same as during nonselective autophagy with one primary distinguishing feature; in selective autophagy, the membrane-bound vesicle targets specific cargos, instead of random cytoplasm. In addition to the core machinery, a cargo ligand (a molecular entity on the surface of the cargo that is recognized by a receptor), receptor and scaffold are involved; the latter act to specifically bind the cargo and provide a bridge between the cargo and the core machinery [79, 80]. Accordingly, during selective autophagy the phagophore is close to the cargo, and the completed autophagosome excludes bulk cytoplasm. As noted above, there are different types of selective autophagy according to the cargo types. Here I will describe Cvt pathway as an example (Table 1.1).

1.4.1 Cvt pathway

With regard to the details of cargo recognition, the Cvt pathway was the first well-studied type of selective autophagy in yeast; it is also the primary example of a biosynthetic rather than degradative use of autophagy [80-83]. The double-membrane sequestering vesicle is termed a Cvt vesicle rather than an autophagosome; as noted above, this vesicle contains selective cargos of the Cvt pathway, but excludes bulk cytoplasm, in accordance with the biosynthetic and constitutive nature of the Cvt pathway compared to starvation-induced autophagy. The Cvt pathway delivers precursor forms of hydrolases, such as Ape1 (aminopeptidase I), Ape4 and Ams1 (α-mannosidase), from the cytoplasm to the vacuole, where they carry out their functions. The formation of the Cvt vesicle at the PAS is driven by the formation of a cargo complex, composed primarily of oligomerized precursor (prApe1) along with a few other resident vacuolar hydrolases

[84, 85]. Atg19 acts as a cargo receptor that binds the ligand (the prApe1 propeptide) and is thus recruited to the complex [86]. Subsequently, the interaction between Atg19 and Atg11, a key scaffold that functions in most or all types of selective autophagy in yeast, mediates the delivery of the cargo complex to the PAS [72, 87]. Atg19 also interacts with Atg8, which might play a role in tethering the Cvt complex to the phagophore [88] and in directing the selective sequestration of the cargo during vesicle formation [72].

1.5 Regulation of Autophagy

Macroautophagy is involved in various aspects of cell physiology, and its dysregulation is associated with a range of diseases. The regulation of macroautophagy is complex, in part reflecting the fact that this process, if not properly modulated, can result in cell death. In this chapter we focus on the current state of knowledge concerning transcriptional and post-transcriptional regulation of macroautophagy in yeast and mammals.

1.5.1 Transcriptional regulation

TOR kinase has long been known as the master regulator of macroautophagy, and as part of TOR complex 1, it controls a range of transcription factors; however, the relevant downstream targets with regard to autophagy regulation have not been well understood. Only recently have researchers started to identify an entire network of transcription factors that are involved in controlling autophagy (summarized in Table 1.3).

Several transcription factors including TP53, STAT3 and NFKB play a dual role in autophagy regulation, through both transcriptional (nuclear interaction) and transcriptional-independent (cytoplasmic interaction) mechanisms, acting as both activators and repressors [89-91]. Thus, it will be interesting to understand the complex transcriptional network involved in

autophagy regulation and to determine precisely what governs the switch between adaptation to stress and the promotion of cell death.

1.5.2 Post-transcriptional regulation of autophagy

Autophagy can be regulated by various post-transcriptional mechanisms, including the action of noncoding microRNAs (miRNAs; summarized in Table 1.4) [92-95]. miRNAs are a class of small endogenous regulatory RNAs that control gene expression at the post-transcriptional level, typically by translational arrest or mRNA cleavage, through interaction mainly at the 3'-untranslated regions (UTRs) of the target mRNAs. miRNAs play important roles in the regulation of development, growth, and metastasis of cancer, and in determining the response of tumor cells to anticancer therapy. Here, we highlight some of the recent data concerning miRNAs and their involvement in regulating different steps of the autophagy core machinery.

The ULK1/2 (yeast Atg1) kinase complex plays a key role in the induction of autophagy. *Mir20a* and *Mir106b*, two members of the *Mir17* microRNA family, may participate in regulating leucine deprivation-induced autophagy via suppression of ULK1 expression in C2C12 myoblasts [96]. There is a putative recognition sequence for *MIR885-3p* in the 5'-UTR of *ULK2*, and this miRNA contributes to the regulation of autophagy via the downregulation of *ULK2* [97].

Nucleation of the phagophore involves the phosphatidylinositol 3-kinase complex that includes PIK3C3/VPS34-PIK3R4/VPS15-BECN1-ATG14. *Mir195* inhibitor treatment increases autophagy activation and suppresses neuron inflammation in vivo and in vitro, which suggests a repressive role of this miRNA [98]. Furthermore, *Atg14* was identified as the functional target of *Mir195*. *MIR205* inhibits *BCL2* expression, thus modulating a key negative regulator of BECN1 function in autophagy [99]. The *BECN1* 3'-UTR binds *MIR30A*, negatively regulating *BECN1* expression, resulting in decreased autophagic activity

MIR30D regulates multiple genes in the autophagy pathway including *BECN1*, *BNIP3L*, *ATG2*, *ATG5*, and *ATG12* based on bioinformatics and miRNA target prediction. *MIR30D* directly suppresses the expression of the corresponding core proteins in the autophagy pathway, inhibiting autophagosome formation and conversion of LC3B-I (a proteolytically processed form) to LC3B-II (a lipidated form) [100]. *MIR376B* controls autophagy by directly regulating intracellular levels of two key autophagy proteins, ATG4C and BECN1 [101]. *MIR101* is a potent inhibitor of basal, etoposide- and rapamycin-induced autophagy, at least in part through downregulation of *RAB5A*, *STMN1* and *ATG4D* [102].

ATG9 is a transmembrane protein required for expansion of the phagophore. Studies in yeast suggest that this protein traffics between donor membranes and the site of phagophore formation [44, 60, 61, 103]. *C. elegans atg-9* contains a binding sequence for *mir-34*, and this miRNA inhibits ATG-9 expression at the post-transcriptional level in vitro [104]. The *C. elegans mir-34* mutation extends life span by enhancing autophagic flux, and in mammalian cells *MIR34A* represses autophagy by directly inhibiting the expression of ATG9A. *MIR130A* reduces autophagosome formation, an effect mediated by downregulation of the *ATG2B* and *DICER1* genes [105]; DICER1 is a key component of the cellular miRNA machinery, suggesting that its downregulation is part of a feedback loop that maintains optimal levels of autophagy. *MIR130A* thus modulates cell survival by controlling autophagic flux.

Besides the miRNA regulation of autophagy, it should also be noted that autophagy, in turn, regulates the biogenesis of miRNAs. DICER1 and AGO2, components involved in miRNA biogenesis, are targeted for selective autophagic degradation through the action of the receptor protein CALCOCO2/NDP52 and the adaptor protein GEMIN4 [106]. Thus, autophagy maintains functional miRNA synthesis by facilitating the removal of inactive DICER1-AGO2 complexes.

Besides miRNA targeting, mRNAs are tightly regulated through other mechanisms, including decapping and degradation of unwanted mRNAs, and storing mRNA in an inaccessible/inactive state in P-bodies. However, it has not been determined whether these post-transcriptional mechanisms regulate autophagy.

1.5.3 Post-translational regulation

Post-translational regulation is essential for modulating autophagy in order to adapt to different types of environmental stress. With regard to autophagy post-translational modifications (PTMs) can be classified into three categories: phosphorylation, ubiquitination and acetylation [107]. These modifications help to regulate autophagy on multiple levels. For example, Atg core components can be directly modified, either being activated or inhibited. In addition, PTMs can also indirectly regulate autophagy by modulating regulators upstream of the Atg proteins. Here, we focus on the direct post-translational regulation of proteins that are part of the Atg core machinery.

1.5.3.1 Phosphorylation

Phosphorylation of Atg proteins is the most well studied PTM. Phosphorylation of Atg proteins either alters the protein's functional activity or changes the protein's structure to modulate the affinity to binding partners. The regulation of the Atg1/ULK1 complex, which is important for autophagy initiation, is a good example where protein function is altered by PTM.

In mammalian cells ULK1 is part of a complex that contains ATG13, RB1CC1 and ATG101 [108]. Previous studies have established that TOR kinase is as a negative regulator of Atg1/ULK1 in nutrient-rich conditions [109, 110]. MTOR phosphorylates ULK1 on Ser757, inhibiting ULK1 activity. Under stress conditions, AMPK phosphorylates ULK1 at Ser317 and

Ser777, thus activating kinase activity and inducing autophagy [111]. AMPK is thus upstream of MTOR and negatively regulates MTOR activity indirectly [112]. In glucose-replete conditions, AMPK is inhibited. Moreover, Ser757 phosphorylation of ULK1 by MTOR results in a weaker interaction between ULK1 and AMPK [111], Thus, the AMPK-MTOR system can regulate ULK1 kinase activity to finely tuning the autophagy process.

In yeast, the Atg1 complex consist of the Atg1 kinase, its regulatory partner Atg13, and the Atg17-Atg31-Atg29 complex [113], TOR participates in the regulation of Atg1 through the direct phosphorylation of the regulatory Atg13 subunit, which is also inhibited by the cAMP-dependent protein kinase A (PKA). Under nutrient-rich conditions Atg13 is phosphorylated at distinct sites by PKA and TOR [48, 51]. The phosphorylation of Atg13 affects both the nature of its interaction with Atg1 and its localization to the phagophore assembly site (PAS). Atg1 is also a direct substrate of PKA, and phosphoryalation also regulates its localization to the PAS. The Atg17-Atg31-Atg29 complex also modulates Atg1 kinase and autophagy activity. Atg29 is phosphorylated along its C terminus and this modification is necessary for interaction with the scaffold protein Atg11, PAS localization and function [15].

Phosphorylation of the phosphatidylinositol (PtdIns) 3-kinase (PtdIns3K) complex, another autophagy core machinery, which is responsible for producing PtdIns3P, also regulates autophagy [107, 114]. In mammals, PIK3C3/VPS34 is the catalytic subunit of a class III PtdIns3K that provides the core function of the complex. PIK3C3 is functional in autophagy when it interacts with BECN1, which in turn is inhibited by anti-apoptotic proteins such as BCL2 [113]. Thus, any PTM that disrupts the interaction between BECN1 and its inhibitory partners has the potential for stimulating autophagy and vice versa. For example, DAPK phosphorylates BECN1 and

MAPK8/JNK1 phosphorylates BCL2 [107, 115, 116]. In both cases the interaction between BECN1 and BCL2 is disrupted, allowing BECN1 to associate with PIK3C3 and induce autophagy.

The protein kinase AKT is also involved in BECN1 phosphorylation. AKT enhances the interaction of BECN1 with YWHA/14-3-3 proteins, thus negatively regulating autophagy [117]. There are multiple PtdIns3K complexes that function in various pathways including autophagy, both stimulating and inhibiting, and their regulation is complex. For example, AMPK phosphorylation inhibits the non-autophagic function of PIK3C3; whereas under glucose starvation conditions, ATG14 functions to decrease the AMPK-dependent phosphorylation of PIK3C3 and increase the phosphorylation of BECN1, which lead to autophagy induction [118]. This differential regulation acts in part to promote activation of the autophagy-specific PIK3C3 complex under stress conditions.

Many other ATG proteins are phosphorylated. For example, LC3-II can be phosphorylated by protein kinase A or protein kinase C [119]. The phosphorylated form has reduced function in autophagosome formation. Yeast Atg9 is a direct target of Atg1 [120]. Phosphorylation of Atg9 is required for recruitment of Atg8 to the PAS, thus ensuring normal expansion of the phagophore. Atg18, a protein involved in Atg9 cycling, is also phosphorylated [121], affecting its affinity for phosphoinositides.

1.5.3.2 Ubiquitination

Ubiquitination is another type of PTM that regulates autophagy. In general ubiquitination can affect the stability of Atg proteins and their upstream regulators. However, ubiquitin can also serve as a signaling molecule, recruiting autophagy receptors. In either case, specific E3 ligases play an important role in ubiquitin function [122].

PARK2/parkin, an E3 ligase that is important for mitochondrial homeostasis, is involved in mitophagy (the selective autophagic degradation of mitochondria) [122, 123]. Once activated by PINK1, PARK2 ubiquitinates multiple mitochondrial proteins on the surface of depolarized mitochondria [124]. Although the precise mechanism is not clear, these events may initiate a cascade that results in the clearance of damaged mitochondria. Conversely, PARK2 has a negative role in non-selective autophagy. PARK2 stabilizes BCL2 via mono-ubiquitination, which strengthens the interaction between BCL2 and BECN1, thus suppressing autophagy [125].

Ubiquitination of the autophagy core machinery can either affect protein function or stability. TRAF6, a RING finger-containing ligase, can ubiquitinate both BECN1 and ULK1 [126, 127]. The K63 linked ubiquitination of BECN1 by TRAF6 is required for TLR4-induced autophagy. In contrast, the deubiquitinating enzyme TNFAIP3/A20 antagonizes the TRAF6 regulation by deubiquitinating BECN1 and repressing autophagy. TRAF6 also ubiquitinates K-63 of ULK1 when interacting with AMBRA1. The ubiquitination of ULK1 leads to the stabilization and activation of the protein. RNF5, another E3 ligase, controls ATG4B; ubiquitination promotes its degradation [128]. Decreased levels of ATG4B result in limited proteolytic processing of LC3 and autophagy suppression.

Although E3 ligases regulate autophagy primarily through their ligation function, these proteins may also regulate autophagy in a ligase-independent manner. A recent study shows a general role of tripartite motif (TRIM) protein family. TRIM proteins contain a, N-terminal RING domain; however, these proteins regulate autophagy mainly through the C-terminal substrate-binding domain [129]. TRIM proteins can bind ATG proteins such as BECN1, ULK1, and LC3 family proteins, as well as receptors including SQSTM1/p62. These findings suggest that TRIM proteins serve as a platform for the association of different ATG proteins.

1.5.3.3 Acetylation

In addition to the epigenetic regulation of autophagy by histone acetylation (discussed below), ATG proteins are also regulated by direct acetylation [130]. During serum starvation, acetyltransferase KAT5/TIP60 is activated by GSK3 and directly acetylates ULK1 [131]. This acetylation is required for ULK1 activation and autophagy initiation. Either inhibition of KAT5 or the presence of an acetylation-insensitive ULK1 mutant will reduce autophagy activity. KAT5 has a yeast ortholog, Esa1, which acetylates Atg3 on K19 and K48 [132]. Blocking this acetylation attenuates Atg8-Atg3 interaction and Atg8 lipidation. The Rpd3 deacetylase counters the effect of Esa1. Rpd3 deletion results in increased acetylation of Atg3 and upregulated autophagy.

Another example of regulatory acetylation/deacetylation in autophagy is seen with EP300/p300 and SIRT1. The EP300 acetyltransferase acetylates a variety of autophagy proteins including ATG5, ATG7, LC3 and ATG12. However, acetylation appears to inhibit the function of these proteins because reduced EP300 stimulates autophagy activity [133]. Conversely, the NAD-dependent deacetylase SIRT1 deacetylates ATG5, ATG7 and LC3 [134]. Deletion of *Sirt1* results in increased acetylation of ATG proteins, negatively affecting autophagosome formation. In addition to the core machinery, acetylation also regulates autophagy by modulating transcription factors upstream of the *ATG* genes. One example is seen with FOXO3, which activates several *ATG* genes as discussed above [135, 136]. Acetylation of FOXO3 cause its dissociation from DNA [137]. SIRT1/2 deacetylate FOXO3 under stress conditions, and this is coordinated with the induction of autophagy [134, 138].

1.5.3.4 Epigenetic regulation

PTMs can also modulate histones and epigenetically regulate autophagy. Histone H3 hyperacetylation on lysine 9, 14 and 18 is accompanied by the repression of *ATG* gene transcription

and autophagic defects [139, 140]. Acetylation on histone H4 lysine16 (H4K16) by KAT8/hMOF downregulates *ATG* genes transcription [141, 142]. Combining those data suggests that acetylation on histones generally interferes with *ATG* gene transcription. Another modification on histone, methylation, also regulates the outcome of *ATG* gene transcription. EHMT2/G9a associates with *ATG* gene promoters and methylates histone H3 in nutrient-rich conditions [143]. This methylation leads to repression of *ATG* gene transcription. During starvation, these marks are removed allowing the induction of *ATG* gene expression. Inhibition of EHMT2 therefore results in upregulated expression of *ATG* genes.

1.5.5 Regulation through protein–protein interactions

Other than by directly modifying ATG proteins, many regulators can also regulate autophagy by interacting with these proteins to modulate their function [114]. One example is TP53. As discussed above, cytosolic TP53 is a negative regulator of autophagy. This population of TP53 interacts with RB1CC1, inhibiting the function of the ULK1 complex in normal conditions [144]. Because TP53 can be translocated to the nucleus, phosphorylation of TP53 decreases the amount in the cytosolic pool, and permits autophagy induction under stress conditions.

Table 1.1 The main types of autophagy in yeast

Name			Cargo	Characteristics
Macroautophagy				
	Nonselective		Random cytoplasm	Autophagosome formation
	Selective	Cvt pathway	Vacuolar hydrolases	Autophagosome or Cvt vesicle formation; Atg19 and Atg34 are receptors, Atg11 is a scaffold
		Mitophagy	Damaged or superfluous mitochondria	Autophagosome formation; Atg32 is a receptor, Atg11 is a scaffold
		Pexophagy	Superfluous peroxisomes	Autophagosome formation; Atg30 and Atg36 are receptors, Atg11 and Atg17 are scaffolds
Microautophagy				
	Nonselective		Random cytoplasm, vacuole membrane	Vacuole invagination
	Selective		Mitochondria	Vacuole invagination or protrusion
			Peroxisomes	Vacuole invagination or protrusion
			Nuclear membrane	Vacuole invagination, requires Nvj1 and Vac8

Table 1.2 Atg/ATG proteins in the core machinery of autophagosome formation

	Yeast	Mammals	Characteristics and functions
Atg1/ULK complex	Atg1	ULK1/2	Ser/Thr protein kinase; phosphorylated by M/TORC1; recruitment of Atg proteins to the PAS
	Atg13	ATG13	Regulatory subunit through phosphorylation by M/TORC1 and/or PKA, linker between Atg1 and Atg17
	Atg17	RBICCI/FIP200 (functional homolog)	Scaffold protein, ternary complex with Atg29 and Atg31. Phosphorylated by ULK1; scaffold for ULK1/2 and ATG13
	Atg29		Ternary complex with Atg17 and Atg31
	Atg31		Ternary complex with Atg17 and Atg29
	Atg11		Scaffold protein in selective autophagy for PAS organization
		C12orf44/Atg101	Component of the conplex with ATG13 and RB1CC1
	Atg2	ATG2	Interacts with Atg18

Atg9 and its cycling system	Atg9	ATG9A/B	Transmembrane protein, directs membrane to the phagophore
	Atg18	WIPI1/2	PtdIns3P binding protein
PtdIns3K complex	Vps34	PIK3C3/VPS34	PtdIns 3-kinase
	Vps15	PIK3R4/VPS15	Ser/Thr protein kinase
	Vps30/Atg6	BECN1	Component of PtdIns3K complex I and II
	Atg14	ATG14	Component of PtdIns3K complex I
Atg8 ubiquitin-like conjugation system	Atg8	LC3A/B/C, GABARAP, GABARAPL1/2	Ubl, conjugated to PE
	Atg7	ATG7	E1-like enzyme
	Atg3	ATG3	E2-like enzyme
	Atg4	ATG4A/B/C/D	Deconjugating enzyme, cysteine proteinase
Atg12 ubiquitin-like conjugation system	Atg12	ATG12	Ubl
	Atg7	ATG7	E1-like enzyme
	Atg10	ATG10	E2-like enzyme
	Atg16	ATG16L1	Interacts with Atg5 and Atg12
	Atg5	ATG5	Conjugated by Atg12

Table 1.3 Transcriptional factors of mammalian autophagy

Transcription factor	**Target**	**Effect**	**Reference**
ATF4	*ATG5*, *LC3* and *ULK1*	+	[145-148]
ATF5	*MTOR*	-	[149]
CEBPB	*BNIP3*, *LC3* and *ULK1*	+	[150]
DDIT3/CHOP	*ATG5* and *LC3*	+	[145]
E2F1	*ATG5*, *BNIP3*, *LC3* and *ULK1*	+	[151-153]
FOXO1	*ATG5*, *ATG12*, *ATG14*, *BECN1*, *BNIP3*, *LC3* and *PIK3C3*/*VPS34*	+	[115, 152, 154]
FOXO3	*ATG4*, *ATG12*, *BECN1*, *BNIP3*, *LC3*, *ULK1*, *ULK2* and *PIK3C3*/*VPS34*	+	[135, 155-158]
GATA1	*LC3*	+	[159]
JUN	*BECN1* and *LC3*	+	[160-162]
NFKB	*BCL2*, *BECN1* and *BNIP3*	+ or -	[152, 163, 164]
TP53	*ATG2*, *ATG4*, *ATG7*, *ATG10*, *BCL2* and *ULK1*	Cytosol-; nucleus +	[71, 165]
SOX2	*ATG10*	+	[166, 167]
SREBF2/SREBP2	*LC3* and *ATG4*	+	[168]
STAT1	*ATG12* and *BECN1*	-	[169]
STAT3	*ATG3*, *BCL2*, and *BNIP3*	-	[170, 171]
TFEB	*ATG4*, *ATG9*, *BCL2*, *LC3* and *WIPI*	+	[172]
ZKSCAN3	*LC3*, *ULK1* and *WIPI*	-	[173]

Table 1.4 miRNAs involved in regulating the autophagy core machinery

miRNA	**Target**	
Mir20a, Mir106b	*Ulk1*	Autophagy induction
MIR885-3p	*ULK2*	
MIR10A	*RB1CC1*	
Mir195	*Atg14*	Phagophore nucleation
MIR30A, *MIR30D*, *MIR376B*, *MIR519A*	*BECN1*	
MIR101, *MIR376B*	*ATG4*	Phagophore elongation
MIR30A, *MIR30D*, *MIR181A*, *MIR374A*	*ATG5*	
MIR17, *MIR375*	*ATG7*	
MIR519A	*ATG10*	
MIR30D, *MIR630*	*ATG12*	
MIR519A, *MIR885-3p*	*ATG16L1*	
MIR204	*LC3*	
MIR30D, *MIR130A*	*ATG2*	Cycling system
MIR34A	*ATG9A*	

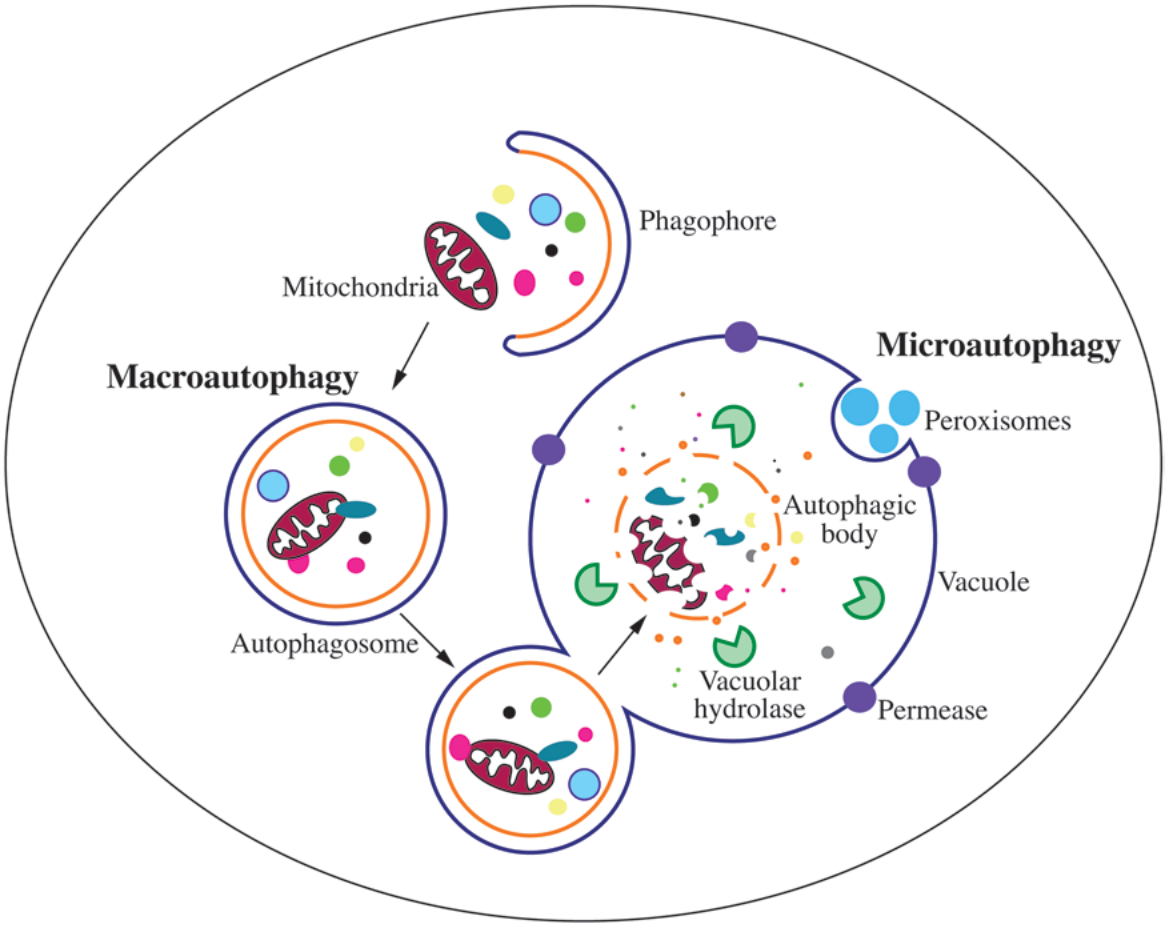

Figure 1.1 Schematic depiction of the two main types of yeast autophagy.
In macroautophagy, random cytoplasm and dysfunctional organelles are sequestered by the expanding phagophore, leading to the formation of the autophagosome. The autophagosome subsequently fuses with the vacuole membrane, releasing the autophagic body into the vacuole lumen. Eventually, the sequestered cargos are degraded or processed by vacuolar hydrolases. In microautophagy, cargos are directly taken up by the invagination of the vacuole membrane, followed by scission, and subsequent lysis, exposing the cargo to vacuolar hydrolases for degradation.

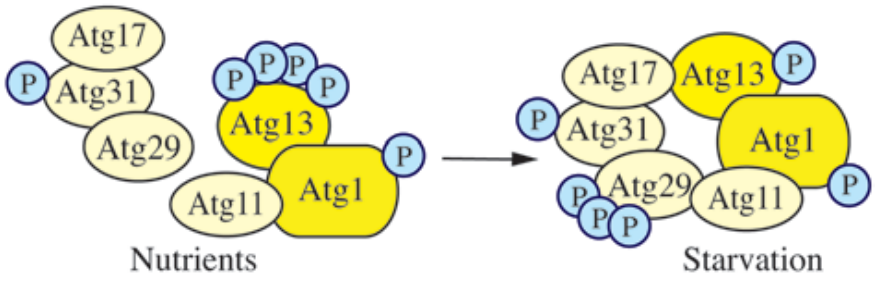

Figure 1.2 Yeast Atg1 kinase complex.
The yeast Atg1 kinase complex includes Atg1, a Ser/Thr protein kinase, Atg13, a regulatory subunit required for Atg1 kinase activity, and the Atg17- Atg31-Atg29 complex, which mayfunction in part as a scaffold. Atg31 bridges Atg17 and Atg29, Atg17 binds Atg13, and Atg29 binds Atg11.

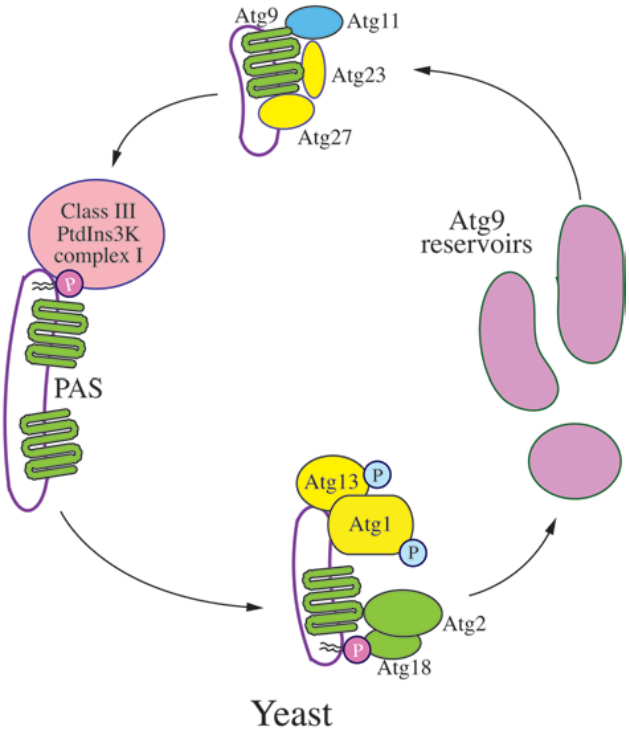

Figure 1.3 Trafficking of yeast Atg9.
In yeast cells, Atg9 is a transmembrane protein that transits between the PAS and peripheral sites (Atg9 reservoirs). Atg9 localization to the PAS from the peripheral sites depends on Atg11, Atg23 and Atg27. Return to the peripheral sites requires Atg1-Atg13, Atg2 and Atg18; PAS recruitment of the latter involves binding to PtdIns3P, the product of the class III PtdIns3K complex.

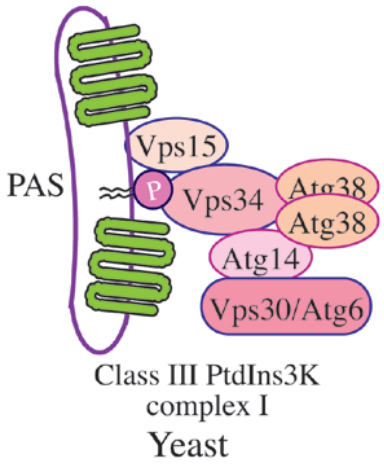

Figure 1.4 Yeast PtdIns3K complex I.
In yeast, Vps15 (a putative regulatory protein kinase that is required for Vps34 membrane association), Vps30/Atg6, Vps34 (the PtdIns3K), Atg14 and Atg38 form the autophagy-specific class III PtdIns3K complex, which localizes at the PAS. Vps15, Vps34 and Vps30 are present in the second class III PtdIns3K complex that includes Vps38 instead of Atg14.

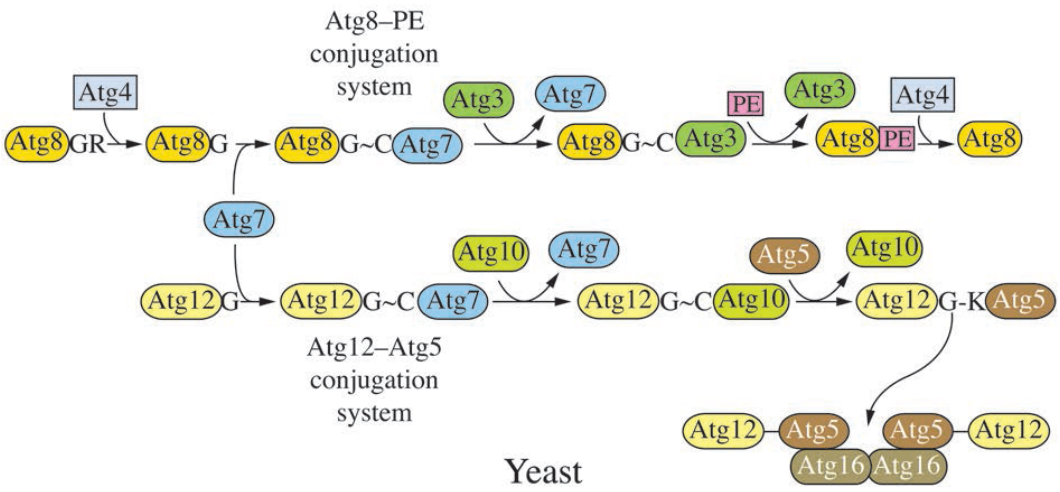

Figure 1.5 Yeast Ubl conjugation systems.
There are two Ubl protein conjugations systems, involving Atg8 and Atg12, whichare used to generate the conjugation products Atg8–PE and Atg12–Atg5, respectively. Atg8 is initially processed by Atg4, a cysteine protease, and during autophagy, Atg8 is released from Atg8–PE by a second Atg4-dependent cleavage. The Atg12–Atg5 conjugate, along with Atg16, facilitates the conjugation of Atg8 to PE. Both of the Ubl protein conjugation systems share a single activating enzyme, Atg7. The conjugating enzymes are Atg3 for Atg8, and Atg10 for Atg12.

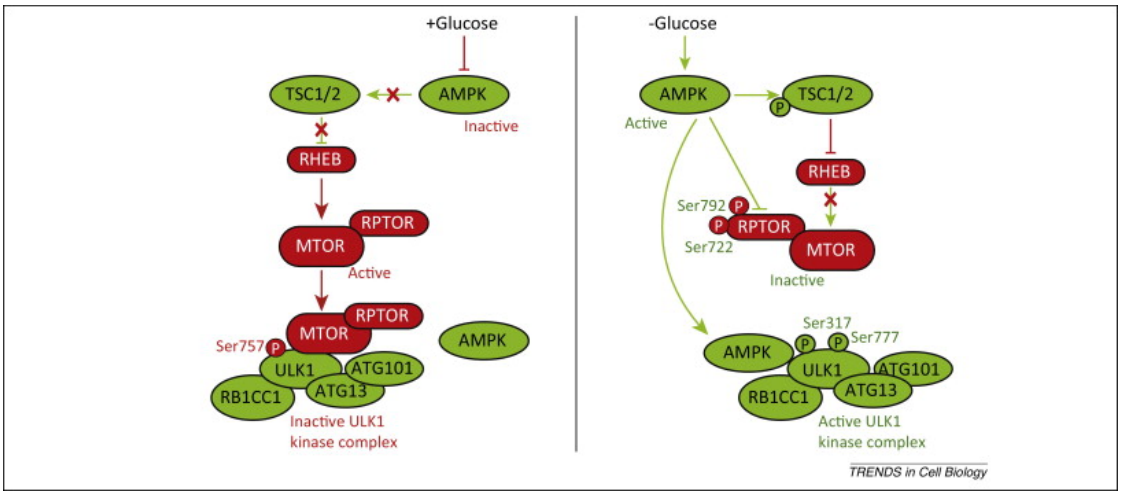

Figure 1.6 Coordinated regulation of ULK1
(unc-51 like autophagy activating kinase 1) by AMPK (AMP-activated protein kinase) and MTOR (mechanistic target of rapamycin). Phosphorylation-dependent regulation of ULK1 by AMPK and MTOR plays crucial roles in modulating autophagy activity. Arrows and bars indicate stimulation and inhibition, respectively. Green or red arrows and bars (or proteins) indicate events (or components) that promote or inhibit autophagy, respective.

Chapter 2 Phosphorylation of Atg9 Regulates Movement to the Phagophore Assembly Site and the Rate of Autophagosome Formation[2]

2.1 Abstract

Macroautophagy is primarily a degradative process that cells use to break down their own components to recycle macromolecules and provide energy under stress conditions, and defects in macroautophagy lead to a wide range of diseases. Atg9, conserved from yeast to mammals, is the only identified transmembrane protein in the yeast core macroautophagy machinery that is required for formation of the sequestering compartment termed the autophagosome. This protein undergoes dynamic movement between the phagophore assembly site (PAS), where the autophagosome precursor is nucleated, and peripheral sites that may provide donor membrane for expansion of the phagophore. Atg9 is a phosphoprotein that is regulated by the Atg1 kinase. We used stable isotope labeling by amino acids in cell culture (SILAC) to identify phosphorylation sites on this protein and identified an Atg1-independent phosphorylation site at serine 122. A non-phosphorylatable Atg9 mutant showed decreased autophagy activity, whereas the phosphomimetic mutant enhanced activity. Electron microscopy analysis suggests that the different levels of autophagy activity reflect differences in autophagosome formation, correlating with the delivery of Atg9 to the PAS. Finally, this phosphorylation regulates Atg9 interaction with Atg23 and Atg27.

[2] This chapter is reprinted from Feng Y, Backues SK, Baba M, Heo JM, Harper JW, Klionsky DJ (2016) Phosphorylation of Atg9 regulates movement to the phagophore assembly site and the rate of autophagosome formation. *Autophagy*;12(4):648-58. doi: 10.1080/15548627.2016.1157237.

2.2 Introduction

Autophagy refers to a group of highly conserved cellular processes in which cytoplasmic components are degraded within the lysosome in most of the higher eukaryotes or the vacuole in yeast and plants. The resulting macromolecular constituents are recycled and used as building blocks for anabolic pathways or to generate energy through catabolism.[1] Autophagy in yeast can be divided into 2 main types, macroautophagy and microautophagy. Macroautophagy (hereafter called autophagy) is the major process in which random cytoplasm is sequestered within a double-membrane structure, the phagophore, which eventually matures into a vesicle termed the autophagosome; generation of the autophagosome is a distinguishing feature between macroautophagy and microautophagy because the latter process involves direct uptake at the vacuole limiting membrane without the use of a phagophore or autophagosome. After fusion of the autophagosome with the vacuole, and degradation in the vacuole lumen, the breakdown products are released back into the cytosol.[113] Autophagy can be selective or nonselective. Nonselective autophagy is used for the turnover of bulk cytoplasm, whereas selective autophagy specifically targets damaged or superfluous organelles, including mitochondria and peroxisomes.[30, 31]

Over the past 2 decades, 41 AuTophaGy-related (*ATG*) genes have been identified in fungi.[34] Among them, one subset including 18 genes is shared by both nonselective and selective autophagy and is required for autophagosome formation, and thus the corresponding gene products are termed the core machinery of autophagosome formation; these proteins can be divided into different functional groups.[113, 174] Although our understanding of the molecular mechanism of autophagy has increased tremendously since the discovery and initial characterization of the Atg proteins, the complex mechanisms involved in the regulation of autophagy are still unclear.

Transcriptional, post-transcriptional and post-translational regulation are all used to modulate autophagy in order to adapt to different types of environmental stress,[107, 175, 176] and several Atg proteins are phosphorylated.[15, 48, 51, 120, 177]

Atg9, conserved from yeast to mammals, is the only transmembrane protein identified in the yeast autophagy core machinery.[178] One of the unique features of Atg9 concerns its subcellular distribution. Whereas most Atg proteins are localized to the PAS, in addition to a cytosolic pool, Atg9 has multiple punctate populations in a yeast cell. Atg9 is detected at the PAS along with most of the other Atg proteins; however, Atg9 is additionally present at peripheral sites, also termed Atg9 reservoirs and tubulovesicular clusters.[44] The Atg9 peripheral sites are found adjacent to mitochondria, but are not directly associated with this organelle, and newly synthesized Atg9 is delivered to these sites through part of the secretory pathway.[23] Studies using high-sensitivity microscopy have shown that most of the punctate Atg9 structures are highly mobile in the cytoplasm.[103] Thus, Atg9 may move between these peripheral sites and the PAS, and earlier studies have suggested that this cycling of Atg9 is required for autophagosome formation, functioning in some manner to direct membrane to the expanding phagophore.[44, 58, 62, 179] In mammalian cells, ATG9 also displays dynamic cycling, moving between the *trans*-Golgi network and endosomes in response to nutritional changes. A subpopulation of ATG9 colocalizes with both LC3, a mammalian homolog of Atg8, and RAB7, a late endosomal protein.[18]

Several Atg proteins have important roles in regulating Atg9 cycling. The anterograde movement of Atg9 from peripheral sites to the PAS requires Atg23, Atg27 and Atg11 (the latter is required primarily in selective types of autophagy).[62] The retrograde trafficking of Atg9 from the PAS depends on the Atg1-Atg13 complex, the Atg2-Atg18 complex and the phosphatidylinositol 3-kinase complex.[44, 58] Self-interaction of Atg9 is also important for its

PAS localization.[59]

Recent studies have shown that the Atg1 kinase directly phosphorylates Atg9 in an early step of regulation.[120] In this study, we identified Atg9 serine 122 (S122), a site that is not a direct target of Atg1, as being important for Atg9 function in autophagy activity. Phosphorylation of S122 regulates Atg9 anterograde trafficking by mediating its interaction with Atg23 and Atg27. These findings provide new evidence of the importance of post-translational modification of Atg9 and regulation of autophagy activity.

2.3 Results

2.3.1 Determination of Atg9 phosphorylation sites

Atg1 is the only protein kinase of the core autophagy machinery,[42] and as such it has received considerable attention. Several of the Atg proteins are phosphorylated, but until recently it was not known if any of these proteins were Atg1 substrates. Many other protein kinases (i.e., proteins that are not part of the autophagy core machinery) also modulate autophagy activity,[180-183] but in most cases the relevant targets have not been identified. Atg9 plays a key role in autophagy, and we recently demonstrated that the amount of the Atg9 protein correlates with the rate of autophagosome formation.[184] The functional pool of Atg9—the part of the population actively engaged in phagophore expansion—is presumed to be that at the PAS. We carried out a SILAC analysis to identify phosphorylation sites on Atg9 that might affect its movement to the PAS, and decided to focus on modifications that were independent of direct Atg1 kinase function, because recent studies have already identified Atg1-dependent sites in this protein.[120]

To identify Atg1-independent phosphorylation sites we performed the SILAC analysis comparing wild-type and *atg1*Δ strains. Phosphorylation scores were defined as mean log2 (*atg1*Δ/wild type [WT]); potential Atg1 targets should have a score <-1, reflecting a decrease in

phosphorylation, whereas changes in phosphorylation that were not directly dependent on Atg1 would have positive scores. From this analysis we identified 4 putative sites in Atg9 that demonstrated alterations in phosphorylation under conditions of nitrogen starvation: S864, T794, S792 and S122 (Fig. 2.1A). Among these sites, only S864 showed a negative enrichment score suggesting it was a direct substrate of Atg1. This site was identified in the study by Papinski et al.,[120] but was relatively unaffected by Atg1 kinase activity. This previous analysis also identified S792 and S122 as being phosphorylated independent of Atg1.

2.3.2 Phosphorylation of Atg9 S122 is important for nonselective autophagy

To determine if any of these phosphorylation sites plays a role in autophagy we generated 3 nonphosphorylatable Atg9 mutants, S122A, S792A/T794A, and S864A, and 3 phosphomimetic mutants, S122D, S792D/T794D and S864D, through site-directed mutagenesis.[185] We then transformed an *atg9*Δ strain with a plasmid encoding either WT Atg9 fused to the green fluorescent protein (Atg9-GFP), the Atg9 mutants or an empty vector, and monitored autophagy activity using the Pho8Δ60 assay.[186] Pho8 is a cytosolic derivative of a vacuolar phosphatase. The truncated version, Pho8Δ60, lacking its N-terminal transmembrane domain, resides in the cytosol and can only be delivered to the vacuole through autophagy, where a propeptide is removed to generate the active enzyme. The *atg9*Δ strain with an empty vector displayed a significant block in autophagy in nitrogen starvation conditions (Fig. 2.1B and 2.6C). In contrast, the strain expressing Atg9-GFP restored the autophagy activity to ~60% of the wild-type strain (Fig. 2.6A and 2.6E); the activity of this strain was set to 100% and used for normalization (Fig. 1B and S1C). Out of the 6 mutants tested, changes at S792, T794 and S864 did not result in significant differences relative to the WT. In contrast, S122A displayed an ~20% decrease, and S122D an ~30% increase, of Pho8Δ60 activity, suggesting that the phosphorylation of Atg9 S122 is important for autophagy.

Atg9 T119 was not identified as a phosphosite in the previous SILAC analysis [120] or in our present study. We decided to mutate this site due to its proximity to S122, in particular to determine whether the addition of a negative charge in this part of the protein would result in a phenotype similar to that seen with the S122D mutation. In contrast to the latter, the T119D mutant did not display an increase in activity, but instead resulted in a slight decrease in Pho8Δ60 activity, suggesting the specificity of the S122D phenotype (Fig. 2.1C and 2.6D). Atg9 homologs have been previously identified in other organisms including plants and humans, [17, 187] and the serine at position 122 is highly conserved among fungi (Fig. 2.6B); similarly, human ATG9A has a serine at position 123. Thus, regulation of Atg9 through post-translational modification at this site might correspond to a conserved mechanism.

2.3.3 Phosphorylation of Atg9 S122 is important for selective autophagy

Atg9 is one of the key proteins in the core machinery that is shared between nonselective and selective autophagy.[83] Accordingly, we next decided to examine the requirement for phosphorylation at S122 in selective types of autophagy. Aminopeptidase I (Ape1), a vacuole resident hydrolase, is initially synthesized as a cytosolic precursor (prApe1), and is delivered to the vacuole through either nonselective autophagy or the cytoplasm-to-vacuole targeting (Cvt) pathway, depending on nutrient conditions;[81, 188-190] in either case delivery is a selective process depending on a receptor protein, Atg19.[34, 86, 191] Upon delivery to the vacuole, the propeptide of prApe1 is enzymatically removed generating the mature hydrolase. This processing event is easily detected as a change in molecular mass following SDS-PAGE. To simplify our analysis, we took advantage of the Cvt pathway phenotype of the *vac8*Δ background to monitor selective autophagy; in the *vac8*Δ strain only prApe1 accumulates in rich conditions, but there is rapid vacuolar delivery following the induction of autophagy.[53] Thus, a shift from rich to

starvation conditions essentially corresponds to a pulse-chase analysis, and prevents the complicating accumulation of mature Ape1 that would otherwise be present. In the *atg9*Δ *vac8*Δ strain only prApe1 could be detected even after the induction of autophagy (Fig. 2.2A). The block of prApe1 maturation during starvation was rescued by integration of WT *ATG9* back into the chromosome. This maturation was partially blocked in cells expressing Atg9^{S122A} after 2 h starvation. At this same time point we could not detect a difference between the strain expressing WT Atg9 and Atg9^{S122D}, because essentially all of the protein was in the mature form. Therefore, we examined earlier time points and found accelerated maturation in the Atg9^{S122D} cells relative to the WT (Fig. 2.2B).

2.3.4 Phosphorylation of Atg9 S122 regulates autophagy by mediating autophagosome formation

At a mechanistic level there are 2 fundamental ways to modulate the magnitude of autophagy: changing the number or the size of autophagosomes. In yeast, the large size of the vacuole makes it possible to accumulate autophagic bodies, which correspond to the single-membrane compartments that result from the fusion of an autophagosome with a vacuole, when their degradation is blocked. The size and number of the accumulated autophagic bodies can then be determined through morphometric analysis by transmission electron microscopy (EM). To carry out this analysis we utilized strains harboring deletions in the *PEP4* gene to prevent autophagic body breakdown. The WT (*pep4*Δ Atg9) and mutant S122A (*pep4*Δ Atg9^{S122A}) and S122D (*pep4*Δ Atg9^{S122D}) strains were grown to mid-log phase and then shifted to nitrogen starvation conditions for 4 h, before being processed for imaging by EM (Fig. 2.3A); the size and number of autophagic bodies were quantified and estimated as described previously.[179]

The average size of the autophagic bodies in both mutants was not significantly different compared to the WT (Fig. 2.7). However, the Atg9^{S122A} strain had fewer autophagic bodies per cell, whereas Atg9^{S122D} displayed an increase (Fig. 2.3B). This result suggests that autophagosome formation was partially impaired in the strain expressing the S122A mutant; there were fewer autophagosomes formed, which corresponds to the lower Pho8Δ60 activity (Fig. 2.1C and 2.6D). In contrast, the higher Pho8Δ60 activity of the S122D mutant (Fig. 2.1C and 2.6D) may be explained by the observation that more autophagosomes were formed. The EM analysis thus suggests that the phosphorylation of Atg9 at S122 is important to maintain an appropriate rate of autophagosome formation, and hence overall level of autophagy.

2.3.5 Phosphorylation of S122 affects autophagy through regulating Atg9 anterograde trafficking

Atg9 cycles between the PAS and other cytosolic punctate structures (the peripheral sites), and has been proposed to be involved in membrane delivery to the PAS for autophagosome formation.[61, 178] To monitor the trafficking of Atg9, we examined cells expressing Atg9 WT, S122A or S122D under the control of the native *ATG9* promoter, and tagged with GFP. We quantified the colocalization of the Atg9 chimeras with red fluorescent protein (RFP)-tagged prApe1 (RFP-Ape1), which serves as a marker for the PAS. In rich conditions (+N) Atg9 localized to multiple puncta, and the abundance of these puncta was increased after cells were shifted to starvation (-N) conditions for 30 min (Fig. 2.4A, B and 2.9A). In rich conditions, ~21% of the WT cells displayed Atg9-GFP colocalized with RFP-Ape1, which represents the distribution of Atg9 during basal autophagy. After starvation for 30 min to induce autophagy this colocalization doubled to ~47%. The colocalization in cells expressing Atg9^{S122A}-GFP was less than half that seen in the WT, and was not substantially elevated after starvation (Fig. 2.4A, B and 2.9A),

suggesting that the trafficking of Atg9^{S122A} was impaired. In contrast, cells expressing Atg9^{S122D} showed the opposite phenotype; these cells displayed ~42% colocalization of Atg9^{S122D}-GFP with RFP-Ape1 in rich conditions, and this increased to ~64% after starvation (Fig. 2.4A, B and 2.9A), suggesting that the constitutive phosphorylation of Atg9 as mimicked by the phosphomimetic mutation promotes the anterograde movement of Atg9 to the PAS during autophagy. These results further indicate that Atg9 S122 phosphorylation plays an important role in regulating autophagy activity by controlling Atg9 trafficking.

Atg9 cycling between peripheral sites and the PAS can be split into 2 steps, corresponding to anterograde and retrograde trafficking.[58] We wanted to determine whether phosphorylation of S122 specifically affects one of these steps. To address this point, we took advantage of a strain developed previously, the multiple-knockout (MKO) strain, which lacks 24 different *ATG* genes that are required for autophagosome formation.[55, 192] The re-addition to this strain of specific genes in various combinations allows the "in vivo reconstitution" of autophagy, and the definition of the minimal set of proteins necessary for a specific step of this process.[193] Recently we showed that the MKO strain expressing Atg9, Atg11, Atg23 and Atg27 was sufficient to promote the anterograde movement of Atg9.[193] We transformed this strain with the RFP-Ape1 plasmid and again examined colocalization. Similar results were observed with the MKO strain as seen as in the WT background; Atg9^{S122A} was partially defective in PAS localization, whereas Atg9^{S122D} had a higher percentage of localization at the PAS, in particular under nutrient-rich conditions (Fig. 2.4C, D and 2.9B). This consistent localization of Atg9 between the WT and MKO (Atg11-Atg19-Atg23-Atg27) strains, where the latter can only carry out anterograde movement, suggests that S122 phosphorylation affects Atg9 anterograde trafficking.

2.3.6 Phosphorylation of S122 regulates Atg9 through its interactions with Atg23 and Atg27

Having determined that S122 phosphorylation affects Atg9 anterograde trafficking, we next wanted to address the question of mechanism. Because of the known role of Atg11, Atg23 and Atg27 in regulating Atg9 movement,[62, 194] and based on our finding that the MKO strain expressing these proteins recapitulates the Atg9 localization phenotype seen with the mutant forms of Atg9, we hypothesized that the interaction of Atg9 with Atg23 and/or Atg27 might be affected in the Atg9 mutants (Atg11 is not essential for nonselective autophagy and the deletion of *ATG11* has little effect on Phho8Δ60 activity[87]). To test this hypothesis, we used the bimolecular fluorescence complementation (BiFC) assay. Briefly, in the BiFC assay, the Venus yellow fluorescent protein (vYFP) is split into 2 fragments, VN (corresponding to the N terminus of vYFP) and VC (the C terminus of vYFP).[195, 196] We fused VN to Atg9 and VC to either Atg23 or Atg27 on the genome. Fluorescence from these 2 chimeras can only be detected when the 2 proteins interact and bring the 2 fragments of vYFP proximal to each other. A plasmid of RFP-Ape1 was transformed into these strains to mark the PAS.

A vYFP signal was observed both before and after N starvation (30 min), indicating that interactions between WT Atg9 and Atg23 or Atg27 exist during both basal and nonselective autophagy (Fig. 2.5). No vYFP fluorescence was detected in VN-Atg9, VC-Atg23 or VC-Atg27 alone (Fig. 2.8), which suggested that the vYFP puncta seen with combinations of these proteins (Fig. 2.5) represented an interaction between Atg9 and Atg23 or Atg27. vYFP signals were also observed in S122A and S122D, suggesting that these interactions were not abolished in either mutant; however, the mutants displayed different numbers of vYFP dots per cell (Fig. 2.5). Calculation of the number of puncta was performed automatically using CellProfiler. Upon nitrogen starvation, with Atg23, $Atg9^{S122A}$ cells had ~20% fewer vYFP dots than WT, whereas

Atg9^{S122D} cells contained almost 50% more puncta (Fig. 2.5B and 2.10A). A similar, but more dramatic, trend was found with Atg27, where the Atg9^{S122D} cells displayed almost 3 times more puncta per cell than WT upon starvation (Fig. 2.5D and 2.10B). These results suggest that phosphorylation of S122 is important for the interaction of Atg9 with Atg23 and Atg27; in particular, this interaction was partially reduced with the S122A mutant and was substantially enhanced with S122D.

We could barely detect the interaction of Atg9 with either Atg23 or Atg27 by co-immunoprecipitation, even with the wild-type proteins, suggesting that the binding may be weak, transient or unstable during the immunoprecipitation procedure.

2.4 Discussion

In this study, Atg9 S122 was identified through a SILAC assay as showing altered phosphorylation during autophagy induction. Among several sites of Atg9 that showed a change of phosphorylation level, S122 was the only one that showed a defect in autophagy activity when altered to a non-phosphorylatable mutant, S122A, and enhanced autophagy activity when constitutive phosphorylation was mimicked with S122D. In addition to nonselective autophagy, our data also showed that the phosphorylation of S122 is important for selective autophagy. However, based on the SILAC results, S122 displayed a 1.45-fold increase of phosphorylation level in the *atg1*Δ strain compared to the WT, which means that it is not a direct target of Atg1 kinase, which was previously shown to phosphorylate Atg9.[120]

We attempted to determine the effect of altering phosphorylation at S122, and the mechanism behind any such effect. We found that the S122A and S122D mutations had opposing effects on autophagy activity, which may be explained by changes in autophagic body (and hence autophagosome) number. That is, more Atg9 at the PAS, as seen with Atg9^{S122D}, correlated with

an increased rate of autophagosome formation. This result agrees with findings from a recent study where the absolute Atg9 levels correspond to the number, but not the size, of autophagosomes generated during autophagy.[184] With the Atg9^{S122D} mutant we altered the amount of Atg9 at the PAS, rather than the total amount of the Atg9 protein. Thus, the present results suggest that it is this pool of Atg9 in particular that accounts for autophagosome formation.

Considering that the PAS-localized pool of Atg9 is the critical one with regard to autophagy activity, how does phosphorylation affect the localization of Atg9? Using fluorescence microscopy, we found that Atg9^{S122A} was defective in PAS localization, whereas Atg9^{S122D} displayed a higher level of localization. Furthermore, using the MKO strain, we determined that anterograde movement was altered with the mutant version of Atg9. Finally, our data suggest that the S122D mutation results in an enhanced interaction between Atg9 and Atg27, one of the components required for efficient anterograde trafficking of Atg9.[179, 193] We note, however, that Atg23 and Atg27 do not appear to be conserved in higher eukaryotes, so different components my take the place of these proteins if this regulatory aspect of Atg9 trafficking is conserved beyond fungi.

In summary, the phosphorylation-dependent regulation of Atg9 anterograde trafficking reveals another mechanism through which autophagy activity can be regulated. At present, the kinase or phosphatase that directly modifies Atg9 S122 remains to be identified, but these studies are currently underway.

2.5 Materials and Methods

2.5.1 Strains, media, and growth conditions

Yeast strains used in this paper are listed in Table 1. Gene deletions or integrations were performed using a standard method.[53] Cells were cultured in rich medium (YPD; 1% [w/v] yeast

extract [ForMedium, YEM04], 2% [w/v] peptone [ForMedium, PEP04], and 2% [w/v] glucose) or synthetic minimal medium (SMD; 0.67% yeast nitrogen base [ForMedium, CYN0410], 2% glucose, and auxotrophic amino acids and vitamins as needed) as indicated. Autophagy was induced through nitrogen starvation by shifting cells in mid-log phase from YPD (or SMD) to SD-N (0.17% yeast nitrogen base without ammonium sulfate or amino acids [ForMedium, CYN0501], and 2% [w/v] glucose) for the indicated times.

2.5.2 Plasmids

Integrating plasmids encoding Atg9-GFP[184] and a centromeric plasmid encoding RFP-Ape1 have been published previously.[197] Plasmids encoding Atg9-GFP with mutations S122A, S122D, T119D were generated by site-directed mutagenesis[198] from Atg9-GFP.

2.5.3 Fluorescence microscopy

For fluorescence microscopy, yeast cells were grown to OD_{600} ~0.5 in SMD and shifted to SD-N for autophagy induction. Images were collected on a Deltavision Elite deconvolution microscope (GEHealthcare/Applied Precision) with a 100× objective and a CCD camera (CoolSnap HQ; Photometrics).

For quantification of Atg9-GFP colocalization with RFP-Ape1, stacks of 15 image planes were collected with a spacing of 0.2 μm to cover the entire yeast cell. Analysis was performed on an average projection of the imaging planes.

2.5.4 Mass spectrometry

WT and *atg1*Δ strains were grown in heavy and light lysine-supplemented SMD media, respectively. Upon reaching OD_{600} = 1.0, WT and *atg1*Δ cells were shifted to nitrogen starvation by culturing in SD-N media supplemented with light and heavy lysine, respectively, for 2 h. Cells

were then harvested and equal numbers of cells were mixed prior to protein extraction, trypsinization, enrichment of phosphopeptides by strong cation exchange chromatography, and purification of phosphopeptides using IMAC columns.[199] Desalted peptides were dissolved in 5% formic acid and analyzed on an LTQ Orbitrap Velos mass spectrometer as described previously.[199] The following instrument parameters were employed: fully tryptic or LysC digestion, up to 2 missed cleavages, precursor mass tolerance of ±25 ppm, 1.0 Da product ion mass tolerance, a static modification of carbamidomethylation on cysteine (+57.0214); and dynamic modifications for phosphorylation on serine, threonine, and tyrosine (+79.9663), methionine oxidation (+15.9949), and 13C6 15N2-lysine (+8.0142). Spectra were searches using SEQUEST and matched to peptides with a 1% FDR using the target decoy approach[200] and subsequently analyzed using linear discriminant analysis to derive Xcorr, ΔCn', precursor mass error, and charge state. The Ascore method[201, 202] was used to assign phosphorylation sites and peptides quantified as described previously.[199]

2.5.5 Transmission electron microscopy

Two separate EM preparations were performed in 2 different labs. The first set of samples was prepared by Dr. M. Baba as described previously[203] with slight modifications: In pre-fixation, the final fixative contained 0.1 M HEPES, pH 6.8, 0.1 M sorbitol, 1 mM $MgCl_2$, 2% glutaraldehyde and 0.5% formaldehyde. 2x fixative was added directly into the starvation medium, and incubated for 5 min at room temperature (RT). Cells were collected by centrifugation and 1x fixative was added, followed by incubation at 4°C for 2.5 h. In post-fixation, 2% $KMnO_4$ was added to the cells for 5 min at RT. Cells were collected by centrifugation and the fixative solution was removed. 2% $KMnO_4$ was added and incubated for approximately 1 h at RT. After washing the cells, 2% low melting agarose was added followed by mixing. Subsequent steps were

performed as described previously.[203] The second set of samples was prepared in our lab as described previously.[179]

2.5.6 Additional assays

Pho8Δ60 assays, western blot, prApe1 processing and EM were performed as described previously.[179, 196, 204, 205] Antibodies against Atg9, Ape1 and Pgk1 (a generous gift from Dr. Jeremy Thorner, University of California, Berkeley), and a commercial antibody that reacts with protein A (no longer available) were used as described previously.[81, 178] Anti-Dpm1 was from Molecular Probes/Invitrogen (A-6429).

2.5.7 Statistical analysis

Two-tailed Student's t test, two-tailed paired Student's t test and ANOVA F-test was used to determine statistical significance.

2.6 Acknowledgments

This work was supported by NIH grant GM053396 to D.J.K. and GM095567 to J.W.H.

Table 2.1 Yeast strains used in this study.

Name	Genotype	Reference
SEY6210	MATα *leu2-3,112 ura3-52 his3-Δ200 trp1-Δ901 suc2-Δ9 lys2-801 GAL*	[206]
SKB257	MKO *RFP-APE1 ATG9-GFP* pATG11-19-23-27	This study
SKB259	MKO *RFP-APE1 ATG9-GFP^{S122A}* pATG11-19-23-27	This study
SKB260	MKO *RFP-APE1 ATG9-GFP^{S122D}* pATG11-19-23-27	This study
WLY176	SEY6210 *pho13Δ pho8Δ60*	[207]
YKF001	WLY176 *atg9Δ::LEU2 ATG9-GFP::URA3*	This study
YKF002	WLY176 *atg9Δ::LEU2 ATG9-GFP^{S122A}::URA3*	This study
YKF003	WLY176 *atg9Δ::LEU2 ATG9-GFP^{S122D}::URA3*	This study
YKF004	WLY176 *atg9Δ::LEU2 ATG9-GFP^{T119D}::URA3*	This study
YKF008	SEY6210 *RFP-APE1::LEU2 atg9Δ::HIS3 ATG9-GFP::URA3*	This study
YKF009	SEY6210 *RFP-APE1::LEU2 atg9Δ::HIS3 ATG9-GFP^{S122A}::URA3*	This study
YKF010	SEY6210 *RFP-APE1::LEU2 atg9Δ::HIS3 ATG9-GFP^{S122D}::URA3*	This study
YKF080	SEY6210 *pep4Δ::LEU2 atg9Δ::HIS3 ATG9-GFP::URA3*	This study
YKF081	SEY6210 *pep4Δ::LEU2 atg9Δ::HI3S ATG9-GFP^{S122A}::URA3*	This study
YKF082	SEY6210 *pep4Δ::LEU2 atg9Δ::HIS3 ATG9-GFP^{S122D}::URA3*	This study
YKF109	BY4742 *RFP-APE1::LEU2 ATG9-GFP::URA3*	This study
YKF110	BY4742 *RFP-APE1::LEU2 ATG9-GFP^{S122A}::URA3*	This study

YKF111	BY4742 *RFP-APE1::LEU2 ATG9-GFP^{S122D}::URA3*	This study
YKF096	SEY6210 *vac8Δ::KAN atg9Δ::LEU2*	This study
YKF396	SEY6210 *vac8Δ::KAN atg9Δ::LEU2 ATG9-GFP::URA3*	This study
YKF397	SEY6210 *vac8Δ::KAN atg9Δ::LEU2 ATG9-GFP^{S122A}::URA3*	This study
YKF398	SEY6210 *vac8Δ::KAN atg9Δ::LEU2 ATG9-GFP^{S122D}::URA3*	This study
YKF417	SEY6210 *Atg9-VN^{WT}::TRP1 Atg23-VC::HIS3 RFP-APE1::LEU2*	This study
YKF413	SEY6210 *Atg9^{S122A}-VN::TRP1 Atg23-VC::HIS3 RFP-APE1::LEU2*	This study
YKF414	SEY6210 *Atg9^{S122D}-VN::TRP1 Atg23-VC::HIS3 RFP-APE1::LEU2*	This study
YKF415	SEY6210 *Atg9^{S122A}-VN::TRP1 Atg27-VC::HIS3 RFP-APE1::LEU2*	This study
YKF416	SEY6210 *Atg9^{S122D}-VN::TRP1 Atg27-VC::HIS3 RFP-APE1::LEU2*	This study
YKF418	SEY6210 *Atg9^{WT}-VN:TRP1 Atg27-VC::HIS3 RFP-APE1::LEU2*	This study

A

Protein	Site	Peptide	Phosphorylation enrichment score (mean log2 (*atg1Δ*/WT))
Atg9	864	PNNEGDSFLNNKY	-2.32
	794	MDEDSLTKKIAVN	3.13
	792	HSMDEDSLTKKIA	3.13
	122	VLETEKSNLERLV	1.45

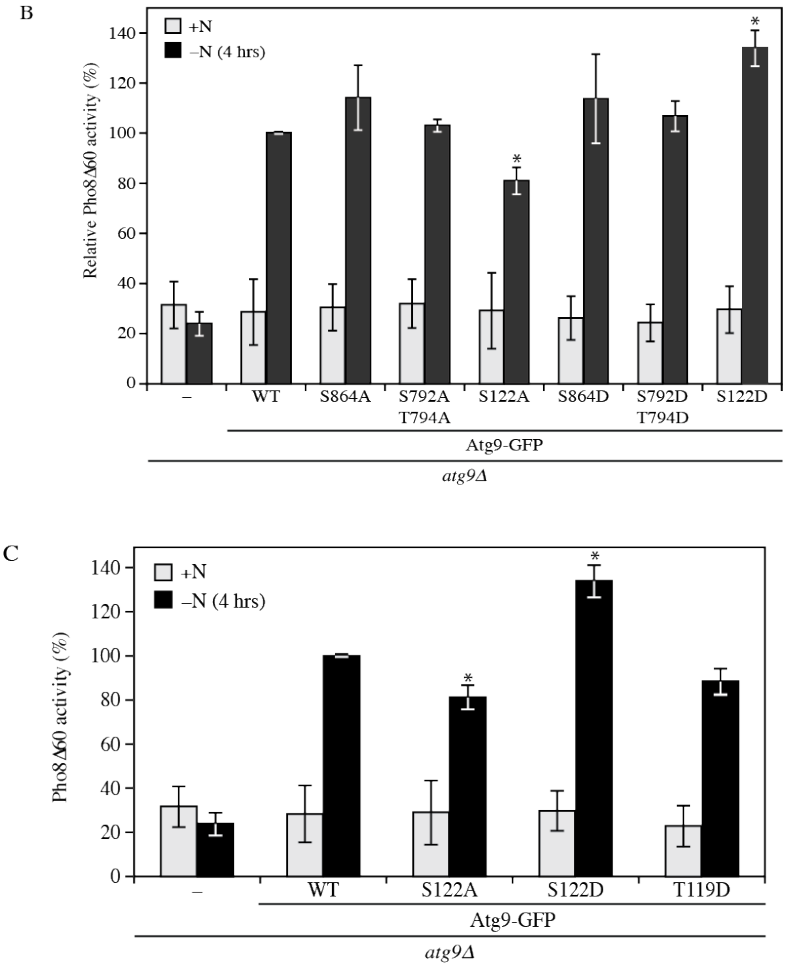

Figure 2.1 Phosphorylation of Atg9 S122 is important for nonselective autophagy. (**A**) Wild-type (WT; SEY6210) and *atg1*Δ cells were collected after 2 h nitrogen starvation and subjected to SILAC analysis. A phosphorylation enrichment score was identified for 4 sites of Atg9. (**B, C**) WLY176 cells were transformed with empty vector (pRS406) or a plasmid containing WT or different phosphorylation mutants of Atg9-GFP as indicated. Cells were cultured in YPD (+N) to midlog phase, and shifted to SD-N (-N) for 4 h. The Pho8Δ60 assay was performed as described in *Materials and Methods.* Error bars correspond to the standard deviation and were obtained from 3 independent repeats. Two-tailed t test was used for statistical significance; ∗p < 0.05.

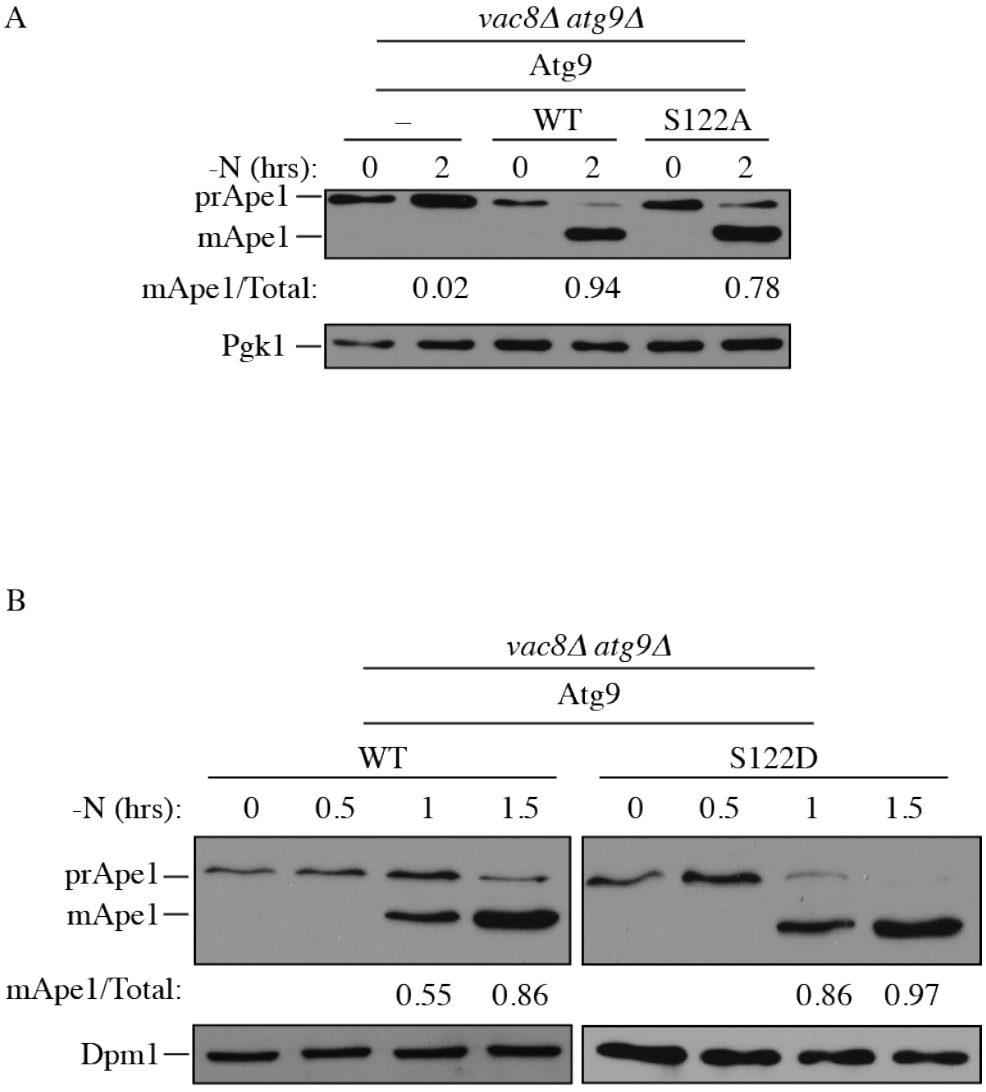

Figure 2.2 Phosphorylation of Atg9 S122 is important for selective autophagy. (**A, B**) Processing of prApe1 was monitored. *atg9*Δ *vac8*Δ cells, transformed with empty vector or a plasmid containing WT Atg9 and either (**A**) $Atg9^{S122A}$ or (**B**) $Atg9^{S122D}$, were cultured in YPD to early log phase ($0D_{600}$ = 0.5) and shifted to SD-N for 0-2 h as indicated. Cells were collected and protein extracts were analyzed by western blot with anti-Ape1 antibody and either anti-Pgk1 or anti-Dpm1 (loading control) antiserum or antibody. The ratio of Ape1: total Ape1 (preApe1 + Ape1) was measured and normalized to that of WT cells, which was set to 100%.

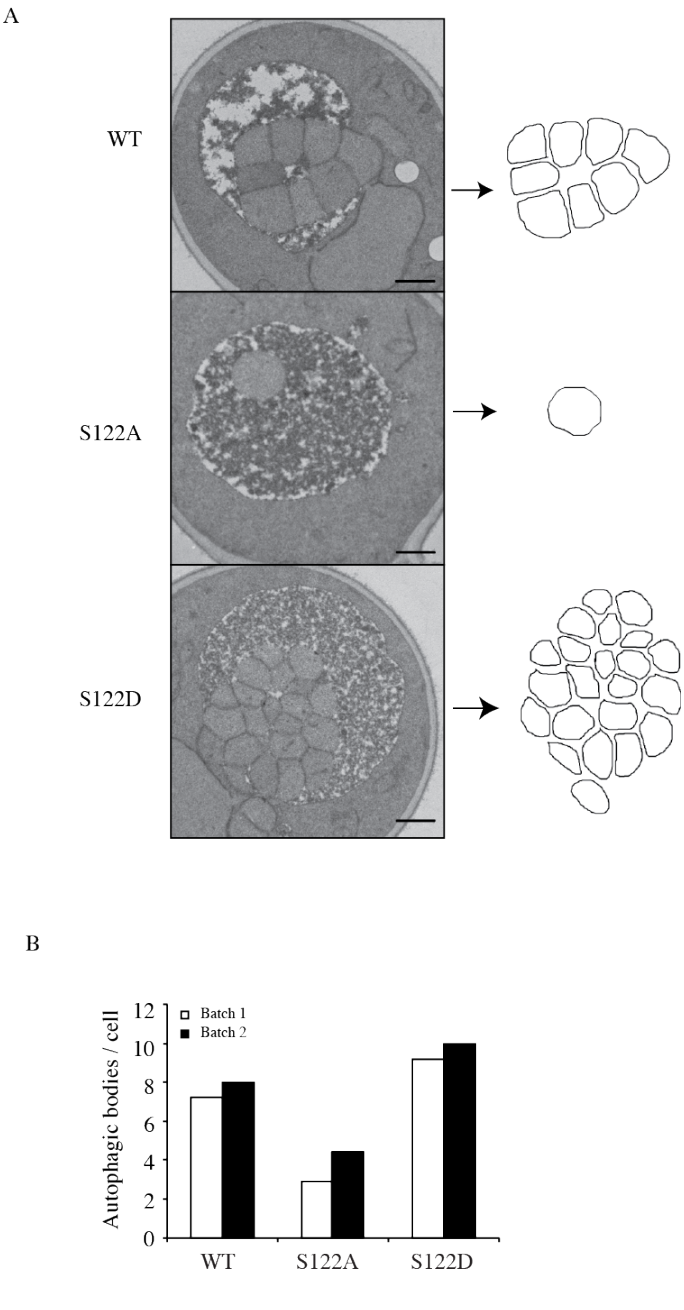

Figure 2.3 Phosphorylation of Atg9 S122 regulates the number of autophagosomes formed/formation rate.
(**A**) Representative TEM images of cells of WT and mutant Atg9 after 4 h of nitrogen starvation. Autophagic bodies are outlined on the right. Scale bar: 500 nm. (**B**) Estimated average number of autophagic body numbers per cell in WT and mutant Atg9 after 4 h of nitrogen starvation. Estimation was based on the number of autophagic body cross sections observed by TEM in 2 independent experiments done by 2 different labs of more than 100 cells each for each strain.

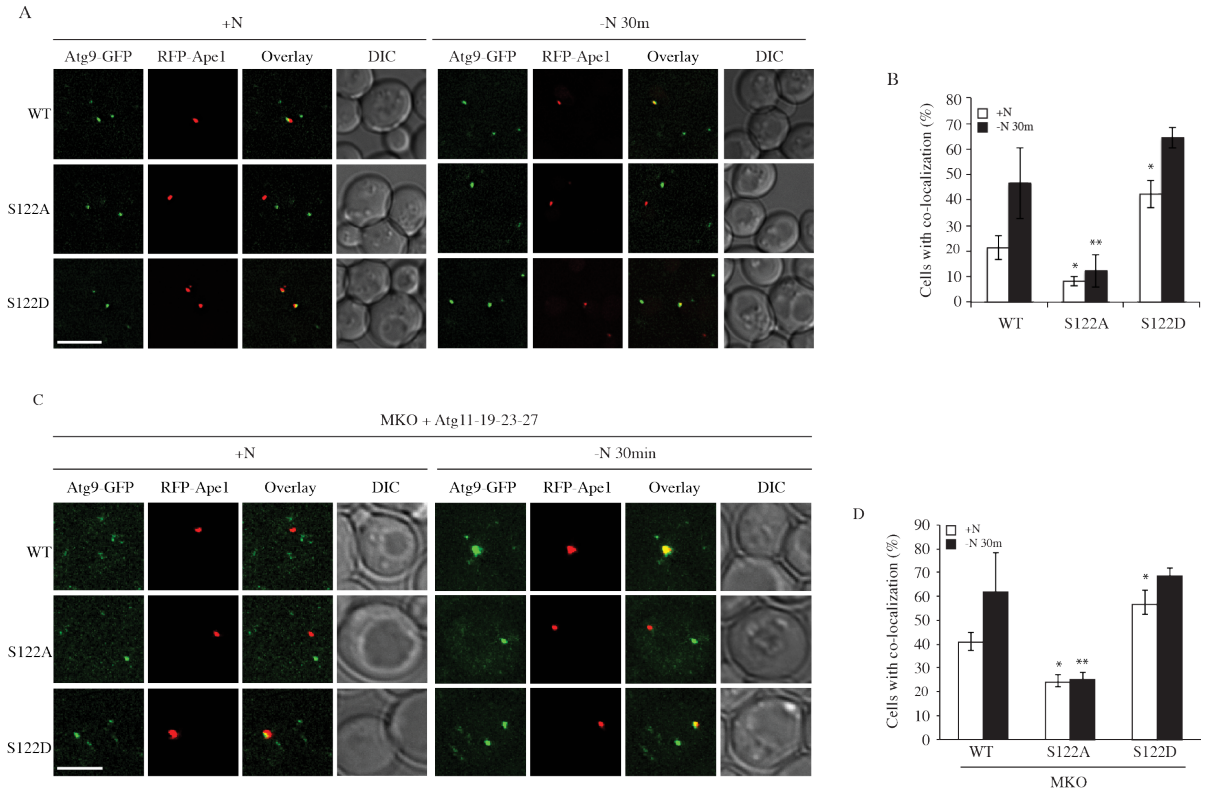

Figure 2.4 Phosphorylation of S122 is important for Atg9 anterograde trafficking. (**A**) Representative florescence microscopy images of *atg9*Δ cells transformed with a plasmid expressing WT or mutant Atg9-GFP. A plasmid expressing RFP-Ape1 was also used to provide a PAS marker. Cells were cultured in YPD, shifted to SD-N and collected at both 0 and 30 min nitrogen starvation. The single z-stack images are displayed at equal intensity for comparison. Scale bars: 5 µm. (**B**) Quantification of colocalization between Atg9-GFP and RFP-Ape1. Error bars correspond to the standard deviation and were obtained from 3 independent repeats. (C) Representative florescence microscopy images of the MKO strain expressing Atg11-Atg19-Atg23-Atg27 and RFP-Ape1, and transformed with a plasmid expressing WT or mutant Atg9-GFP. Cells were cultured, collected and imaged as in (**A**). (**D**) Quantification of colocalization between Atg9-GFP and RFP-Ape1 was performed as in (**B**). ANOVA F test was used for statistical significance. *, $p < 0.05$; **, $p < 0.01$

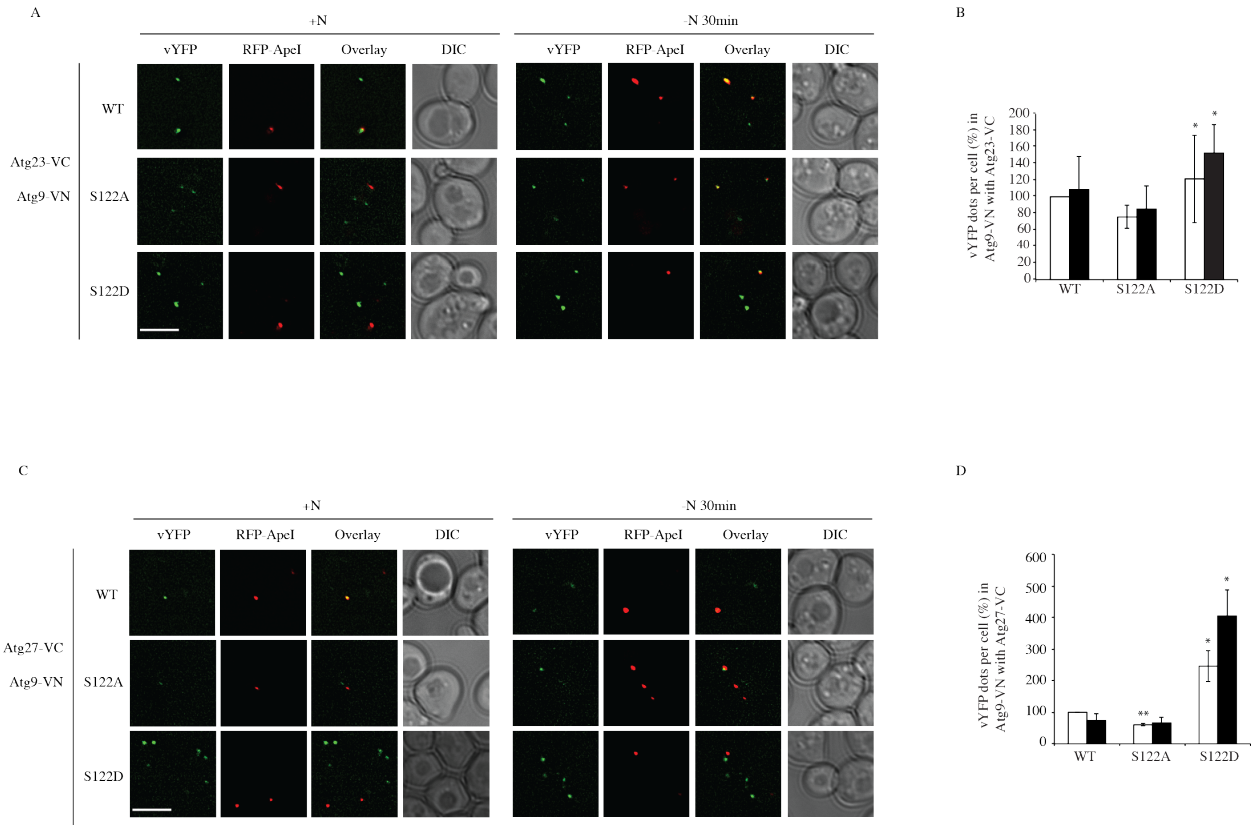

Figure 2.5 Phosphorylation of Atg9 S122 is important for the interaction of Atg9 with Atg23 and Atg27.

(**A, B**) Representative florescence microscopy images (**A**) of WT or mutant Atg9-VN expressed with Atg23-VC. RFP-Ape1 was used as a PAS marker. Cells were cultured and collected as in Figure 4. Scale bars: 5 μm. (**B**) Quantification of vYFP puncta/cell was performed using CellProfiler. (**C, D**) Representative florescence microscopy images (**C**) of WT or mutant Atg9-VN expressed with Atg27-VC. (**D**) Quantification of vYFP puncta/cell was performed using CellProfiler. ANOVA F test was used for statistical significance. *, $p < 0.05$; **, $p < 0.01$.

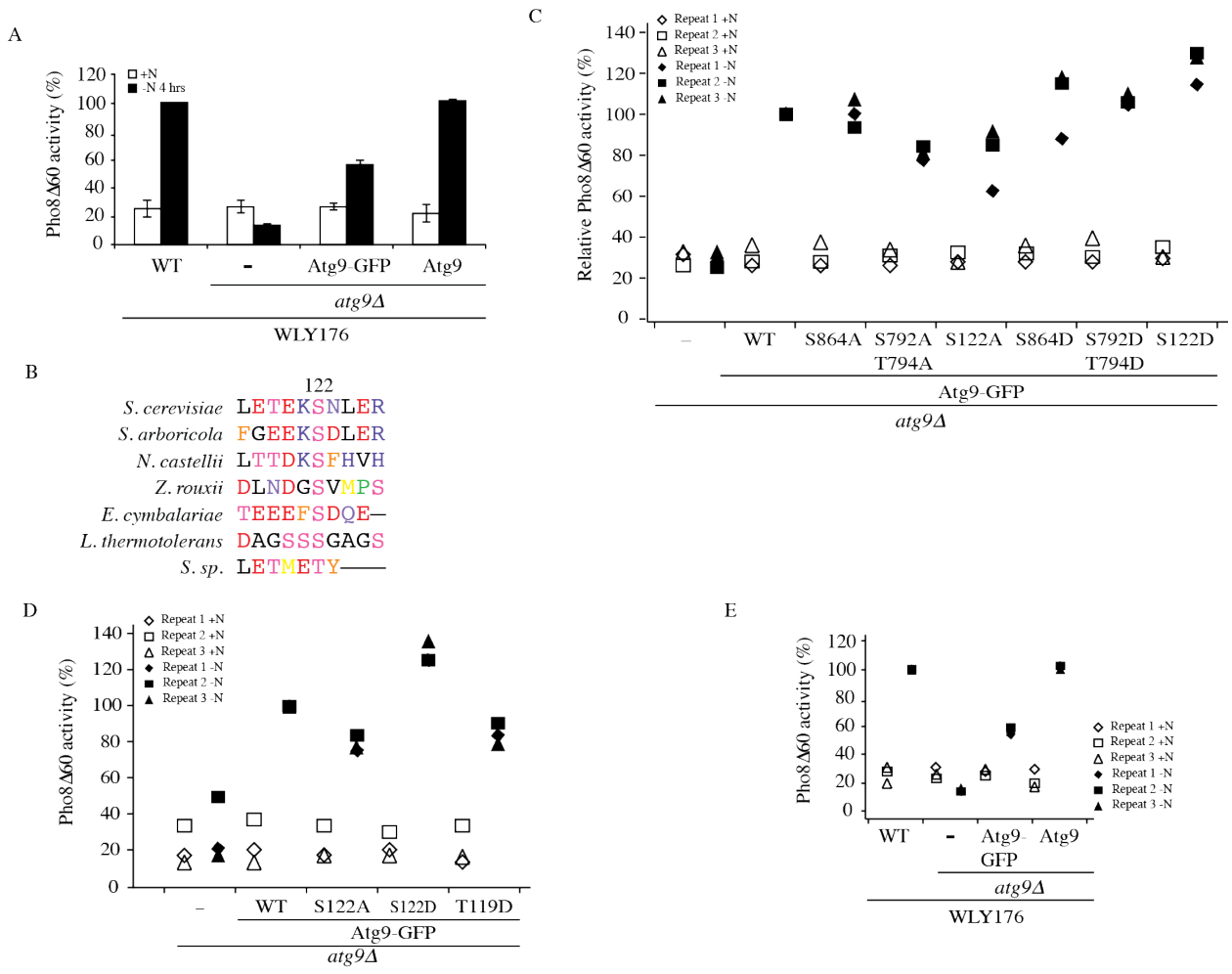

Figure 2.6 Phosphorylation of Atg9 S122 is important for nonselective autophagy. (**A**) Untransformed WLY176 (WT) or WLY176 *atg9*Δ cells transformed with an empty vector or a pRS406 plasmid expressing either untagged Atg9 or Atg9-GFP, and assayed for Pho8Δ60 activity after 4 h nitrogen starvation as described in *Materials and Methods*. Error bars correspond to the standard deviation and were obtained from 3 independent repeats. (**B**) Alignment of the N terminus of Atg9 throughout different species. (**C-E**) Results of (**C**) Figure 1B, (**D**) Figure 1C and (**E**) Figure S1 are displayed, showing 3 independent repeats as scatterplots.

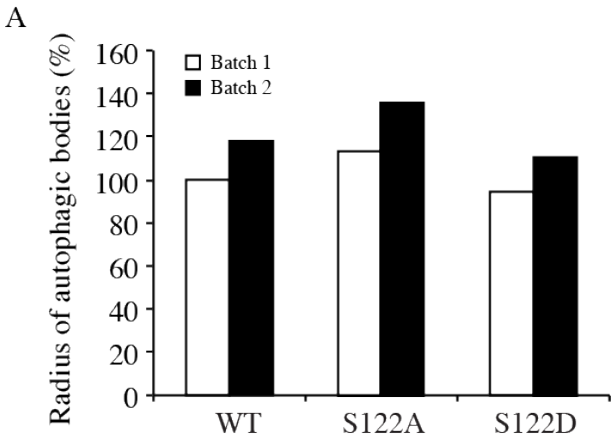

Figure 2.7 Phosphorylation of Atg9 S122 does not affect the size of autophagosomes. Estimated average radius of autophagic bodies in WT and mutant Atg9 after 4 h of nitrogen starvation. The estimation was based on the radius of autophagic body cross sections observed by TEM in 2 independent experiments done by 2 different labs of more than 100 cells each for each strain.

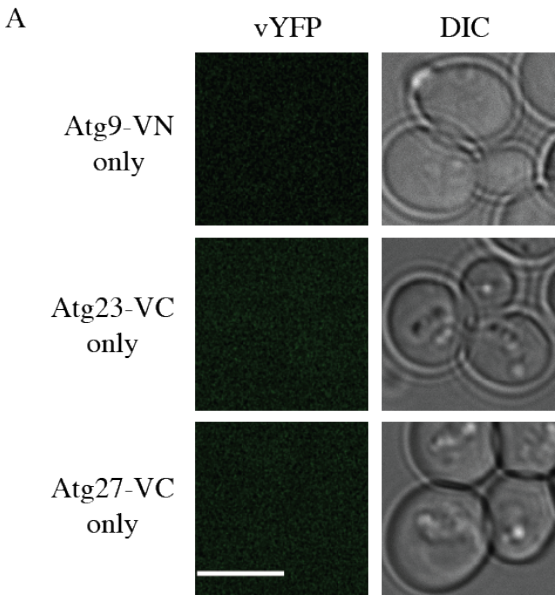

Figure 2.8 Phosphorylation of S122 is important for the interaction of Atg9 with Atg23 and Atg27.

Representative florescence microscopy images of cells expressing only WT Atg9-VN, Atg23-VC or Atg27-VC. Cells were cultured, collected and imaged as in Figure 5. Scale bars: 5 μm.

A

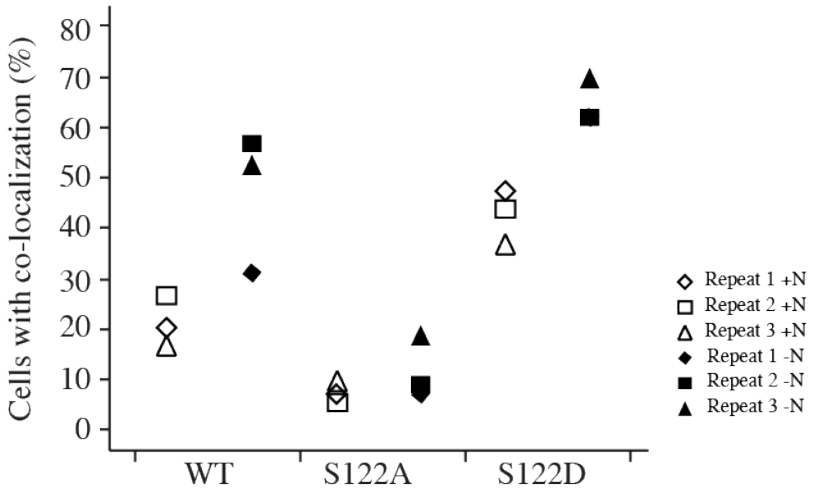

B

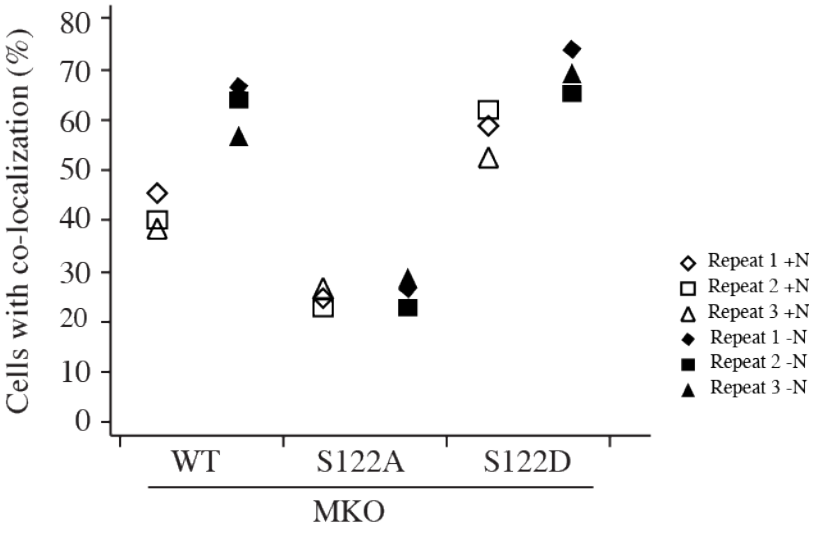

Figure 2.9 Phosphorylation of S122 is important for Atg9 anterograde trafficking. (**A-B**) Results of the quantification of colocalization between Atg9-GFP and RFP-Ape1 from (**A**) Figure 4B and (**B**) Figure 4D are displayed, showing 3 independent repeats as scatterplots.

A

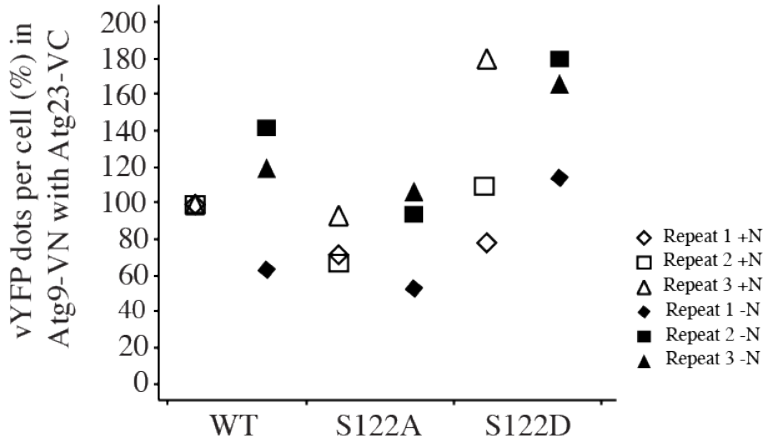

B

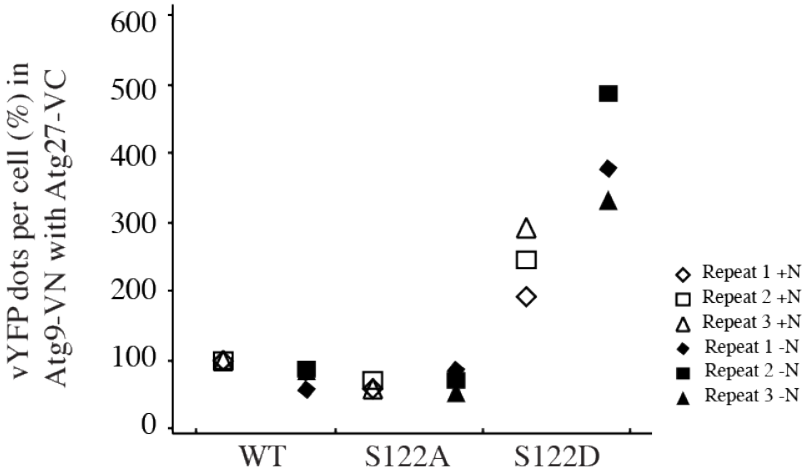

Figure 2.10 Phosphorylation of Atg9 S122 is important for the interaction of Atg9 with Atg23 and Atg27.
Results of the quantification of colocalization between Atg9-GFP and RFP-Ape1 in (**A**) Figure 5B and (**B**) Figure 5D are displayed, showing 3 independent repeats as scatter.

Chapter 3 Downregulation of Autophagy by Met30-Mediated Atg9 Turnover[3]

3.1 Abstract

Macroautophagy/autophagy is primarily a self-eating process that recycles cytosolic components such as misfolded or aggregated proteins and dysfunctional organelles for homeostasis, and for survival in unfavorable conditions. Autophagy is stringently regulated at different levels including transcriptionally, post-transcriptionally, translationally and post-translationally. A thorough understanding of the mechanisms involved is crucial to allow the manipulation of autophagy for the treatment of diseases. Post-translational modifications (PTMs) represent a subset of regulatory mechanisms that are critical for modulating autophagy in order to adapt to different types of environmental stress. In summary, we identified a novel mechanism of Atg9 regulation in autophagy through PTMs. In growing conditions, Atg9 is synthesized at a basl level and cells are primed for autophagy. We show that in this situation Atg9 is ubiquitinated and targeted for degradation in a proteasome-dependent manner, thereby limiting autophagy to a basal level. However, when cells are deprived of nutrients, autophagy is highly induced, necessitating an increase in the amount of Atg9; the proteasome-dependent reduction of Atg9 protein levels is subsequently reduced to facilitate the increase in autophagy. Thus, the post-translational ubiquitination of Atg9 provides an additional mechanism that allows cells to maintain appropriate levels of autophagy, and—by ending this modification—to rapidly respond and adapt to environmental stresses.

[3] A modified version of this chapter has been submitted for publication.

3.2 Introduction

Depending on the type of cargo that is sequestered, autophagy can be nonselective or selective; examples of the latter include the cytoplasm-to-vacuole targeting (Cvt) pathway, mitophagy, and pexophagy [113, 208]. One of the key features of autophagy is the generation of the phagophore, a dynamic and transient compartment that carries out the sequestration of cytoplasm; during maturation, the phagophore seals, becoming a double-membrane spherical structure referred to as an autophagosome. At present, in the complex network of autophagy-related (*ATG*) genes that are present in all eukaryotes, over 40 unique components have been identified that make up the autophagy machinery; the core components refer to those proteins that are critical for autophagosome formation [208]. However, many questions remain concerning the mechanism of autophagosome biogenesis, including the source of the membrane used for nucleation and expansion of the phagophore. Among the core machinery, AtgG9 is the only transmembrane protein (and one of only two Atg membrane proteins in fungi) [103]. Unlike most other Atg proteins that mainly localize as a diffuse population in the cytosol and as a discrete punctum that corresponds to the phagophore assembly site (PAS)—where the phagophore nucleates—Atg9 is found at multiple punctate structures in yeast cells in addition to the PAS. Various studies have indicated that Atg9 travels through and/or remains in proximity to the endoplasmic reticulum, the Golgi apparatus, endosomes, and mitochondria [58, 209, 210]. When autophagy is induced, the percent of the total Atg9 population that localizes at the PAS is significantly increased [211]. This observation suggests that during autophagy, Atg9 is constantly cycling between the PAS and peripheral sites [193], presumably facilitating the delivery of membranes from donor organelles that is used for autophagosome formation [103]. Therefore,

characterizing Atg9 thoroughly is of great importance in understanding the membrane origin, and the mechanism of phagophore expansion in autophagy.

The highly conserved and constitutive autophagy pathway has to be critically regulated; disruption of this balance leads to various diseases that include neurodegeneration, cancer and infection, as well as aging-related disorders [212, 213]. It is essential that we gain a detailed understanding of the regulatory mechanisms that control autophagy to enable its safe modulation for therapeutic purposes. Studies have shown that Atg9 is transcriptionally repressed in growing conditions; this regulation correlates with the number of autophagosomes formed [184], in agreement with the model that Atg9 plays a critical role in membrane delivery to the PAS.

In addition to transcriptional control, post-translational modifications (PTMs) such as glycosylation, ubiquitination, phosphorylation, acetylation, lipidation, and proteolysis, represent a subset of regulatory mechanisms that are critical for controlling the level of autophagy activity that allows cells to adapt to various stress conditions [122, 176, 214, 215]. Ubiquitination involves the addition of the 8-kDa ubiquitin (Ub) moiety to a targeted protein; different linkages direct the target for subsequent proteasome-dependent degradation, signal transduction or other cellular processes. The completion of the reaction cascade requires an E1 Ub activating enzyme, an E2 Ub conjugating enzyme (E2), an E3 Ub ligase, and, in some cases, an E4 Ub chain elongation factor [216]. Recent studies have reported a role for the CUL3-KLHL20 complex, which acts as a ubiquitin ligase in mammalian cells; the activity of this enzyme leads to the degradation of the PIK3C3/VPS34 and ULK1 complexes, and the subsequent downregulation of autophagy [217]. Lys63-linked ubiquitination of BECN1 by TRAF6 or by AMBRA1 regulate its binding to BCL2 as well as subsequent phosphatidylinositol 3-kinase complex activity. TRAF6-mediaed ubiquitination of BECN1 amplifies lipopolysaccharide-, IFNG/interferon γ- and amino acid

starvation-induced autophagy in mouse macrophages [218]. In addition, deubiquitinating enzymes such as USP10 and USP13 are involved in the regulation of BECN1 ubiquitination in human and mouse cells, which promotes autophagy [219]. In our study, we discovered a novel role of ubiquitination on Atg9 in the regulation of autophagy in basal conditions; termination of this modification allows cells to rapidly respond and adapt to environmental stresses.

Based on a large-scale analysis predicting that yeast Atg9 is ubiquitinated and is short-lived [220], we studied the regulation of this protein through ubiquitination. We found that…

3.3 Results

3.3.1 Atg9 is ubiquitinated in nutrient-rich conditions

In the study by Radivojac et al., Atg9 is proposed to be ubiquitinated on lysine (K) 113 and K138, both of which are localized at the N terminus of Atg9, which is predicted to face the cytosol (Fig. 1A). To detect Atg9 ubiquitination at the endogenous level, we used TUBEs (Tandem Ubiquitin Binding Entities) agarose beads for isolation and detection of poly-ubiquitinated Atg9 [221]. Due to the low abundance of Atg9 molecules in a cell, we adopted an extra step of Atg9-MYC affinity isolation with anti-MYC magnetic beads to enrich Atg9 from the cell extract, and used it as input for the subsequent TUBEs precipitation; thus, we refer to this procedure as a two-step affinity isolation of poly-ubiquitinated Atg9. Ubc6, a known proteasome substrate, was also included as a positive control [222]. Similar to Ubc6, Atg9-MYC was detected after TUBEs affinity isolation, suggesting that Atg9 was ubiquitinated (Fig. 3.1B, Step 2, IP). We repeated the affinity isolation using a gradient of TUBEs agarose beads to determine the point of saturation (Fig. S1B). Using a gradient of TUBEs agarose beads we found that the amount of Atg9 that was affinity isolated increased, suggesting that at low levels the TUBEs beads may be saturated (Fig. 3.8B). When we examined the same number of cells from nutrient-depleted conditions, we

detected a substantial decrease in the amount of affinity-isolated (ubiquitinated) Atg9 (Fig. 3.8B). These results indicate that Atg9 is a ubiquitinated protein and this ubiquitination occurs primarily in rich conditions.

3.3.2 Atg9 is targeted for proteasome dependent degradation

Next, we decided to investigate whether the ubiquitination of Atg9 is a signal for proteasomal degradation or if it plays a role in regulating other cellular processes including protein translocation from peripheral sites to the PAS and protein-protein interaction. Accordingly, we looked at Atg9 steady-state protein levels in a proteasome mutant compared with the wild-type (WT) isogenic control strain. The *PRE1* gene, encodes the beta 4 subunit of the 20S proteasome, and is essential; therefore, we used a temperature-sensitive *pre1-1* mutant to analyze the stability of Atg9 when proteasome activity is compromised. When cultured at a permissive temperature (24°C), Atg9 protein levels were essentially the same in the *pre1-1* mutant compared to the WT cells, and the same was true during 1 h of nitrogen starvation (Fig. 3.2A). In contrast, at a nonpermissive temperature (34°C), the Atg9 protein level in the *pre1-1* mutant was increased compared to the WT or to the mutant at 24°C (Fig. 3.2A). Furthermore, this increase in the Atg9 protein amount was reversed after shifting the cells back to 24°C.

To extend this analysis, we also chemically inhibited proteasome activity through MG132 treatment and examined the effect on Atg9 turnover. In this experiment, cycloheximide (CHX) was added, allowing us to monitor degradation in the absence of new protein synthesis. In growing conditions, Atg9 was degraded by approximately 50% after 1.5 h in the presence of CHX. In contrast, this degradation was largely blocked following treatment with MG132 (Fig. 3.2B). The turnover of Ubc6 was monitored as a positive control and showed a half-life of approximately 1 h

(Fig. 3.9), in agreement with published studies [222] with nearly complete rescue in the presence of MG132 (Fig. 3.9).

Based on our findings in Figure 1, which showed that Atg9 ubiquitination decreased in nitrogen starvation conditions (i.e., when autophagy was induced), we decided to test if this decrease of ubiquitination also corresponded to a decrease of degradation. We carried out the same analysis to examine degradation in the presence of CHX in nitrogen starvation conditions and found that Atg9 degradation was indeed essentially blocked (Fig. 3.2C). Next, we determined whether the putative ubiquitination sites, K113 and K138, were involved in the degradation event. To do this, we generated an $Atg9^{K113,138R}$ double mutant ($Atg9^{KKRR}$) that is no longer subject to ubiquitination at these sites and repeated the same analysis. In agreement with these sites serving as ubiquitination targets, the $Atg9^{KKRR}$ mutant displayed a substantial stabilization in the presence of CHX in nutrient-rich conditions (Fig. 3.3A). These results collectively suggest that Atg9 is a target of the ubiquitin-proteasome system in growing conditions, when autophagy is maintained at a basal level.

Atg9 undergoes dynamic cycling during autophagy, shuttling between the peripheral sites and the PAS [58, 61, 178]. Anterograde trafficking to the PAS from the peripheral sites is dependent on various proteins including Atg23 [62], whereas the retrograde trafficking from the PAS to the peripheral sites depends on Atg1-Atg13 and Atg2-Atg18 [44]. To understand the timing and subcellular location of Atg9 ubiquitination, we generated *atg23*Δ, and *atg1*Δ cells, where Atg9 is either blocked at the peripheral sites or at the PAS, respectively. Again, we examined Atg9 stability at either location. In *atg23*Δ cells, Atg9 was degraded similar to the situation seen in the WT and to an even greater level, and this degradation was blocked by MG132 treatment (Fig. 3.3B). Similar result is seen in atg27Δ cells (Fig. 3.10A). In contrast, in *atg1*Δ, Atg9 appeared to

be stabilized in the absence or presence of MG132 (Fig. 3.3C). It is also consistent with results in atg18Δ cells (Fig. 3.10B). These findings suggest that Atg9 degradation happens primarily at the peripheral sites, which is consistent with our previous finding that Atg9 degradation primarily occurs in growing conditions.

3.3.3 Atg9 ubiquitination affects autophagy activity

To test if the two putative ubiquitination sites, K113 and K138, play a role with regard to autophagy activity, we examined the $Atg9^{KKRR}$ double mutant using an assay that monitors the processing of GFP-Atg8. GFP-Atg8 is initially present on both the convex and concave surfaces of the phagophore; the GFP-Atg8 that is localized on the concave surface becomes trapped within the autophagosome, is transported into the vacuole during autophagy, and is subsequently degraded. GFP is relatively stable to hydrolysis compared to the full-length chimera, so the free GFP produced reflects the level of autophagy [223]. Compared to the WT, the double mutant $Atg9^{KKRR}$ showed a statistically significant increase in autophagy-dependent GFP-Atg8 processing, particularly when looking at the basal level (0 h) and the 1 h time point; by 2 h of starvation, when the Atg9 protein level was increasing in the WT strain due to the block in ubiquitination, the difference became insignificant (Fig. 3.4A).

The GFP-Atg8 processing assay measures both selective and nonselective autophagy. To examine the effect of $Atg9^{KKRR}$ on selective autophagy activity we used the precursor aminopeptidase I (prApe1) maturation assay in *vac8*Δ cells. Ape1 is a vacuolar enzyme that is initially synthesized in the cytosol as a precursor containing a propeptide; delivery of prApe1 to the vacuole can occur via either the Cvt pathway or nonselective autophagy, depending on nutrient conditions [81, 188]; in either case, the efficient trafficking of prApe1 depends on a receptor protein, Atg19, making the delivery a selective process [86]. Following the release of prApe1 into

the vacuole lumen, the propeptide is removed, which generates the mature Ape1 hydrolase. This maturation event—removal of the propeptide—is easily detected by SDS-PAGE due to the resulting change in molecular mass. In this experiment, we relied on the phenotype of the *vac8*Δ strain; in the absence of Vac8, prApe1 accumulates in cells during vegetative growth, due to an essentially complete block in the Cvt pathway; however, following a shift to starvation conditions there is rapid vacuolar delivery and maturation of prApe1 [53]. Thus, shifting *vac8*Δ cells from vegetative to starvation conditions mimics a pulse-chase analysis. In the *atg9*Δ *vac8*Δ strain we could detect only prApe1 even after autophagy was induced by starvation (Fig. 3.4B). This block in prApe1 maturation that was seen under autophagy-inducing conditions was rescued by chromosomal re-integration of the wild-type *ATG9* gene, and prApe1 maturation was increased in the presence of $Atg9^{KKRR}$ after 1 h starvation (Fig. 3.4B). These results suggest that the ubiquitination of Atg9 has consequences for Atg9 function in both selective and nonselective autophagy.

3.3.4 The Atg9 ubiquitination mutant has increased PAS localization

To follow the movement of Atg9, we monitored cells expressing wild-type Atg9 or $Atg9^{KKRR}$ driven by the native *ATG9* promoter, and tagged with GFP on the C terminus. We used red fluorescent protein (RFP)-tagged prApe1 (RFP-Ape1) as a marker of the PAS, and quantified the colocalization with the Atg9 chimeras. During vegetative growth, Atg9-GFP localized to multiple puncta per cell, and approximately 20% of the cells examined had Atg9-GFP puncta localized to the PAS; this distribution of Atg9 during basal autophagy agrees with our previously published data [211]. The percent colocalization at the PAS (i.e., the population of active Atg9) was increased to approximately 50% after cells were shifted to starvation (-N) conditions for 30 min. In contrast, the colocalization of Atg9-GFP in cells expressing $Atg9^{KKRR}$-GFP was

substantially higher than WT in growing conditions and it remained at the WT level after autophagy was induced (Fig. 3.5A). This result suggests that the partial block of Atg9 degradation due to the block in ubiquitination at K113 and K138 leads to an increase in the population that is localized to the PAS.

To test if the increased PAS localization of $Atg9^{KKRR}$ bypasses the normal requirement of its interacting proteins, we carried out the same experiment in either the *atg1*Δ strain, where Atg9 accumulates at the PAS or in *atg27*Δ cells, where Atg9 remains at the peripheral sites. In this case, by again monitoring the colocalization of Atg9-GFP and RFP-Ape1, we found no significant differences between the KKRR mutant and WT with regard to Atg9 localization in these two deletion backgrounds (Fig. 3.5B-D). Taken together, these data suggest that the increased PAS localization of $Atg9^{KKRR}$-GFP does not bypass the role of Atg proteins involved in Atg9 trafficking, and that it depends on the higher protein level of Atg9 resulting from the block in degradation.

3.3.5 Atg9 degradation is mediated by Met30

To identify for the E3 ligase that covalently link ubiquitin to Atg9, we performed a screen of yeast strains harboring knockouts or conditional mutations in the genes encoding the E3 enzymes. Atg9 was tagged with protein A (PA) on the genome in each mutant and Atg9-PA stability was monitored in the presence of CHX. In WT cells, after 3 h of CHX treatment, the Atg9 protein level decreased to approximately 20% of that present at time 0. Most of the E3 mutants that we screened, such as *yjl149w*Δ and *rad7*Δ, displayed a similar stability of Atg9 as seen in WT (Fig. 3.11). A few of the mutants had a partial effect on Atg9 degradation, resulting in over 50% of Atg9 being present at the 3-h time point. Among all of the mutants tested, the *met30-6* temperature-sensitive mutant displayed the most significant block; more than 80% of Atg9

remained after 3 h in the presence of CHX (Fig. 3.6A). This result suggests that Atg9 degradation is mediated at least in part by Met30.

Met30 is an F-box protein working in a SCF (Skp, Cullin, F-box containing) ubiquitin complex, which contributes to substrate specificity by targeting a specific protein [224]. The association between E3 and substrate is weak and transient due to the fact that F-box proteins are not abundant, or stable and also as a result of the rapid de-ubiquitination process. To test if Atg9 is a substrate of the Met30 SCF, we used a bimolecular fluorescence complementation (BiFC) assay. Briefly, this assay involves the separation of the Venus yellow fluorescent protein (vYFP) into two fragments, VN and VC, corresponding to the N and C termini of vYFP, respectively [195]. If the two halves of vYFP are brought into proximity due to interaction of the respective chimeras, fluorescence is restored. We genomically fused VN to Atg9 on the C terminus and overexpressed VC under the *RPL1* promoter to Met30 on the N terminus. In growing conditions, a vYFP signal was observed only in cells that expressed both Atg9-VN and VC-Met30 (Fig. 3.6B), suggesting that interactions between Atg9 and Met30 existed in basal autophagy conditions. The interaction of Atg9-VN and Atg23-VC was included as a positive control (Fig. 3.6B) [211]. The interaction between Atg9-VN and VC-Met30 was also seen in starvation conditions; however, we think this observation reflects the fact that vYFP is extremely stable in the BiFC complex. In contrast, we could barely detect the interaction between these two proteins through co-immunoprecipitation even in growing conditions, suggesting this binding is weak and/or transient (data not shown).

Phosphorylation can promote or inhibit subsequent protein ubiquitination [225], and previous studies showed Atg9 is a phosphoprotein [120, 211]. Accordingly, we examined ubiquitination-dependent degradation of Atg9 in phosphorylation site mutants. We observed that

Atg9^{S122A} was degraded in a similar pattern as in WT cells with 1 or 2 h of CHX chase (Fig. 3.6C). This result suggests that phosphorylation of S122A in Atg9 is not involved in the regulation of its ubiquitination.

3.4 Discussion

Atg9 is the only membrane protein in the autophagy core machinery, and it plays a significant role in phagophore/autophagosome formation; thus, it is important to know how this protein is regulated in order to understand the mechanism of autophagy. Based on a large-scale analysis that predicts Atg9 is a ubiquitinated protein with a short half-life, we first verified this ubiquitination by two-step affinity isolation using TUBEs, and observed a higher amount of Atg9 being pulled down in nutrient-rich conditions compared to starvation, which indicates Atg9 is primarily ubiquitinated in growing conditions. By checking the protein stability of Atg9 in cells where proteasome function was compromised either genetically or through chemically inhibition, we further determined that this ubiquitination is a signal for proteasome-dependent degradation of Atg9 in growing conditions, which maintains autophagy at a low basal level. This hypothesis is consistent with our later findings that Atg9 was degraded in *atg23*Δ cells when it was restricted to peripheral sites; whereas, it was stabilized in *atg1*Δ cells when Atg9 is primarily localized at the PAS. These findings suggest that the "active" population of Atg9 (i.e., Atg9 that has orchestrated the delivery of membrane) at the PAS is not subject to degradation, while that part of the Atg9 pool localized at peripheral sites, or on its way to the PAS, is subject to degradation.

We also generated Atg9 lysine-to-arginine double mutants K113,138R (KKRR) based on the predicted ubiquitination sites. These two sites are conserved across different species of fungi (Fig. 3.8A) and this type of modification and regulation may be also conserved among more complex eukaryotes. Using both GFP-Atg8 processing and prApe1 processing assays, we found

that autophagy activity was increased in the mutant compared to WT, which maybe due to a higher level of Atg9. This is consistent with previous findings showing that the amount of Atg9 correlates with the number of autophagosomes formed (i.e., the frequency of formation) and hence with autophagy activity [184]. Knowing Atg9 is undergoing dynamic trafficking during autophagy, we also looked at its PAS localization as a readout of its trafficking and found there was a higher PAS localization in the presence of KKRR mutant Atg9 compared to WT cells in growing conditions. We hypothesized that this higher autophagy activity and higher PAS localization of Atg9 was due to the higher Atg9 protein level as a result of a partial block of ubiquitination. However, the KKRR mutant was not able to travel to the PAS without Atg27 or Atg1. To look for the E3 ligase responsible for conjugating ubiquitin to Atg9 in growing conditions, we performed a screen using an E3 knockout library to look for a mutant that stabilizes Atg9. Among 37 E3s we screened, Atg9 was stabilized the most significantly in *met30 ts,* suggesting Atg9 degradation is mediated by Met30. We further validated this hypothesis by testing interactions between Atg9 and Met30 by BiFC, and indeed observed interacting signals in growing conditions.

In summary, we identified a novel mechanism of Atg9 regulation in autophagy through ubiquitination. In growing conditions, Atg9 is synthesized and cells are primed for autophagy. We showed that Atg9 is ubiquitinated and targeted for degradation in a proteasome-dependent manner during nutrient-rich conditions, therefore limiting autophagy to a basal level. However, when cells are nutritionally deprived, autophagy is highly induced, necessitating an increase in the amount of Atg9; the proteasome-dependent reduction of Atg9 protein levels is reduced to give cells a jumpstart for autophagy. Thus, the post-translational ubiquitination of Atg9 provides an additional mechanism that allows cells to maintain appropriate levels of autophagy, and to rapidly respond and adapt to environmental stresses.

3.5 Materials and Methods

3.5.1 Strains, media, and growth conditions

Yeast strains used in this paper are listed in Table 1. Gene deletions or integrations were performed using a standard method [226, 227]. Cells were cultured in rich medium (YPD; 1% [w:v] yeast extract [ForMedium, YEM04], 2% [w:v] peptone [ForMedium, PEP04], and 2% [w:v] glucose), or synthetic minimal medium (SMD; 0.67% yeast nitrogen base [ForMedium, CYN0410], 2% glucose, and auxotrophic amino acids and vitamins as needed) as indicated, referred to as nutrient-rich conditions. Autophagy was induced through nitrogen starvation by shifting cells in mid-log phase from YPD (or SMD) to SD-N (0.17% yeast nitrogen base without ammonium sulfate or amino acids [ForMedium, CYN0501], and 2% [w:v] glucose) for the indicated times, referred to as starvation conditions.

3.5.2 Plasmids

Integrating plasmids encoding Atg9-GFP [184] and a centromeric plasmid encoding pCu-GFP-ATG8 or RFP-Ape1 have been published previously [223]. Plasmids encoding Atg9-GFP with mutations K113R and K138R was generated by site-directed mutagenesis [198] from Atg9-GFP.

3.5.3 Ubiquitination assay

Step 1: Yeast cells (50 OD units; equivalent to 50 ml of cells at OD_{600} = 1.0) grown in YPD to OD_{600} =1.0 were lysed using glass beads in 1.5 ml IP buffer (PBS, 200 mM Sorbitol, 1 mM $MgCl_2$, 0.1% Tween 20), supplemented with a mixture of protease inhibitor cocktail (Complete EDTA-free, Roche; 1 tablet per 50 ml lysis buffer) and 1 mM PMSF. After mixing by vortex for 8 min and centrifugation for 10 min at 15,000 rpm (20,879 x g), the resulting supernatant was

removed and incubated with 100 µl of anti-MYC/c-Myc magnetic beads (Thermo Scientific) for 4 h at 4°C. Magnetic beads are washed 3 times with IP buffer and collected using a magnetic stand. MYC-tagged protein was eluted by incubating 3 times with 100 µl of 0.5 mg/ml MYC/c-Myc peptide (Sigma) at 37°C, 10 min. The eluate concentration was measured using NanoDrop. Step 2: The eluate was incubated with agarose-TUBEs beads (LifeSensors) according to the manufacturer's protocol overnight at 4°C. Beads were washed 3 times with IP buffer and then suspended in SDS-PAGE loading buffer (50 mM Tris-Cl, pH 6.8, 100 Mm DTT, 2% SDS, 0.1% bromophenol blue, 10% glycerol) and analyzed by western blot.

3.5.4 Additional assays

GFP-Atg8 processing, prApe1 processing, western blot, fluorescence microscopy and BiFC assays were performed as described previously [211, 223]. Antibodies against GFP, Atg9, Ape1 and Pgk1 (a generous gift from Dr. Jeremy Thorner, University of California, Berkeley) were used as described previously. A commercial antibody that reacts with protein A (Jackson Immunoresearch) was used at 1:40,000 dilution and anti-MYC/c-Myc (Invitrogen) was used at 1:5,000 dilution.

3.5.5 Statistical analysis

Two-way ANOVA test was used to determine statistical significance.

* $p<0.05$, ** $p<0.01$, *** $p<0.001$, N.S., not statistically significant

3.6 Acknowledgements

The authors thank Dr. Mara Duncan (University of Michigan) and Dr. Taras Nazarko (University of California, San Diego) for helpful comments. This work was supported by NIH grant GM053396 to DJK.

Table 3.1. Yeast strains used in this study.

Name	Genotype	Reference
SEY6210	MATα *leu2-3,112 ura3-52 his3-Δ200 trp1-Δ901 suc2-Δ9 lys2-801 GAL*	[206]
YKF548	WLY176 *pdr5ΔdrKAN UBC6-13MYC::HIS3*	This study
YKF539	WLY176 *ATG9-MYC::TRP1 doa4Δ::KAN*	This study
YKF511	WLY176 *ATG9-MYC::TRP1*	This study
YKF557	WLY176 *pdr5Δ::KAN UBC6-MYC::HIS3*	This study
YKF512	BY4741 *ATG9-PA:: HIS3*	This study
YKF513	BY4741 *pre1-1ts::KAN ATG9-PA::HIS3*	This study
YKF515	BY4741 *UBC6-PA::HIS3 pdr5Δ::KAN*	This study
YKF508	WLY176 *pdr5Δ::KAN ATG9-PA::HIS3*	This study
YKF619	WLY176 *atg9Δ::LEU2 pRS314 ATG9-PA ::TRP1*	This study
YKF620	WLY176 *atg9Δ::LEU2 pRS314 ATG9* $^{K113R\,K138R}$ *-PA::TRP1*	This study
YKF530	WLY176 *pdr5Δ::KAN ATG9-PA::HIS3 atg23Δ::URA*	This study
YKF547	WLY176 *pdr5Δ::KAN ATG9-PA::HIS3 atg18Δ::URA3*	This study
YKF531	WLY176 *pdr5Δ::KAN ATG9-PA::HIS3 atg27Δ::URA3*	This study
YKF528	WLY176 *pdr5Δ::KAN ATG9-PA::HIS3 atg1Δ::URA*	This study
YKF083	WLY176 *atg9Δ::LEU2 ATG9-GFP::URA RFP-APE1:TRP1*	This study
YKF516	WLY176 *atg9Δ::LEU2 ATG9*^{K113RK138R}*-GFP::URA3 RFP-APE1::TRP1*	This study
YKF496	WLY176 *atg9Δ::LEU2 ATG9-GFP::URA3 RFP-APE1::TRP1 atg1Δ::HIS3*	This study

YKF500	WLY176 *atg9Δ::LEU2 ATG9-GFP::URA3 RFP-APE1::TRP1 atg27Δ::HIS3*	This study
YKF538	WLY176 *atg9Δ::LEU2 ATG9^{K113RK138R}-GFP::URA3 RFP-APE1::TRP1 atg1Δ::HIS3*	This study
YKF506	WLY176 *atg9Δ::LEU2 ATG9^{K113RK138R}-GFP::URA3 RFP-APE1::TRP1 atg27Δ::HIS3*	This study
YKF621	WLY176 *pRPL-VC-MET30::KAN*	This study
YKF640	WLY176 *pRPL-VC-MET30::KAN ATG9-VN::HIS3*	This study
YKF631	WLY176 *ATG9-VN::HIS3*	This study
YKF001	WLY176 *atg9Δ::LEU2 ATG9-GFP WT::URA3*	[211]
YKF002	WLY176 *atg9Δ::LEU2 ATG9-GFP S122A::URA3*	[211]

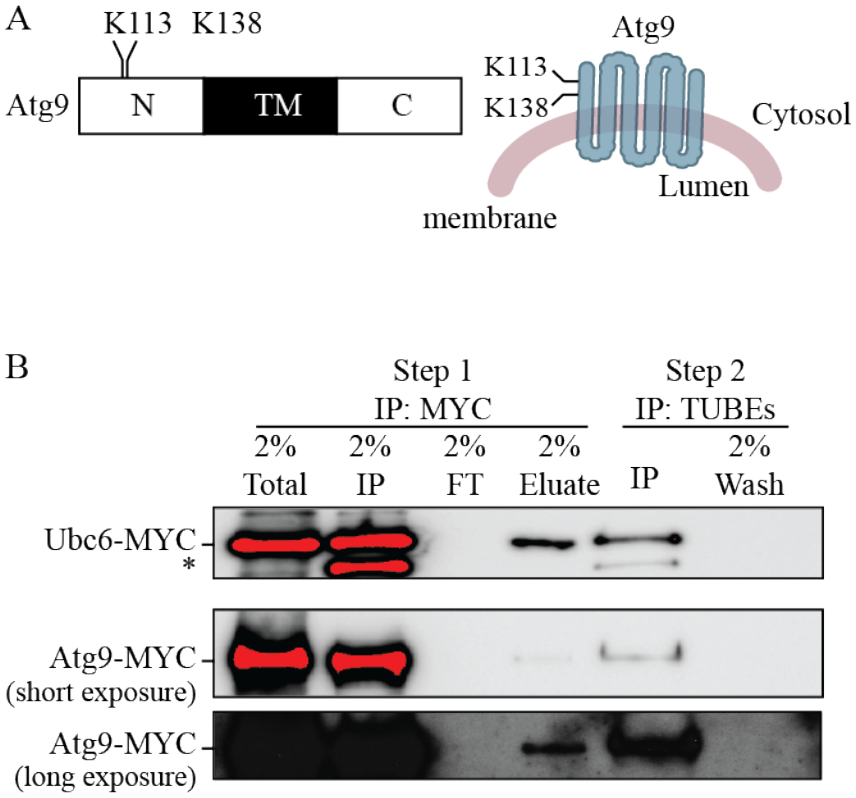

Figure 3.1 Atg9 is ubiquitinated in nutrient-rich conditions.
(A) Schematic representation of Atg9 highlighting positions of K113 and K138 on the N terminal cytosolic domain. (B) TUBEs affinity isolation of ubiquitinated Ubc6 and Atg9 in growing conditions

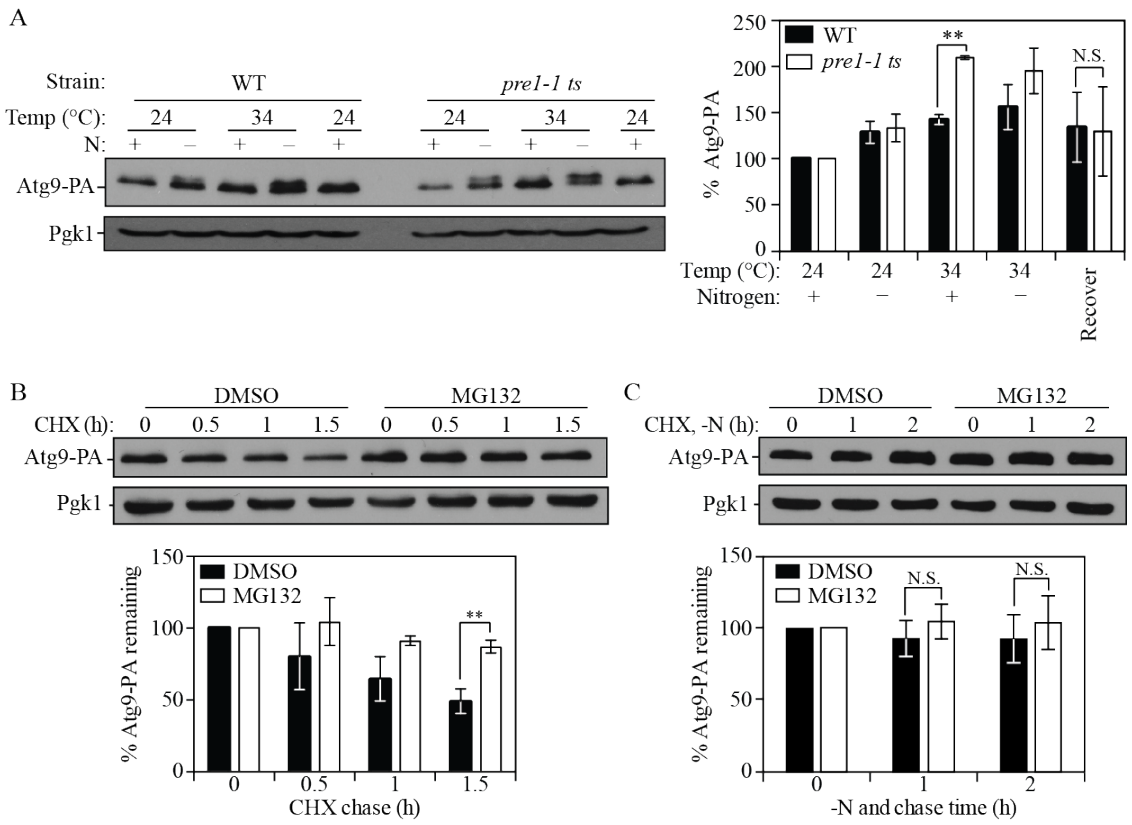

Figure 3.2 Atg9 is targeted for proteasome-dependent degradation.
(A) Atg9-PA protein level in WT and proteasome-mutant *pre1-1 ts* cells under permissive (24°C) and non-permissive (34°C) temperatures. Quantification of the data is shown on the right. (B, C) Atg9-PA protein stability in (B) growing or (C) starvation conditions in control (DMSO) and proteasome inhibitor (MG132; 75 µM)-treated cells at the indicated time points of CHX (100 µg/ml) chase time. Quantification of the data is shown below each set of blots.

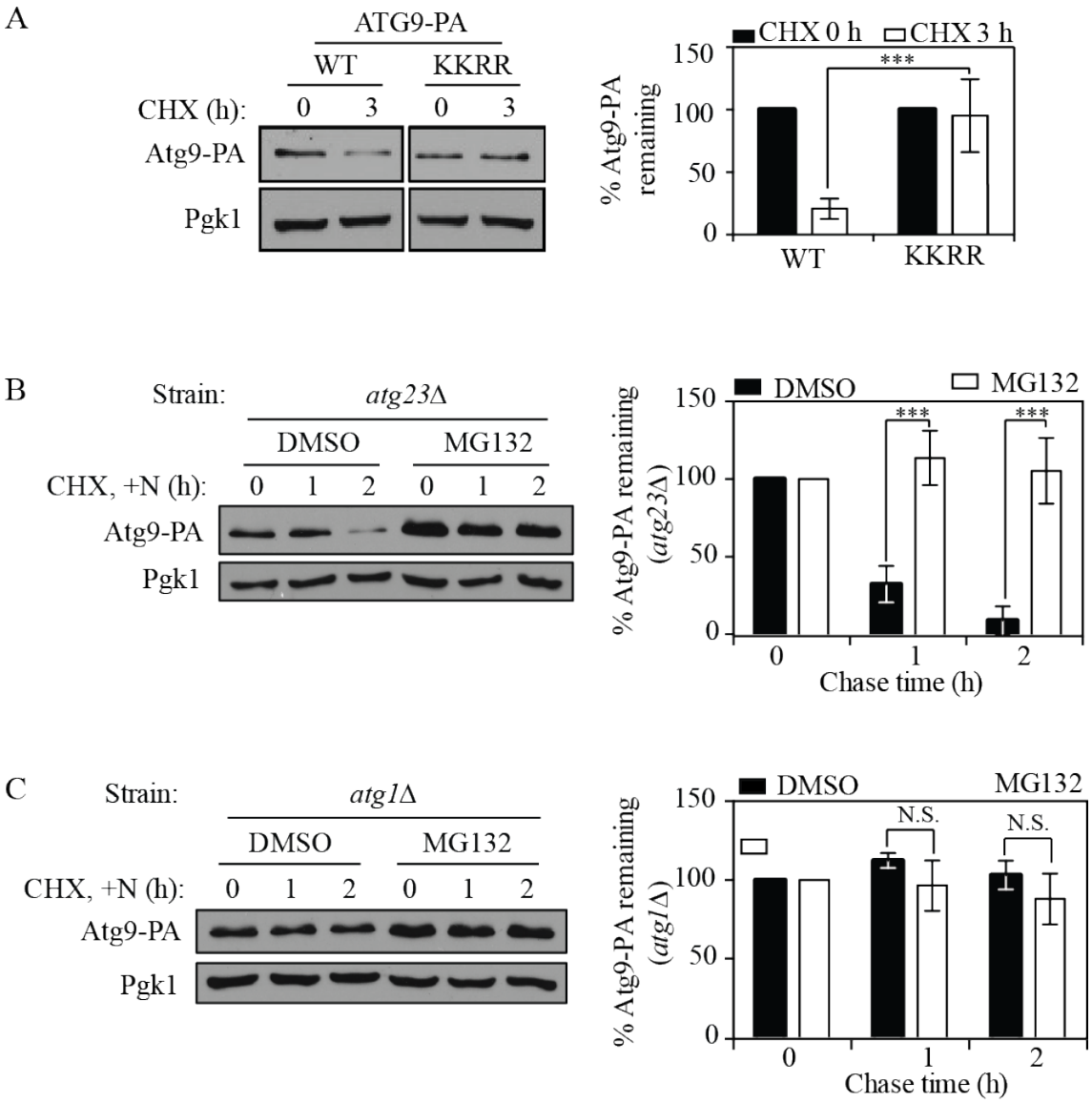

Figure 3.3 Atg9 is primarily degraded at peripheral sites.
(A) Atg9-PA protein stability in WT and KKRR mutant cells at the indicated time points of CHX chase time. (B, C) Atg9-PA protein stability in (B) *atg23*Δ or (C) *atg1*Δ cells in control (DMSO) and proteasome inhibitor (MG132) treatment conditions at the indicated time points of CHX chase time. The quantification for each set of blots is shown on the right.

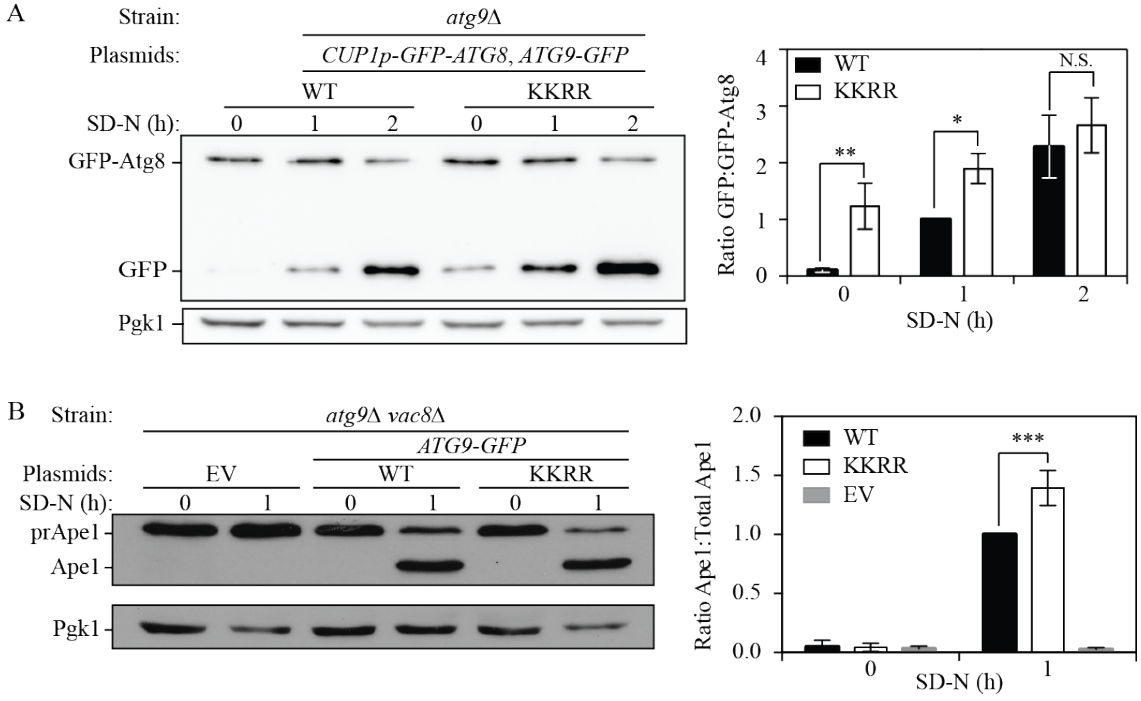

Figure 3.4 Atg9 ubiquitination is important for autophagy activity.
(A) Western blot analysis of a GFP-Atg8 processing assay in *atg9*Δ cells transformed with a plasmid expressing Atg9-GFP WT or the KKRR mutant. Cells were cultured in YPD, shifted to SD-N and collected at the indicated time points of nitrogen starvation. The quantification of free GFP:total GFP ratio is shown on the right. (B) Western blot analysis of prApe1 processing assay in *atg9*Δ *vac8*Δ cells transformed with an empty vector (EV) or with a plasmid expressing Atg9-GFP WT or the KKRR mutant. Cells were grown and processed as in A. The quantification of Ape1:total Ape1 (Ape1 + prApe1) ratio is shown on the right.

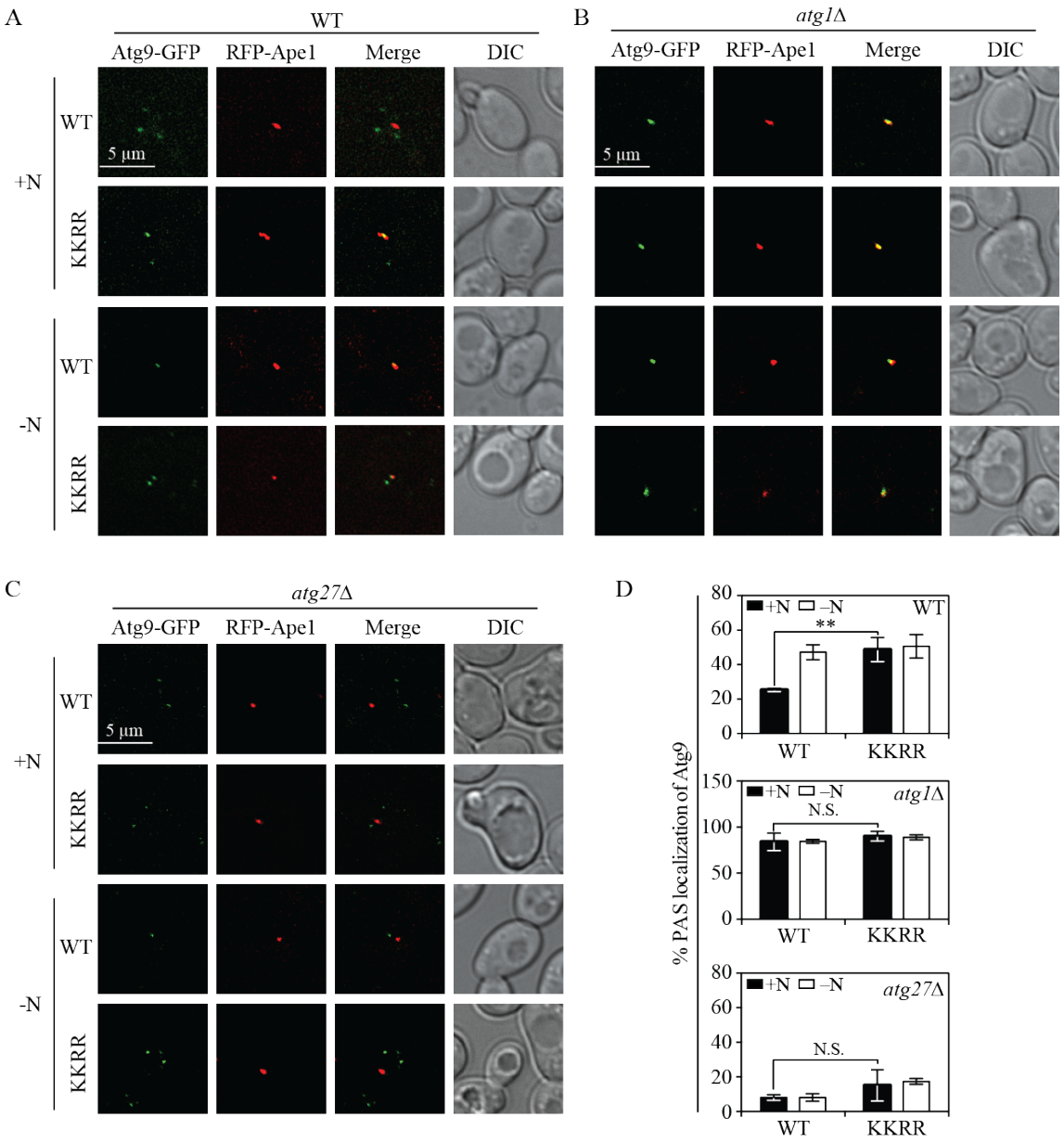

Figure 3.5 The Atg9 ubiquitination mutant displays a higher frequency of PAS localization. (A-C) Representative florescence microscopy images of (A) *atg9*Δ (WT), (B) *atg1*Δ or (C) *atg27*Δ cells transformed with a plasmid expressing WT or KKRR mutant Atg9-GFP. A plasmid expressing RFP-Ape1 was also used to provide a PAS marker. Cells were cultured in YPD, shifted to SD-N and collected at both 0 and 30 min nitrogen starvation. The single z-stack images are displayed at equal intensity for comparison. Scale bars: 5 µm. (D) Quantification of colocalization between Atg9-GFP and RFP-Ape1 in each of the respective strains. Error bars correspond to the standard deviation and were obtained from 3 independent repeats.

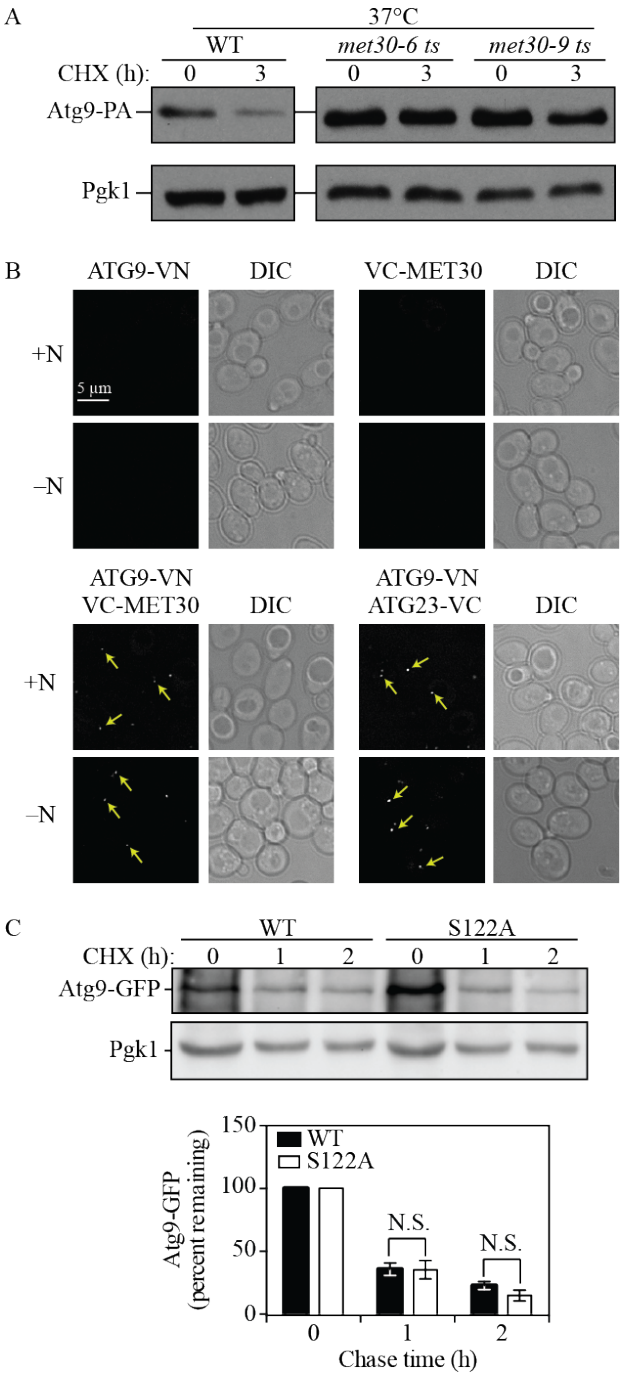

Figure 3.6 Atg9 degradation is mediated by Met30.
(A) Representative western blot images of Atg9-PA stability in two alleles of the *met30 ts* mutant. Pgk1 was used as a loading control. (B) Representative florescence microscopy images of cells expressing the BiFC constructs ATG9-VN, VC-MET30, or both, cultured in YPD and shifted to SD-N for 1 h. ATG9-VN ATG23VC was included as a positive control. Images are from single Z-sections. DIC, differential interference contrast. Scale bar: 5 µm. (C) Atg9-GFP protein stability in growing conditions in control WT and S122A mutant cells at the indicated time points of CHX chase time. A quantification of the western blots is shown below the panels.

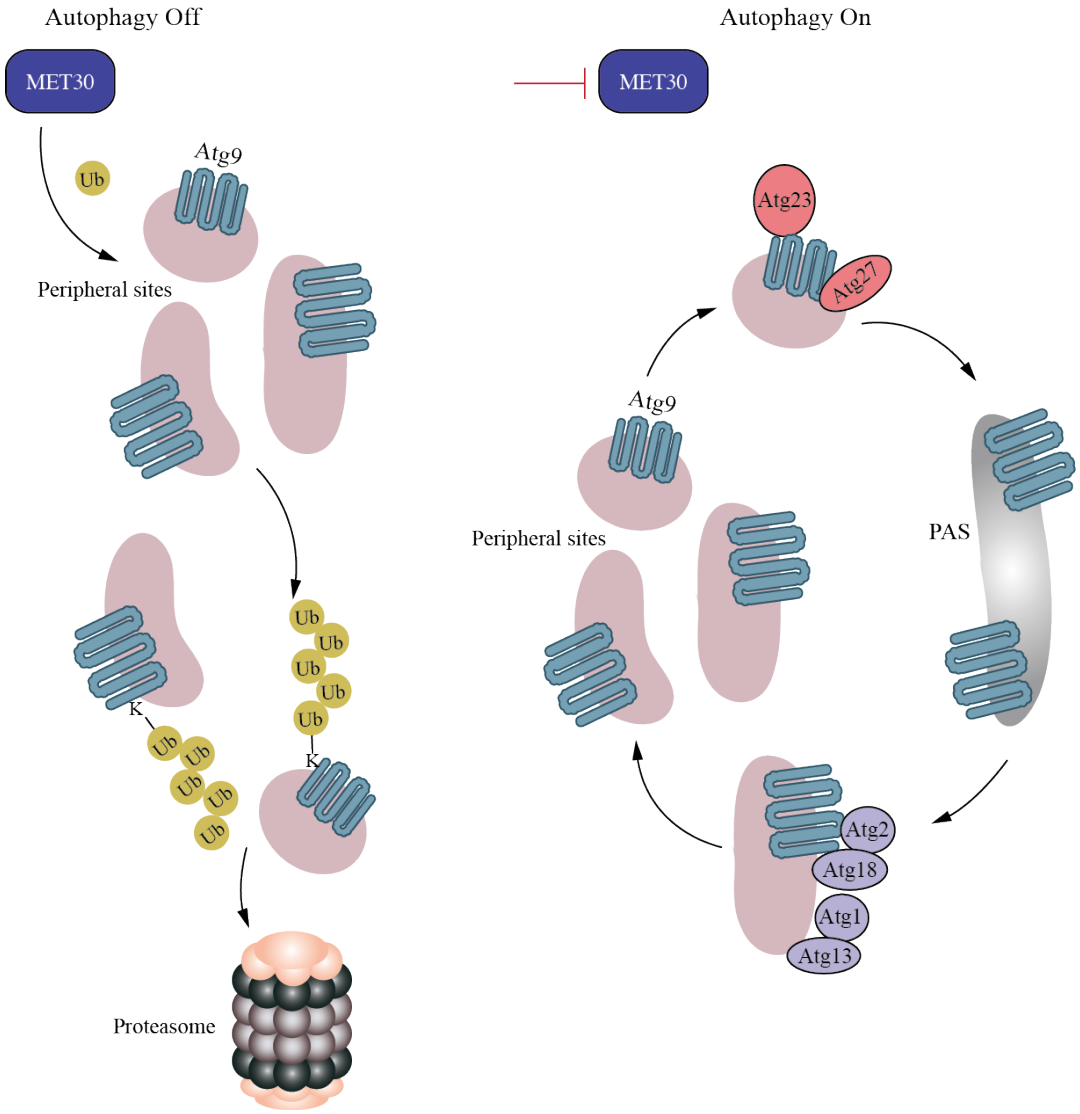

Figure 3.7 Schematic model for downregulation of autophagy through UPS-dependent degradation of Atg9.
In nutrient-rich conditions, Atg9 is synthesized and cells are primed for autophagy. The excessive Atg9 is ubiquitinated and targeted for degradation in a proteasome-dependent manner, therefore limiting autophagy to a basal level. However, when cells are nutritionally deprived, autophagy is highly induced, necessitating an increase in the amount of Atg9; the proteasome-dependent reduction of Atg9 protein levels is reduced to allow cells to induce a higher level of autophagy.

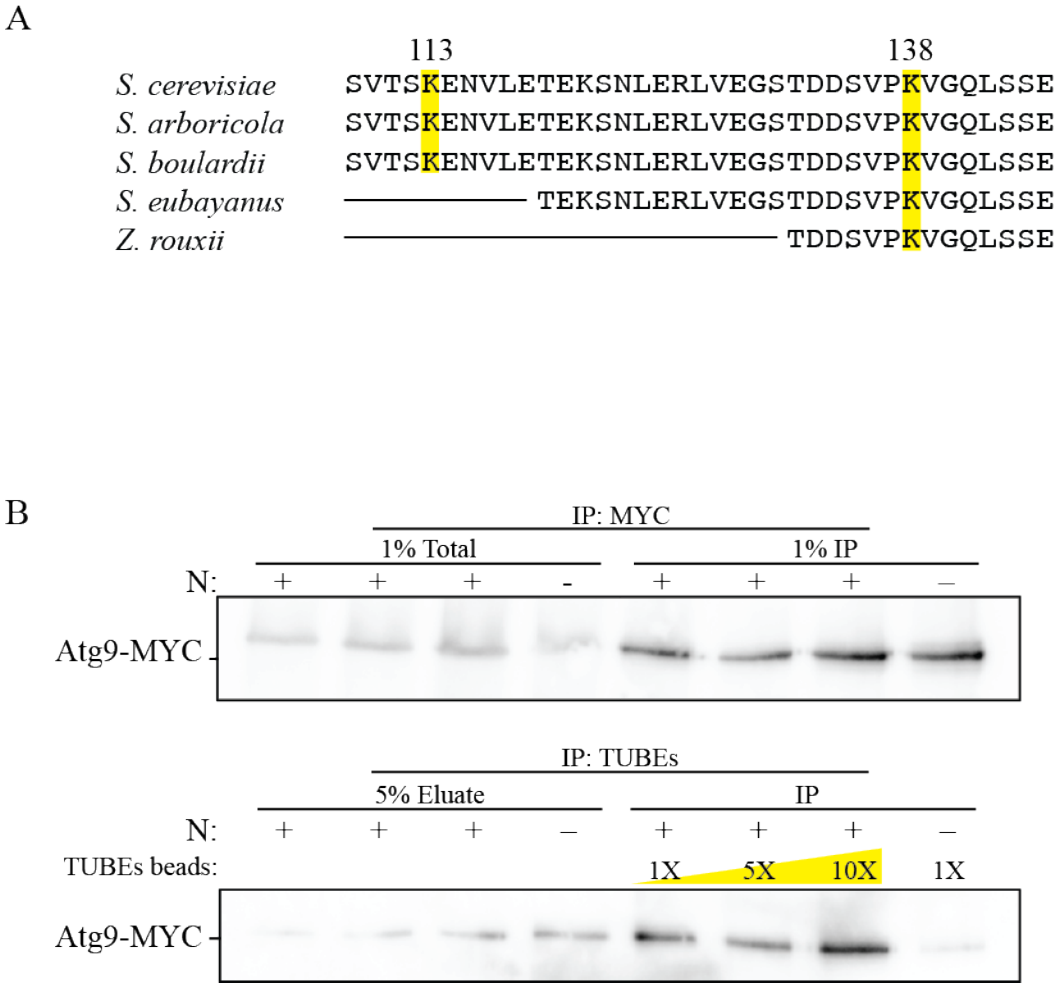

Figure 3.8 The Atg9 N terminus is conserved among fungi, and Atg9 ubiquitination is suppressed in starvation conditions.
(A)Amino acid sequence alignment of the N terminus of Atg9 across different species. The mutated lysine residues are highlighted in yellow. *S.*, *Saccharomyces*; *Z.*, *Zygosaccharomyces*. (B) TUBEs affinity isolation of ubiquitinated Atg9 in growing conditions with increasing amount of TUBEs beads and ubiquitinated Atg9 in nitrogen starvation for 1 h.

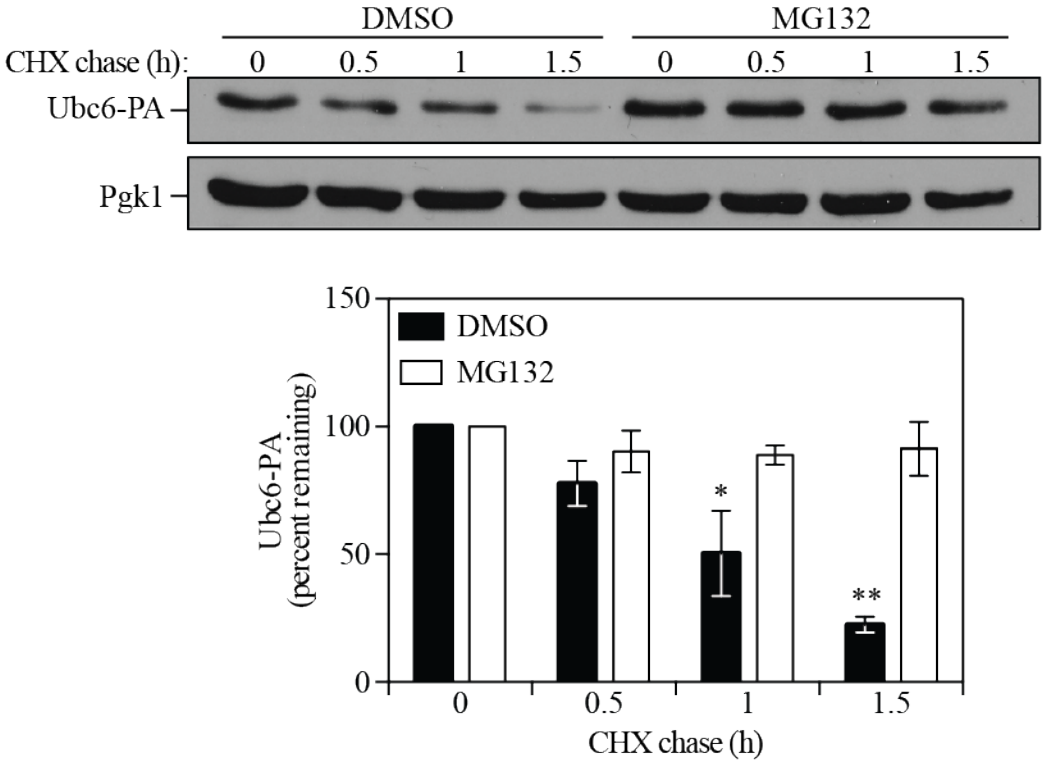

Figure 3.9 Ubc6 is degraded in a proteasome-dependent manner.
Ubc6-PA protein stability in control (DMSO) and proteasome inhibitor (MG132)-treated cells at the indicated time points of CHX chase time.

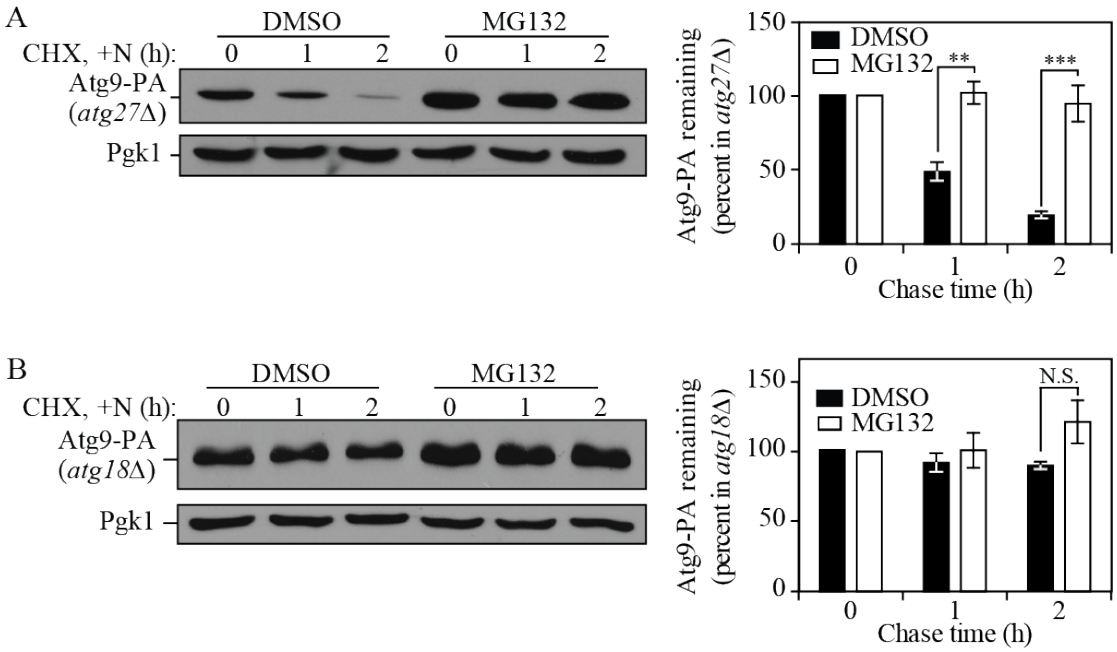

Figure 3.10 Atg9 is primarily degraded at peripheral sites.
(A, B) Atg9-PA protein stability in (A) *atg27*Δ or (B) *atg27*Δ cells in control (DMSO) and proteasome inhibitor (MG132) treatment conditions at the indicated time points of CHX chase time.

A

Percent of Atg9 remaining after 3 h

>80%	50-80%	<50%		
met30	*cdc44*	*ama1*	*pib1*	*stf13*
	hrt3	*asi1*	*prp19*	*tom1*
	mdm30	*asi3*	*rad5*	*tul1*
	san1	*bre3*	*rad7*	*ubr1*
	ssm4	*cdc20*	*rad18*	*ufd2*
	ubr2	*cdh1*	*rcy1*	*ufd4*
	ylr352w	*ela1*	*rkr1*	*ydr306c*
		hrd1	*rsp5*	*yjl149w*
		hul4	*saf1*	*ymr119w*
		hul5	*skp2*	

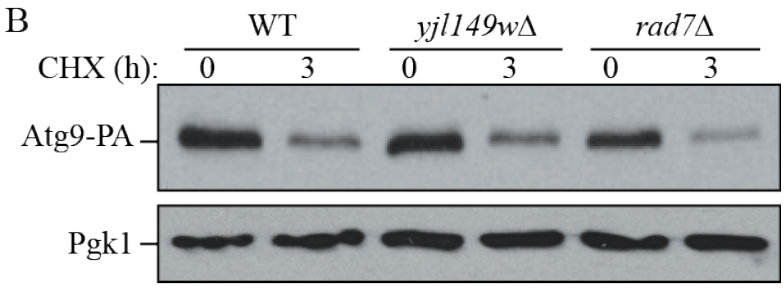

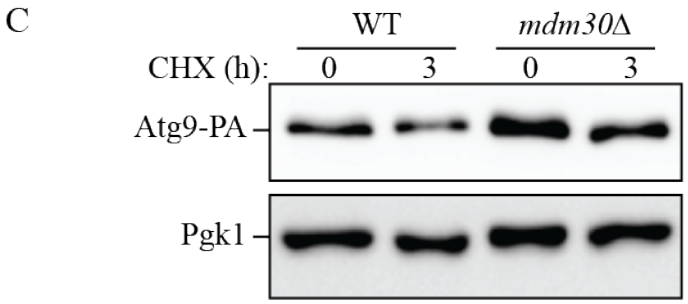

Figure 3.11 Atg9 degradation is mediated by Met30.
(A) 37 E3 ligase mutants were screened for stability of Atg9 by western blot analysis, quantified and grouped into categories of <50%, 50-80% and >80% stability after 3 h of CHX chase. (B, C) Representative western blot images of Atg9-PA stability in (B) WT, *yjl149w*Δ and *rad7*Δ cells representing the group <50% and in (C) WT and *mdm30*Δ cells representing the group 50-80%.

Chapter 4 Summary

Autophagy is a self-eating process in which cells engulf portions of the cytosol or organelles via phagophores. After maturation, the resulting double-membrane autophagosomes deliver the cargo to the lysosome or vacuole, where it is ultimately degraded; the resulting breakdown products are released back into the cytosol and recycled to allow the cells to survive unfavorable conditions and maintain cellular homeostasis. One of the key questions regarding macroautophagy/autophagy is the mechanism through which the transmembrane protein Atg9 functions in delivering membrane to the expanding phagophore, the sequestering compartment that matures into an autophagosome.

Previous studies have indicated that multiple membrane sources contribute to autophagosome formation, including the endoplasmic reticulum (ER) [228-230], the Golgi apparatus [231] and the plasma membrane [232]. Atg9 is the only transmembrane protein in the autophagy core machinery and has been proposed to play a key role in directing membrane from donor organelles for autophagosome formation. Thus, understanding the mechanism of Atg9 regulation is fundamental.

In this chapter, I summarize findings of chapters 2 and 3, and discuss future directions.

4.1 Phosphorylation of Atg9 regulates movement to the phagophore assembly site and the rate of autophagosome formation

In chapter 2, we characterized a phosphorylation-dependent regulation of Atg9 anterograde trafficking that mediates autophagy activity. We first identified S122 on Atg9 as a phosphorylation site independent of Atg1 kinase from a SILAC assay. Alteration of this residue to a non-

phosphorylatable mutant, S122A, reduces autophagy activity, whereas the phospho-mimetic mutant S122D increases autophagy activity. Besides non-selective autophagy, this phosphorylation is also important in selective autophagy. We subsequently examined the mechanisms behind such an effect by EM analysis and found that the number of autophagosomes formed in these mutants is also altered. Consistent with autophagy activity, cells expressing $Atg9^{S122A}$ generate fewer autophagosomes, whereas cells expressing $Atg9^{S122D}$ have the opposite phenotype. Based on previous studies that propose Atg9 cycles between the PAS and other cytosolic punctate structures, we also find this phosphorylation is important for Atg9 trafficking as shown in its localization at the PAS by fluorescence microscopy. More Atg9 at the PAS, as seen with $Atg9^{S122D}$, correlates with an increased rate of autophagosome formation. This result agrees with findings from a recent study where the absolute Atg9 levels correspond to the number, but not the size, of autophagosomes generated during autophagy [233]. Furthermore, using the MKO strain, we determined that anterograde movement is altered with the mutant version of Atg9. Finally, our data suggest that the S122D mutation results in an enhanced interaction between Atg9 and Atg27, one of the components required for efficient anterograde trafficking of Atg9 [179, 193].

We are not able to show this interaction by co-immunoprecipitation due to the fact that it may be weak, transient or unstable during the immunoprecipitation procedure. Also, the kinase or phosphatase that directly modifies Atg9 S122 remains to be identified.

4.2 Downregulation of autophagy through Met30-mediated Atg9 turnover

In chapter 3, we identified a novel mechanism of restricting autophagy to a basal level through ubiquitination and proteasome-dependent degradation of Atg9 in nutrient-rich conditions. Based on a large-scale analysis that predicts Atg9 is a ubiquitinated protein, we first verified this

ubiquitination by two-step affinity isolation using TUBEs, and observed a higher amount of ubiquitinated Atg9 in growing conditions compared to starvation conditions, which indicates Atg9 is primarily ubiquitinated in the former. We further identified this ubiquitin as being a proteasome-dependent degradation signal in growing conditions by finding an increase of Atg9 steady state protein level in cells with a genetically defective proteasome or one that was chemically compromised. A chase analysis to monitor Atg9 stability in *atg23*Δ (Atg9 is present at peripheral sites) or *atg1*Δ (Atg9 is localized at the PAS) cells further supports our hypothesis that the population of Atg9 either at peripheral sites or on its way to the PAS is subject to degradation, but the population at the PAS, which is actively working in autophagy, is protected and not subject to degradation. A lysine-to-arginine double mutant K113R K138R generated based on the predicted ubiquitination sites promoted increased non-selective and selective autophagy activity at early time points relative to the wild-type strain. Subsequent fluorescence microscopy analysis revealed an increased PAS localization of $Atg9^{K113,138R}$, which explained the higher autophagy activity. However, trafficking of $Atg9^{K113,138R}$ still depended on interaction with Atg23, Atg27 and Atg1, suggesting that this alteration was specifically affecting protein level rather than protein movement. Based on these findings, we performed a screen for the E3 ligase that modifies Atg9 and found that Atg9 is stabilized the most significantly in the *met30 ts* strain, indicating that the ubiquitination is at least partly mediated by Met30. The interaction between Atg9 and Met30 was verified by BiFC assay.

In summary, we identified a novel mechanism of Atg9 regulation in autophagy through ubiquitination. In growing conditions, Atg9 is synthesized and cells are primed for autophagy. We showed that Atg9 is ubiquitinated and targeted for degradation in a proteasome-dependent manner during nutrient-rich conditions, therefore limiting autophagy to a basal level. However, when cells

are nutritionally deprived, autophagy is highly induced, necessitating an increase in the amount of Atg9; the proteasome-dependent reduction of Atg9 protein levels is reduced to give cells a jump start for autophagy. Thus, the post-translational ubiquitination of Atg9 provides an additional mechanism that allows cells to maintain appropriate levels of autophagy, and to rapidly respond and adapt to environmental stresses.

4.3 Discussion and perspectives

Although increasing details about the post-translational regulation of autophagy have been revealed in recent years, many questions remain to be answered. Modulation of proteins by phosphorylation and ubiquitination is a dynamic process; both conjugation and removal of the modulating groups are crucial to maintaining normal autophagy flux. However, information about dephosphorylation and deubiquitination is relatively limited. For example, the relevant phosphatases that affect the autophagy core machinery proteins are still unknown. Similarly, the role of deubiquitinating enzymes in the regulation of autophagy needs further investigation. In addition, the regulation of autophagy is connected to the control of apoptosis, and these two processes share many regulatory components. How these two processes are coordinated and co-regulated needs further analysis. Finally, more research about the relationship between the regulation of autophagy and human disease is required.

Bibliography

1. Klionsky, D.J., et al., *A comprehensive glossary of autophagy-related molecules and processes (2nd edition).* Autophagy, 2011. 7(11): p. 1273-94.

2. Klionsky, D.J., *The molecular machinery of autophagy: unanswered questions.* J Cell Sci, 2005. 118(Pt 1): p. 7-18.

3. Yorimitsu, T. and D.J. Klionsky, *Autophagy: molecular machinery for self-eating.* Cell Death Differ, 2005. 12 Suppl 2: p. 1542-52.

4. Baba, M., M. Osumi, and Y. Ohsumi, *Analysis of the membrane structures involved in autophagy in yeast by freeze-replica method.* Cell Struct Funct, 1995. 20(6): p. 465-71.

5. Fimia, G.M., et al., *Ambra1 regulates autophagy and development of the nervous system.* Nature, 2007. 447(7148): p. 1121-5.

6. Dunn, W.A., Jr., *Studies on the mechanisms of autophagy: maturation of the autophagic vacuole.* J Cell Biol, 1990. 110(6): p. 1935-45.

7. He, C. and D.J. Klionsky, *Atg9 trafficking in autophagy-related pathways.* Autophagy, 2007. 3(3): p. 271-4.

8. Suzuki, K., et al., *The pre-autophagosomal structure organized by concerted functions of APG genes is essential for autophagosome formation.* EMBO J, 2001. 20(21): p. 5971-81.

9. Kim, J., et al., *Convergence of multiple autophagy and cytoplasm to vacuole targeting components to a perivacuolar membrane compartment prior to de novo vesicle formation.* J Biol Chem, 2002. 277(1): p. 763-73.

10. Seglen, P.O., P.B. Gordon, and I. Holen, *Non-selective autophagy.* Semin Cell Biol, 1990. 1(6): p. 441-8.

11. Huang, W.P., et al., *The itinerary of a vesicle component, Aut7p/Cvt5p, terminates in the yeast vacuole via the autophagy/Cvt pathways.* J Biol Chem, 2000. 275(8): p. 5845-51.

12. Kirisako, T., et al., *Formation process of autophagosome is traced with Apg8/Aut7p in yeast.* J Cell Biol, 1999. 147(2): p. 435-46.

13. Suzuki, K., et al., *Hierarchy of Atg proteins in pre-autophagosomal structure organization.* Genes Cells, 2007. 12(2): p. 209-18.

14. Cheong, H. and D.J. Klionsky, *Dual role of Atg1 in regulation of autophagy-specific PAS assembly in Saccharomyces cerevisiae.* Autophagy, 2008. 4(5): p. 724-6.

15. Mao, K., et al., *Atg29 phosphorylation regulates coordination of the Atg17-Atg31-Atg29 complex with the Atg11 scaffold during autophagy initiation.* Proc Natl Acad Sci U S A, 2013. 110(31): p. E2875-84.

16. Mizushima, N., et al., *Dissection of autophagosome formation using Apg5-deficient mouse embryonic stem cells.* J Cell Biol, 2001. 152(4): p. 657-68.

17. Yamada, T., et al., *Endothelial nitric-oxide synthase antisense (NOS3AS) gene encodes an autophagy-related protein (APG9-like2) highly expressed in trophoblast.* J Biol Chem, 2005. 280(18): p. 18283-90.

18. Young, A.R., et al., *Starvation and ULK1-dependent cycling of mammalian Atg9 between the TGN and endosomes.* J Cell Sci, 2006. 119(Pt 18): p. 3888-900.

19. Noda, T., K. Suzuki, and Y. Ohsumi, *Yeast autophagosomes: de novo formation of a membrane structure.* Trends Cell Biol, 2002. 12(5): p. 231-5.

20. Kovacs, A.L., et al., *Sequestration revisited: integrating traditional electron microscopy, de novo assembly and new results.* Autophagy, 2007. 3(6): p. 655-62.

21. Gordon, P.B. and P.O. Seglen, *Prelysosomal convergence of autophagic and endocytic pathways.* Biochem Biophys Res Commun, 1988. 151(1): p. 40-7.

22. Geng, J. and D.J. Klionsky, *The Atg8 and Atg12 ubiquitin-like conjugation systems in macroautophagy. 'Protein modifications: beyond the usual suspects' review series.* EMBO Rep, 2008. 9(9): p. 859-64.

23. Mari, M., et al., *An Atg9-containing compartment that functions in the early steps of autophagosome biogenesis.* J Cell Biol, 2010. 190(6): p. 1005-22.

24. van der Vaart, A., J. Griffith, and F. Reggiori, *Exit from the Golgi is required for the expansion of the autophagosomal phagophore in yeast Saccharomyces cerevisiae.* Mol Biol Cell, 2010. 21(13): p. 2270-84.

25. Yen, W.L., et al., *The conserved oligomeric Golgi complex is involved in double-membrane vesicle formation during autophagy.* J Cell Biol, 2010. 188(1): p. 101-14.

26. Taylor, R., Jr., et al., *KCS1 deletion in Saccharomyces cerevisiae leads to a defect in translocation of autophagic proteins and reduces autophagosome formation.* Autophagy, 2012. 8(9): p. 1300-11.

27. Axe, E.L., et al., *Autophagosome formation from membrane compartments enriched in phosphatidylinositol 3-phosphate and dynamically connected to the endoplasmic reticulum.* J Cell Biol, 2008. 182(4): p. 685-701.

28. Shintani, T. and D.J. Klionsky, *Autophagy in health and disease: a double-edged sword.* Science, 2004. 306(5698): p. 990-5.

29. Kunz, J.B., H. Schwarz, and A. Mayer, *Determination of four sequential stages during microautophagy in vitro.* J Biol Chem, 2004. 279(11): p. 9987-96.

30. Deffieu, M., et al., *Glutathione participates in the regulation of mitophagy in yeast.* J Biol Chem, 2009. 284(22): p. 14828-37.

31. Dunn, W.A., Jr., et al., *Pexophagy: the selective autophagy of peroxisomes.* Autophagy, 2005. 1(2): p. 75-83.

32. Thumm, M., et al., *Isolation of autophagocytosis mutants of Saccharomyces cerevisiae.* FEBS Lett, 1994. 349(2): p. 275-80.

33. Tsukada, M. and Y. Ohsumi, *Isolation and characterization of autophagy-defective mutants of Saccharomyces cerevisiae.* FEBS Lett, 1993. 333(1-2): p. 169-74.

34. Klionsky, D.J., et al., *A unified nomenclature for yeast autophagy-related genes.* Dev Cell, 2003. 5(4): p. 539-45.

35. Harding, T.M., et al., *Isolation and characterization of yeast mutants in the cytoplasm to vacuole protein targeting pathway.* J Cell Biol, 1995. 131(3): p. 591-602.

36. Mizushima, N., *Autophagy: process and function.* Genes Dev, 2007. 21(22): p. 2861-73.

37. Mizushima, N., T. Yoshimori, and Y. Ohsumi, *The role of Atg proteins in autophagosome formation.* Annu Rev Cell Dev Biol, 2011. 27: p. 107-32.

38. Xie, Z. and D.J. Klionsky, *Autophagosome formation: core machinery and adaptations.* Nat Cell Biol, 2007. 9(10): p. 1102-9.

39. Cheong, H., et al., *Atg17 regulates the magnitude of the autophagic response.* Mol Biol Cell, 2005. 16(7): p. 3438-53.

40. Kabeya, Y., et al., *Atg17 functions in cooperation with Atg1 and Atg13 in yeast autophagy.* Mol Biol Cell, 2005. 16(5): p. 2544-53.

41. Kabeya, Y., et al., *Cis1/Atg31 is required for autophagosome formation in Saccharomyces cerevisiae.* Biochem Biophys Res Commun, 2007. 356(2): p. 405-10.

42. Kamada, Y., et al., *Tor-mediated induction of autophagy via an Apg1 protein kinase complex.* J Cell Biol, 2000. 150(6): p. 1507-13.

43. Kawamata, T., et al., *Characterization of a novel autophagy-specific gene, ATG29.* Biochem Biophys Res Commun, 2005. 338(4): p. 1884-9.

44. Reggiori, F., et al., *The Atg1-Atg13 complex regulates Atg9 and Atg23 retrieval transport from the pre-autophagosomal structure.* Dev Cell, 2004. 6(1): p. 79-90.

45. Matsuura, A., et al., *Apg1p, a novel protein kinase required for the autophagic process in Saccharomyces cerevisiae.* Gene, 1997. 192(2): p. 245-50.

46. Abeliovich, H., et al., *Chemical genetic analysis of Apg1 reveals a non-kinase role in the induction of autophagy.* Mol Biol Cell, 2003. 14(2): p. 477-90.

47. Nair, U. and D.J. Klionsky, *Molecular mechanisms and regulation of specific and nonspecific autophagy pathways in yeast.* J Biol Chem, 2005. 280(51): p. 41785-8.

48. Stephan, J.S., et al., *The Tor and PKA signaling pathways independently target the Atg1/Atg13 protein kinase complex to control autophagy.* Proc Natl Acad Sci U S A, 2009. 106(40): p. 17049-54.

49. Yeh, Y.Y., K. Wrasman, and P.K. Herman, *Autophosphorylation within the Atg1 activation loop is required for both kinase activity and the induction of autophagy in Saccharomyces cerevisiae.* Genetics, 2010. 185(3): p. 871-82.

50. Kijanska, M., et al., *Activation of Atg1 kinase in autophagy by regulated phosphorylation.* Autophagy, 2010. 6(8): p. 1168-78.

51. Kamada, Y., et al., *Tor directly controls the Atg1 kinase complex to regulate autophagy.* Mol Cell Biol, 2010. 30(4): p. 1049-58.

52. Budovskaya, Y.V., et al., *An evolutionary proteomics approach identifies substrates of the cAMP-dependent protein kinase.* Proc Natl Acad Sci U S A, 2005. 102(39): p. 13933-8.

53. Scott, S.V., et al., *Apg13p and Vac8p are part of a complex of phosphoproteins that are required for cytoplasm to vacuole targeting.* J Biol Chem, 2000. 275(33): p. 25840-9.

54. Kraft, C., et al., *Binding of the Atg1/ULK1 kinase to the ubiquitin-like protein Atg8 regulates autophagy.* EMBO J, 2012. 31(18): p. 3691-703.

55. Cao, Y., et al., *A multiple ATG gene knockout strain for yeast two-hybrid analysis.* Autophagy, 2009. 5(5): p. 699-705.

56. Kabeya, Y., et al., *Characterization of the Atg17-Atg29-Atg31 complex specifically required for starvation-induced autophagy in Saccharomyces cerevisiae.* Biochem Biophys Res Commun, 2009. 389(4): p. 612-5.

57. Ragusa, M.J., R.E. Stanley, and J.H. Hurley, *Architecture of the Atg17 complex as a scaffold for autophagosome biogenesis.* Cell, 2012. 151(7): p. 1501-1512.

58. Reggiori, F., et al., *Atg9 cycles between mitochondria and the pre-autophagosomal structure in yeasts.* Autophagy, 2005. 1(2): p. 101-9.

59. He, C., et al., *Self-interaction is critical for Atg9 transport and function at the phagophore assembly site during autophagy.* Mol Biol Cell, 2008. 19(12): p. 5506-16.

60. He, C., et al., *Recruitment of Atg9 to the preautophagosomal structure by Atg11 is essential for selective autophagy in budding yeast.* J Cell Biol, 2006. 175(6): p. 925-35.

61. Legakis, J.E., W.L. Yen, and D.J. Klionsky, *A cycling protein complex required for selective autophagy.* Autophagy, 2007. 3(5): p. 422-32.

62. Yen, W.L., et al., *Atg27 is required for autophagy-dependent cycling of Atg9.* Mol Biol Cell, 2007. 18(2): p. 581-93.

63. Krick, R., et al., *Structural and functional characterization of the two phosphoinositide binding sites of PROPPINs, a beta-propeller protein family.* Proc Natl Acad Sci U S A, 2012. 109(30): p. E2042-9.

64. Watanabe, Y., et al., *Structure-based analyses reveal distinct binding sites for Atg2 and phosphoinositides in Atg18.* J Biol Chem, 2012. 287(38): p. 31681-90.

65. Baskaran, S., et al., *Two-site recognition of phosphatidylinositol 3-phosphate by PROPPINs in autophagy.* Mol Cell, 2012. 47(3): p. 339-48.

66. Dove, S.K., et al., *Svp1p defines a family of phosphatidylinositol 3,5-bisphosphate effectors.* EMBO J, 2004. 23(9): p. 1922-33.

67. Rieter, E., et al., *Atg18 function in autophagy is regulated by specific sites within its beta-propeller.* J Cell Sci, 2013. 126(Pt 2): p. 593-604.

68. Obara, K., T. Sekito, and Y. Ohsumi, *Assortment of phosphatidylinositol 3-kinase complexes--Atg14p directs association of complex I to the pre-autophagosomal structure in Saccharomyces cerevisiae.* Mol Biol Cell, 2006. 17(4): p. 1527-39.

69. Kihara, A., et al., *Two distinct Vps34 phosphatidylinositol 3-kinase complexes function in autophagy and carboxypeptidase Y sorting in Saccharomyces cerevisiae.* J Cell Biol, 2001. 152(3): p. 519-30.

70. Araki, Y., et al., *Atg38 is required for autophagy-specific phosphatidylinositol 3-kinase complex integrity.* J Cell Biol, 2013. 203(2): p. 299-313.

71. Xie, Z., U. Nair, and D.J. Klionsky, *Atg8 controls phagophore expansion during autophagosome formation.* Mol Biol Cell, 2008. 19(8): p. 3290-8.

72. Shintani, T., et al., *Mechanism of cargo selection in the cytoplasm to vacuole targeting pathway.* Dev Cell, 2002. 3(6): p. 825-37.

73. Kirisako, T., et al., *The reversible modification regulates the membrane-binding state of Apg8/Aut7 essential for autophagy and the cytoplasm to vacuole targeting pathway.* J Cell Biol, 2000. 151(2): p. 263-76.

74. Kim, J., et al., *Apg7p/Cvt2p is required for the cytoplasm-to-vacuole targeting, macroautophagy, and peroxisome degradation pathways.* Mol Biol Cell, 1999. 10(5): p. 1337-51.

75. Ichimura, Y., et al., *A ubiquitin-like system mediates protein lipidation.* Nature, 2000. 408(6811): p. 488-92.

76. Mizushima, N., et al., *A protein conjugation system essential for autophagy.* Nature, 1998. 395(6700): p. 395-8.

77. Tanida, I., et al., *Apg7p/Cvt2p: A novel protein-activating enzyme essential for autophagy.* Mol Biol Cell, 1999. 10(5): p. 1367-79.

78. Shintani, T., et al., *Apg10p, a novel protein-conjugating enzyme essential for autophagy in yeast.* EMBO J, 1999. 18(19): p. 5234-41.

79. Mijaljica, D., et al., *Receptor protein complexes are in control of autophagy.* Autophagy, 2012. 8(11): p. 1701-5.

80. Lynch-Day, M.A. and D.J. Klionsky, *The Cvt pathway as a model for selective autophagy.* FEBS Lett, 2010. 584(7): p. 1359-66.

81. Klionsky, D.J., R. Cueva, and D.S. Yaver, *Aminopeptidase I of Saccharomyces cerevisiae is localized to the vacuole independent of the secretory pathway.* J Cell Biol, 1992. 119(2): p. 287-99.

82. Oda, M.N., et al., *Identification of a cytoplasm to vacuole targeting determinant in aminopeptidase I.* J Cell Biol, 1996. 132(6): p. 999-1010.

83. Scott, S.V., et al., *Cytoplasm-to-vacuole targeting and autophagy employ the same machinery to deliver proteins to the yeast vacuole.* Proc Natl Acad Sci U S A, 1996. 93(22): p. 12304-8.

84. Baba, M., et al., *Two distinct pathways for targeting proteins from the cytoplasm to the vacuole/lysosome.* J Cell Biol, 1997. 139(7): p. 1687-95.

85. Scott, S.V., et al., *Aminopeptidase I is targeted to the vacuole by a nonclassical vesicular mechanism.* J Cell Biol, 1997. 138(1): p. 37-44.

86. Scott, S.V., et al., *Cvt19 is a receptor for the cytoplasm-to-vacuole targeting pathway.* Mol Cell, 2001. 7(6): p. 1131-41.

87. Kim, J., et al., *Cvt9/Gsa9 functions in sequestering selective cytosolic cargo destined for the vacuole.* J Cell Biol, 2001. 153(2): p. 381-96.

88. Geng, J. and D.J. Klionsky, *Quantitative regulation of vesicle formation in yeast nonspecific autophagy.* Autophagy, 2008. 4(7): p. 955-7.

89. Kreuzaler, P.A., et al., *Stat3 controls lysosomal-mediated cell death in vivo.* Nat Cell Biol, 2011. 13(3): p. 303-9.

90. Guerriero, J.L., D. Ditsworth, and W.X. Zong, *Non-apoptotic routes to defeat cancer.* Oncoimmunology, 2012. 1(1): p. 94-96.

91. Jiang, L., M.S. Sheikh, and Y. Huang, *Decision Making by p53: Life versus Death.* Mol Cell Pharmacol, 2010. 2(2): p. 69-77.

92. Lee, R.C., R.L. Feinbaum, and V. Ambros, *The C. elegans heterochronic gene lin-4 encodes small RNAs with antisense complementarity to lin-14.* Cell, 1993. 75(5): p. 843-54.

93. Wightman, B., I. Ha, and G. Ruvkun, *Posttranscriptional regulation of the heterochronic gene lin-14 by lin-4 mediates temporal pattern formation in C. elegans.* Cell, 1993. 75(5): p. 855-62.

94. He, L. and G.J. Hannon, *MicroRNAs: small RNAs with a big role in gene regulation.* Nat Rev Genet, 2004. 5(7): p. 522-31.

95. Yu, Y., et al., *microRNA 30A promotes autophagy in response to cancer therapy.* Autophagy, 2012. 8(5): p. 853-5.

96. Wu, H., et al., *MiR-20a and miR-106b negatively regulate autophagy induced by leucine deprivation via suppression of ULK1 expression in C2C12 myoblasts.* Cell Signal, 2012. 24(11): p. 2179-86.

97. Huang, Y., A.Y. Chuang, and E.A. Ratovitski, *Phospho-DeltaNp63alpha/miR-885-3p axis in tumor cell life and cell death upon cisplatin exposure.* Cell Cycle, 2011. 10(22): p. 3938-47.

98. Shi, G., et al., *Increased miR-195 aggravates neuropathic pain by inhibiting autophagy following peripheral nerve injury.* Glia, 2013. 61(4): p. 504-12.

99. Verdoodt, B., et al., *MicroRNA-205, a novel regulator of the anti-apoptotic protein Bcl2, is downregulated in prostate cancer.* Int J Oncol, 2013. 43(1): p. 307-14.

100. Yang, X., et al., *mir-30d Regulates multiple genes in the autophagy pathway and impairs autophagy process in human cancer cells.* Biochem Biophys Res Commun, 2013. 431(3): p. 617-22.

101. Korkmaz, G., et al., *miR-376b controls starvation and mTOR inhibition-related autophagy by targeting ATG4C and BECN1.* Autophagy, 2012. 8(2): p. 165-76.

102. Frankel, L.B., et al., *microRNA-101 is a potent inhibitor of autophagy.* EMBO J, 2011. 30(22): p. 4628-41.

103. Yamamoto, H., et al., *Atg9 vesicles are an important membrane source during early steps of autophagosome formation.* J Cell Biol, 2012. 198(2): p. 219-33.

104. Yang, J., et al., *MiR-34 modulates Caenorhabditis elegans lifespan via repressing the autophagy gene atg9.* Age (Dordr), 2013. 35(1): p. 11-22.

105. Kovaleva, V., et al., *miRNA-130a targets ATG2B and DICER1 to inhibit autophagy and trigger killing of chronic lymphocytic leukemia cells.* Cancer Res, 2012. 72(7): p. 1763-72.

106. Gibbings, D., et al., *Selective autophagy degrades DICER and AGO2 and regulates miRNA activity.* Nat Cell Biol, 2012. 14(12): p. 1314-21.

107. Boya, P., F. Reggiori, and P. Codogno, *Emerging regulation and functions of autophagy.* Nat Cell Biol, 2013. 15(7): p. 713-20.

108. Levine, B., N. Mizushima, and H.W. Virgin, *Autophagy in immunity and inflammation.* Nature, 2011. 469(7330): p. 323-35.

109. Jung, C.H., et al., *mTOR regulation of autophagy.* FEBS Lett, 2010. 584(7): p. 1287-95.

110. Chang, Y.Y., et al., *Nutrient-dependent regulation of autophagy through the target of rapamycin pathway.* Biochem Soc Trans, 2009. 37(Pt 1): p. 232-6.

111. Kim, J., et al., *AMPK and mTOR regulate autophagy through direct phosphorylation of Ulk1.* Nat Cell Biol, 2011. 13(2): p. 132-41.

112. Rubinsztein, D.C., P. Codogno, and B. Levine, *Autophagy modulation as a potential therapeutic target for diverse diseases.* Nat Rev Drug Discov, 2012. 11(9): p. 709-30.

113. Feng, Y., et al., *The machinery of macroautophagy.* Cell Res, 2014. 24(1): p. 24-41.

114. Marino, G., et al., *Self-consumption: the interplay of autophagy and apoptosis.* Nat Rev Mol Cell Biol, 2014. 15(2): p. 81-94.

115. Xu, P., et al., *JNK regulates FoxO-dependent autophagy in neurons.* Genes Dev, 2011. 25(4): p. 310-22.

116. Zalckvar, E., et al., *DAP-kinase-mediated phosphorylation on the BH3 domain of beclin 1 promotes dissociation of beclin 1 from Bcl-XL and induction of autophagy.* EMBO Rep, 2009. 10(3): p. 285-92.

117. Wang, R.C., et al., *Akt-mediated regulation of autophagy and tumorigenesis through Beclin 1 phosphorylation.* Science, 2012. 338(6109): p. 956-9.

118. Kim, J., et al., *Differential regulation of distinct Vps34 complexes by AMPK in nutrient stress and autophagy.* Cell, 2013. 152(1-2): p. 290-303.

119. Cherra, S.J., 3rd, et al., *Regulation of the autophagy protein LC3 by phosphorylation.* J Cell Biol, 2010. 190(4): p. 533-9.

120. Papinski, D., et al., *Early steps in autophagy depend on direct phosphorylation of Atg9 by the Atg1 kinase.* Mol Cell, 2014. 53(3): p. 471-83.

121. Tamura, N., et al., *Atg18 phosphoregulation controls organellar dynamics by modulating its phosphoinositide-binding activity.* J Cell Biol, 2013. 202(4): p. 685-98.

122. Kuang, E., J. Qi, and Z. Ronai, *Emerging roles of E3 ubiquitin ligases in autophagy.* Trends Biochem Sci, 2013. 38(9): p. 453-60.

123. Narendra, D., et al., *Parkin is recruited selectively to impaired mitochondria and promotes their autophagy.* J Cell Biol, 2008. 183(5): p. 795-803.

124. Geisler, S., et al., *PINK1/Parkin-mediated mitophagy is dependent on VDAC1 and p62/SQSTM1.* Nat Cell Biol, 2010. 12(2): p. 119-31.

125. Chen, D., et al., *Parkin mono-ubiquitinates Bcl-2 and regulates autophagy.* J Biol Chem, 2010. 285(49): p. 38214-23.

126. Nazio, F., et al., *mTOR inhibits autophagy by controlling ULK1 ubiquitylation, self-association and function through AMBRA1 and TRAF6.* Nat Cell Biol, 2013. 15(4): p. 406-16.

127. Shi, C.S. and J.H. Kehrl, *Traf6 and A20 differentially regulate TLR4-induced autophagy by affecting the ubiquitination of Beclin 1.* Autophagy, 2010. 6(7): p. 986-7.

128. Kuang, E., et al., *Regulation of ATG4B stability by RNF5 limits basal levels of autophagy and influences susceptibility to bacterial infection.* PLoS Genet, 2012. 8(10): p. e1003007.

129. Mandell, M.A., et al., *TRIM Proteins Regulate Autophagy and Can Target Autophagic Substrates by Direct Recognition.* Dev Cell, 2014. 30(4): p. 394-409.

130. Banreti, A., M. Sass, and Y. Graba, *The emerging role of acetylation in the regulation of autophagy.* Autophagy, 2013. 9(6): p. 819-29.

131. Lin, S.Y., et al., *GSK3-TIP60-ULK1 signaling pathway links growth factor deprivation to autophagy.* Science, 2012. 336(6080): p. 477-81.

132. Yi, C., et al., *Function and molecular mechanism of acetylation in autophagy regulation.* Science, 2012. 336(6080): p. 474-7.

133. Lee, I.H. and T. Finkel, *Regulation of autophagy by the p300 acetyltransferase.* J Biol Chem, 2009. 284(10): p. 6322-8.

134. Lee, I.H., et al., *A role for the NAD-dependent deacetylase Sirt1 in the regulation of autophagy.* Proc Natl Acad Sci U S A, 2008. 105(9): p. 3374-9.

135. Zhao, J., et al., *FoxO3 coordinately activates protein degradation by the autophagic/lysosomal and proteasomal pathways in atrophying muscle cells.* Cell Metab, 2007. 6(6): p. 472-83.

136. Attaix, D. and D. Bechet, *FoxO3 controls dangerous proteolytic liaisons.* Cell Metab, 2007. 6(6): p. 425-7.

137. Daitoku, H., J. Sakamaki, and A. Fukamizu, *Regulation of FoxO transcription factors by acetylation and protein-protein interactions.* Biochim Biophys Acta, 2011. 1813(11): p. 1954-60.

138. Wang, F., et al., *SIRT2 deacetylates FOXO3a in response to oxidative stress and caloric restriction.* Aging Cell, 2007. 6(4): p. 505-14.

139. Eisenberg, T., et al., *A histone point mutation that switches on autophagy.* Autophagy, 2014. 10(6): p. 1143-5.

140. Eisenberg, T., et al., *Nucleocytosolic depletion of the energy metabolite acetyl-coenzyme a stimulates autophagy and prolongs lifespan.* Cell Metab, 2014. 19(3): p. 431-44.

141. Fullgrabe, J., et al., *The histone H4 lysine 16 acetyltransferase hMOF regulates the outcome of autophagy.* Nature, 2013. 500(7463): p. 468-71.

142. Fullgrabe, J., D.J. Klionsky, and B. Joseph, *Histone post-translational modifications regulate autophagy flux and outcome.* Autophagy, 2013. 9(10): p. 1621-3.

143. Artal-Martinez de Narvajas, A., et al., *Epigenetic regulation of autophagy by the methyltransferase G9a.* Mol Cell Biol, 2013. 33(20): p. 3983-93.

144. Tasdemir, E., et al., *Regulation of autophagy by cytoplasmic p53.* Nat Cell Biol, 2008. 10(6): p. 676-87.

145. Rouschop, K.M., et al., *The unfolded protein response protects human tumor cells during hypoxia through regulation of the autophagy genes MAP1LC3B and ATG5.* J Clin Invest, 2010. 120(1): p. 127-41.

146. Milani, M., et al., *The role of ATF4 stabilization and autophagy in resistance of breast cancer cells treated with Bortezomib.* Cancer Res, 2009. 69(10): p. 4415-23.

147. Pike, L.R., et al., *Transcriptional up-regulation of ULK1 by ATF4 contributes to cancer cell survival.* Biochem J, 2013. 449(2): p. 389-400.

148. Pike, L.R., et al., *ATF4 orchestrates a program of BH3-only protein expression in severe hypoxia.* Mol Biol Rep, 2012. 39(12): p. 10811-22.

149. Sheng, Z., et al., *BCR-ABL suppresses autophagy through ATF5-mediated regulation of mTOR transcription.* Blood, 2011. 118(10): p. 2840-8.

150. Ma, D., S. Panda, and J.D. Lin, *Temporal orchestration of circadian autophagy rhythm by C/EBPbeta.* EMBO J, 2011. 30(22): p. 4642-51.

151. Polager, S., M. Ofir, and D. Ginsberg, *E2F1 regulates autophagy and the transcription of autophagy genes.* Oncogene, 2008. 27(35): p. 4860-4.

152. Shaw, J., et al., *Antagonism of E2F-1 regulated Bnip3 transcription by NF-kappaB is essential for basal cell survival.* Proc Natl Acad Sci U S A, 2008. 105(52): p. 20734-9.

153. Yurkova, N., et al., *The cell cycle factor E2F-1 activates Bnip3 and the intrinsic death pathway in ventricular myocytes.* Circ Res, 2008. 102(4): p. 472-9.

154. Liu, H.Y., et al., *Hepatic autophagy is suppressed in the presence of insulin resistance and hyperinsulinemia: inhibition of FoxO1-dependent expression of key autophagy genes by insulin.* J Biol Chem, 2009. 284(45): p. 31484-92.

155. Mammucari, C., et al., *FoxO3 controls autophagy in skeletal muscle in vivo.* Cell Metab, 2007. 6(6): p. 458-71.

156. Xiong, X., et al., *The autophagy-related gene 14 (Atg14) is regulated by forkhead box O transcription factors and circadian rhythms and plays a critical role in hepatic autophagy and lipid metabolism.* J Biol Chem, 2012. 287(46): p. 39107-14.

157. Sanchez, A.M., et al., *AMPK promotes skeletal muscle autophagy through activation of forkhead FoxO3a and interaction with Ulk1.* J Cell Biochem, 2012. 113(2): p. 695-710.

158. Schips, T.G., et al., *FoxO3 induces reversible cardiac atrophy and autophagy in a transgenic mouse model.* Cardiovasc Res, 2011. 91(4): p. 587-97.

159. Kang, Y.A., et al., *Autophagy driven by a master regulator of hematopoiesis.* Mol Cell Biol, 2012. 32(1): p. 226-39.

160. Sun, T., et al., *c-Jun NH2-terminal kinase activation is essential for up-regulation of LC3 during ceramide-induced autophagy in human nasopharyngeal carcinoma cells.* J Transl Med, 2011. 9: p. 161.

161. Jia, G., et al., *Insulin-like growth factor-1 and TNF-alpha regulate autophagy through c-jun N-terminal kinase and Akt pathways in human atherosclerotic vascular smooth cells.* Immunol Cell Biol, 2006. 84(5): p. 448-54.

162. Li, D.D., et al., *The pivotal role of c-Jun NH2-terminal kinase-mediated Beclin 1 expression during anticancer agents-induced autophagy in cancer cells.* Oncogene, 2009. 28(6): p. 886-98.

163. Copetti, T., et al., *p65/RelA modulates BECN1 transcription and autophagy.* Mol Cell Biol, 2009. 29(10): p. 2594-608.

164. Ling, J., et al., *KrasG12D-induced IKK2/beta/NF-kappaB activation by IL-1alpha and p62 feedforward loops is required for development of pancreatic ductal adenocarcinoma.* Cancer Cell, 2012. 21(1): p. 105-20.

165. Yee, K.S., et al., *PUMA- and Bax-induced autophagy contributes to apoptosis.* Cell Death Differ, 2009. 16(8): p. 1135-45.

166. Kenzelmann Broz, D., et al., *Global genomic profiling reveals an extensive p53-regulated autophagy program contributing to key p53 responses.* Genes Dev, 2013. 27(9): p. 1016-31.

167. Rosenbluth, J.M. and J.A. Pietenpol, *mTOR regulates autophagy-associated genes downstream of p73.* Autophagy, 2009. 5(1): p. 114-6.

168. Seo, Y.K., et al., *Genome-wide localization of SREBP-2 in hepatic chromatin predicts a role in autophagy.* Cell Metab, 2011. 13(4): p. 367-75.

169. McCormick, J., et al., *STAT1 deficiency in the heart protects against myocardial infarction by enhancing autophagy.* J Cell Mol Med, 2012. 16(2): p. 386-93.

170. Dauer, D.J., et al., *Stat3 regulates genes common to both wound healing and cancer.* Oncogene, 2005. 24(21): p. 3397-408.

171. Lipinski, M.M., et al., *A genome-wide siRNA screen reveals multiple mTORC1 independent signaling pathways regulating autophagy under normal nutritional conditions.* Dev Cell, 2010. 18(6): p. 1041-52.

172. Settembre, C., et al., *TFEB controls cellular lipid metabolism through a starvation-induced autoregulatory loop.* Nat Cell Biol, 2013. 15(6): p. 647-58.

173. Moresi, V., et al., *Histone deacetylases 1 and 2 regulate autophagy flux and skeletal muscle homeostasis in mice.* Proc Natl Acad Sci U S A, 2012. 109(5): p. 1649-54.

174. Reggiori, F. and D.J. Klionsky, *Autophagic processes in yeast: mechanism, machinery and regulation.* Genetics, 2013. 194(2): p. 341-61.

175. Feng, Y., Z. Yao, and D.J. Klionsky, *How to control self-digestion: transcriptional, post-transcriptional, and post-translational regulation of autophagy.* Trends Cell Biol, 2015. 25(6): p. 354-363.

176. Xie, Y., et al., *Posttranslational modification of autophagy-related proteins in macroautophagy.* Autophagy, 2015. 11(1): p. 28-45.

177. Wilkinson, D.S., et al., *Phosphorylation of LC3 by the Hippo kinases STK3/STK4 is essential for autophagy.* Mol Cell, 2015. 57(1): p. 55-68.

178. Noda, T., et al., *Apg9p/Cvt7p is an integral membrane protein required for transport vesicle formation in the Cvt and autophagy pathways.* J Cell Biol, 2000. 148(3): p. 465-80.

179. Backues, S.K., et al., *Estimating the size and number of autophagic bodies by electron microscopy.* Autophagy, 2014. 10(1): p. 155-64.

180. Noda, T. and Y. Ohsumi, *Tor, a phosphatidylinositol kinase homologue, controls autophagy in yeast.* J Biol Chem, 1998. 273(7): p. 3963-6.

181. Pfaffenwimmer, T., et al., *Hrr25 kinase promotes selective autophagy by phosphorylating the cargo receptor Atg19.* EMBO Rep, 2014. 15(8): p. 862-70.

182. Tanaka, C., et al., *Hrr25 triggers selective autophagy-related pathways by phosphorylating receptor proteins.* J Cell Biol, 2014. 207(1): p. 91-105.

183. Yang, Z., et al., *Positive or negative roles of different cyclin-dependent kinase Pho85-cyclin complexes orchestrate induction of autophagy in Saccharomyces cerevisiae.* Mol Cell, 2010. 38(2): p. 250-64.

184. Jin, M., et al., *Transcriptional regulation by Pho23 modulates the frequency of autophagosome formation.* Curr Biol, 2014. 24(12): p. 1314-1322.

185. Liu, H. and J.H. Naismith, *An efficient one-step site-directed deletion, insertion, single and multiple-site plasmid mutagenesis protocol.* BMC Biotechnol, 2008. 8: p. 91.

186. Klionsky, D.J., *Monitoring autophagy in yeast: the Pho8Delta60 assay.* Methods Mol Biol, 2007. 390: p. 363-71.

187. Hanaoka, H., et al., *Leaf senescence and starvation-induced chlorosis are accelerated by the disruption of an Arabidopsis autophagy gene.* Plant Physiol, 2002. 129(3): p. 1181-93.

188. Yorimitsu, T. and D.J. Klionsky, *Atg11 links cargo to the vesicle-forming machinery in the cytoplasm to vacuole targeting pathway.* Mol Biol Cell, 2005. 16(4): p. 1593-605.

189. Reggiori, F., et al., *Early stages of the secretory pathway, but not endosomes, are required for Cvt vesicle and autophagosome assembly in Saccharomyces cerevisiae.* Mol Biol Cell, 2004. 15(5): p. 2189-204.

190. Suzuki, K., Y. Kamada, and Y. Ohsumi, *Studies of cargo delivery to the vacuole mediated by autophagosomes in Saccharomyces cerevisiae.* Dev Cell, 2002. 3(6): p. 815-24.

191. Leber, R., et al., *Yol082p, a novel CVT protein involved in the selective targeting of aminopeptidase I to the yeast vacuole.* J Biol Chem, 2001. 276(31): p. 29210-7.

192. Cao, Y., et al., *In vivo reconstitution of autophagy in Saccharomyces cerevisiae.* J Cell Biol, 2008. 182(4): p. 703-13.

193. Backues, S.K., et al., *Atg23 and Atg27 act at the early stages of Atg9 trafficking in S. cerevisiae.* Traffic, 2015. 16(2): p. 172-90.

194. Tucker, K.A., et al., *Atg23 is essential for the cytoplasm to vacuole targeting pathway and efficient autophagy but not pexophagy.* J Biol Chem, 2003. 278(48): p. 48445-52.

195. Sung, M.K. and W.K. Huh, *Bimolecular fluorescence complementation analysis system for in vivo detection of protein-protein interaction in Saccharomyces cerevisiae.* Yeast, 2007. 24(9): p. 767-75.

196. Mao, K., et al., *The progression of peroxisomal degradation through autophagy requires peroxisomal division.* Autophagy, 2014. 10(4): p. 652-61.

197. Wang, K., et al., *Phosphatidylinositol 4-kinases are required for autophagic membrane trafficking.* J Biol Chem, 2012. 287(45): p. 37964-72.

198. Zheng, L., U. Baumann, and J.L. Reymond, *An efficient one-step site-directed and site-saturation mutagenesis protocol.* Nucleic Acids Res, 2004. 32(14): p. e115.

199. Dephoure, N. and S.P. Gygi, *A solid phase extraction-based platform for rapid phosphoproteomic analysis.* Methods, 2011. 54(4): p. 379-86.

200. Huttlin, E.L., et al., *A tissue-specific atlas of mouse protein phosphorylation and expression.* Cell, 2010. 143(7): p. 1174-89.

201. Elias, J.E. and S.P. Gygi, *Target-decoy search strategy for increased confidence in large-scale protein identifications by mass spectrometry.* Nat Methods, 2007. 4(3): p. 207-14.

202. Beausoleil, S.A., et al., *A probability-based approach for high-throughput protein phosphorylation analysis and site localization.* Nat Biotechnol, 2006. 24(10): p. 1285-92.

203. Wright, R., *Transmission electron microscopy of yeast.* Microsc Res Tech, 2000. 51(6): p. 496-510.

204. Noda, T. and D.J. Klionsky, *The quantitative Pho8Delta60 assay of nonspecific autophagy.* Methods Enzymol, 2008. 451: p. 33-42.

205. Noda, T., et al., *Novel system for monitoring autophagy in the yeast Saccharomyces cerevisiae.* Biochem Biophys Res Commun, 1995. 210(1): p. 126-32.

206. Robinson, J.S., et al., *Protein sorting in Saccharomyces cerevisiae: isolation of mutants defective in the delivery and processing of multiple vacuolar hydrolases.* Mol Cell Biol, 1988. 8(11): p. 4936-48.

207. Kanki, T., et al., *A genomic screen for yeast mutants defective in selective mitochondria autophagy.* Mol Biol Cell, 2009. 20(22): p. 4730-8.

208. Yin, Z., C. Pascual, and D.J. Klionsky, *Autophagy: machinery and regulation.* Microb Cell, 2016. 3(12): p. 588-596.

209. He, S., et al., *PtdIns(3)P-bound UVRAG coordinates Golgi-ER retrograde and Atg9 transport by differential interactions with the ER tether and the beclin 1 complex.* Nat Cell Biol, 2013. 15(10): p. 1206-1219.

210. Tooze, S.A. and T. Yoshimori, *The origin of the autophagosomal membrane.* Nat Cell Biol, 2010. 12(9): p. 831-5.

211. Feng, Y., et al., *Phosphorylation of Atg9 regulates movement to the phagophore assembly site and the rate of autophagosome formation.* Autophagy, 2016. 12(4): p. 648-58.

212. Levine, B. and G. Kroemer, *Autophagy in the pathogenesis of disease.* Cell, 2008. 132(1): p. 27-42.

213. Choi, A.M., S.W. Ryter, and B. Levine, *Autophagy in human health and disease.* N Engl J Med, 2013. 368(7): p. 651-62.

214. Deribe, Y.L., T. Pawson, and I. Dikic, *Post-translational modifications in signal integration.* Nat Struct Mol Biol, 2010. 17(6): p. 666-72.

215. Shaid, S., et al., *Ubiquitination and selective autophagy.* Cell Death Differ, 2013. 20(1): p. 21-30.

216. Swatek, K.N. and D. Komander, *Ubiquitin modifications.* Cell Res, 2016. 26(4): p. 399-422.

217. Liu, C.C., et al., *Cul3-KLHL20 Ubiquitin Ligase Governs the Turnover of ULK1 and VPS34 Complexes to Control Autophagy Termination.* Mol Cell, 2016. 61(1): p. 84-97.

218. Shi, C.S. and J.H. Kehrl, *TRAF6 and A20 regulate lysine 63-linked ubiquitination of Beclin-1 to control TLR4-induced autophagy.* Sci Signal, 2010. 3(123): p. ra42.

219. Liu, J., et al., *Beclin1 controls the levels of p53 by regulating the deubiquitination activity of USP10 and USP13.* Cell, 2011. 147(1): p. 223-34.

220. Radivojac, P., et al., *Identification, analysis, and prediction of protein ubiquitination sites.* Proteins, 2010. 78(2): p. 365-80.

221. Hjerpe, R., et al., *Efficient protection and isolation of ubiquitylated proteins using tandem ubiquitin-binding entities.* EMBO Rep, 2009. 10(11): p. 1250-8.

222. Ravid, T., S.G. Kreft, and M. Hochstrasser, *Membrane and soluble substrates of the Doa10 ubiquitin ligase are degraded by distinct pathways.* EMBO J, 2006. 25(3): p. 533-43.

223. Shintani, T. and D.J. Klionsky, *Cargo proteins facilitate the formation of transport vesicles in the cytoplasm to vacuole targeting pathway.* J Biol Chem, 2004. 279(29): p. 29889-94.

224. Smothers, D.B., et al., *The abundance of Met30p limits SCF(Met30p) complex activity and is regulated by methionine availability.* Mol Cell Biol, 2000. 20(21): p. 7845-52.

225. Hunter, T., *The age of crosstalk: phosphorylation, ubiquitination, and beyond.* Mol Cell, 2007. 28(5): p. 730-8.

226. Gueldener, U., et al., *A second set of loxP marker cassettes for Cre-mediated multiple gene knockouts in budding yeast.* Nucleic Acids Res, 2002. 30(6): p. e23.

227. Longtine, M.S., et al., *Additional modules for versatile and economical PCR-based gene deletion and modification in Saccharomyces cerevisiae.* Yeast, 1998. 14(10): p. 953-61.

228. Hamasaki, M., et al., *Autophagosomes form at ER-mitochondria contact sites.* Nature, 2013. 495(7441): p. 389-93.

229. Hayashi-Nishino, M., et al., *Electron tomography reveals the endoplasmic reticulum as a membrane source for autophagosome formation.* Autophagy, 2010. 6(2): p. 301-3.

230. Yla-Anttila, P., et al., *3D tomography reveals connections between the phagophore and endoplasmic reticulum.* Autophagy, 2009. 5(8): p. 1180-5.

231. Ge, L., et al., *The ER-Golgi intermediate compartment is a key membrane source for the LC3 lipidation step of autophagosome biogenesis.* Elife, 2013. 2: p. e00947.

232. Ravikumar, B., et al., *Plasma membrane contributes to the formation of pre-autophagosomal structures.* Nat Cell Biol, 2010. 12(8): p. 747-57.

233. Jin, M., et al., *Transcriptional regulation by Pho23 modulates the frequency of autophagosome formation.* Curr Biol, 2014. 24(12): p. 1314-22.